

---

# **Calcium-regulated Processes in Plant Organelles: Role of Calmodulin in Mitochondrial Protein Translocation**

---

Dissertation

der Fakultät für Biologie  
der Ludwig Maximilians Universität  
München

Vorgelegt von

Nargis Parvin

Aus Bolpur, Indien

München, den 17.06.2015

Gutachter/in: 1. Prof. Dr. Ute C. Vothknecht

2. Prof. Dr. Jörg Nickelsen

Datum der Einreichung: 17.06.2015

Datum der Promotion: 21.08.2015

## **Ehrenwörtliche Versicherung**

Ich versichere hiermit an Eides statt, dass die vorliegende Dissertation von mir selbstständig und ohne unerlaubte Hilfe angefertigt wurde.

## **Erklärung**

Diese Dissertation wurde keiner weiteren Prüfungskommission weder in Teilen noch als Ganzes vorgelegt. Ich habe nicht versucht, anderweitig eine Dissertation einzureichen oder mich einer Doktorprüfung zu unterziehen.

München, den 17. Juni 2015

---

*Ort, Datum*

---

*Nargis Parvin*

---

**Table of Contents**

1	Introduction .....	1
1.1	Mitochondrial Protein Import .....	1
1.1.2	Protein Translocation into Plant Mitochondria .....	5
1.2	Aim of this study .....	9
2	Materials .....	10
2.1	Chemicals .....	10
2.2	Enzymes and kits .....	11
2.3	Molecular weight and size markers .....	11
2.4	Plasmid DNA vectors .....	12
2.5	Bacteria strains .....	12
2.6	Oligonucleotides .....	13
2.7	List of constructs .....	13
2.8	Accession numbers .....	14
2.9	Radioisotopes .....	15
2.10	Antibodies .....	15
2.11	Plant material and growth conditions .....	16
3	Methods .....	17
3.1	Nucleic acid methods .....	17
3.1.1	General nucleic acid methods .....	17
3.1.2	Molecular cloning and construction of expression plasmids .....	17
3.1.3	Construction of plasmids to generate transgenic plants .....	18
3.2	Protein methods .....	18
3.2.1	General protein methods .....	18
3.2.2	Purification of mitochondria .....	19
3.2.3	Purification of stromal extracts from Arabidopsis .....	19
3.2.4	Expression and purification of recombinant proteins .....	20
3.2.5	Affinity chromatography on CaM-agarose .....	20
3.2.6	Bioinformatical analyses .....	21
3.2.7	Chemical cross-linking using EDC or DSP .....	21
3.2.8	Co-immunoprecipitation .....	22
3.2.9	Microscale Thermophoresis (MST) .....	22
3.2.10	Blue Native PAGE .....	23

---

3.2.11	<i>In vitro</i> protein import into <i>Arabidopsis thaliana</i> mitochondria .....	23
3.2.12	Fractionation of Arabidopsis stroma proteins by FPLC .....	24
3.2.13	<i>In vitro</i> phosphorylation assays of recombinant proteins .....	24
3.3	Plant methods .....	24
3.3.1	Generation of transgenic plants .....	24
3.3.2	Phenotypic analysis of mutant plants .....	25
3.3.3	Microarray analysis .....	25
3.3.4	Quantitative real-time PCR .....	26
3.3.5	Self-assembly GFP assay .....	26
3.4	Bacteria methods .....	27
3.4.1	Preparation of chemical-competent <i>E. coli</i> .....	27
3.4.2	Preparation of electro-competent <i>Agrobacteria</i> .....	27
4	Results .....	28
4.1	Isolation of CaM-binding proteins from plant mitochondria .....	28
4.1.1	Identification of CaM binding proteins by mass spectrometry .....	29
4.2	Confirmation of TOM9.2 binding to CaM .....	30
4.3	TOM9.2 binds to CaM at its cytosolic domain .....	32
4.3.1	<i>In silico</i> identification of a potential CaMBD of TOM9.2 .....	34
4.3.2	Experimental confirmation of the CaMBD .....	35
4.4	The TOM9 CaMBD is conserved among dicots .....	37
4.4.1	AtTOM9.1 can also interact with CaM .....	39
4.5	CaM-binding to TOM9.2 affects its interaction with TOM20 .....	40
4.5.1	TOM9 interacts with TOM20 <i>in vivo</i> .....	42
4.6	Role of CaM for the targeting of TOM9 to mitochondria .....	43
4.7	Screening for T-DNA insertion lines in the <i>TOM9.2</i> gene locus .....	46
4.8	Generation of <i>TOM9.2</i> knock-down plants RNA silencing .....	48
4.8.1	TOM9 knock-down plants exhibit several phenotypes .....	49
4.9	<i>TOM9.2</i> knock-down plants have up-regulated expression of genes related to floral development .....	52
4.10	<i>TOM9.2</i> knock-down plants display differential mitochondrial protein abundance .....	57
4.11	<i>TOM9.2</i> knock-down plants show a reduction in assembled TOM and TIM23 complex .....	58

---

4.12	Mitochondria from <i>TOM9.2</i> knock-down plants are import competent.....	60
4.13	Calcium-dependent protein phosphorylation.....	61
4.13.1	Calcium-dependent phosphorylation site of CaS .....	61
4.13.2	Calcium dependency of CaS phosphorylation.....	63
4.14	Isolation of potential stromal calcium-dependent kinases .....	64
4.14.1	Analysis of subcellular localization of the identified kinases .....	66
5	Discussion .....	68
5.1	The plant specific protein import system.....	68
5.2	Importance of TOM9 in the plant development .....	70
5.2	Essentiality of TOM9 for the TOM complex organization .....	73
5.3	TOM9 as a CaM-binding protein.....	74
5.4	CaM regulation of mitochondrial protein import.....	75
6.	References .....	77
	Summary.....	87
	Zusammenfassung .....	88
	Acknowledgements .....	89
	Appendices .....	90
	Appendix I: List of oligomers .....	90
	Appendix II: Microarray data.....	92
	Appendix III: Mass spectrometric data.....	100

## 1 Introduction

Plants as sessile organism cannot escape their immediate location. In order to properly adapt to stresses and changes in their environment they evolved specific signalling transduction mechanisms to regulate various cellular processes in response to these stimuli. In many cases these complex strategies involve cross-talk between different signalling networks and metabolic pathways, acting in a stimuli-specific and orchestrated manner. In eukaryotic cells, calcium plays an important role in regulating a great variety of cellular processes by acting as a secondary messenger. However, very little is known about calcium-mediated regulation within endosymbiotic organelles, i.e. mitochondria and chloroplasts. In both organelles the regulation of the protein import by calcium/calmodulin (CaM) was shown, but only for chloroplasts the mediating calmodulin-binding protein (CaMBP) was identified. Therefore, the mediator of the CaM signaling in the mitochondrial protein import is yet to be elucidated.

### 1.1 Mitochondrial Protein Import

The major portion of the mitochondrial proteins are encoded in the nuclear genome and synthesised on cytosolic ribosomes. Those cytosol-synthesized peptides, also called precursor proteins or presequences contain signal sequences that are recognized by multi-subunit protein translocases located in the mitochondrial membranes and thereby facilitate their import into the organelle (Milenkovic et al., 2007; Chacinska et al., 2009; Dudek et al., 2013). The mitochondrial signal sequences are usually amphiphillic helices that are positively charged at one surface of the helix and hydrophobic on the other surface. The first step of mitochondrial protein import is recognition by receptors of the translocase of the outer membrane of mitochondria (TOM complex) followed by insertion through the TOM complex channel. After passing through the TOM complex the precursor proteins can be directed to one of the two translocase complexes present in the inner membrane (TIM23 and TIM22 complex), to the sorting and assembly machinery (SAM complex) on the outer membrane or to the mitochondrial intermembrane space assembly (MIA) complex. The machinery for importing proteins into mitochondria is well described in yeasts and is more or less conserved among eukaryotes from fungi and animals to plants

(Liu et al., 2011; Eckers et al., 2012). However significant changes in structure and function of some components as well as the absence of some direct orthologs have been noted in plants in comparison to yeasts, indicating a modulation of the system to function as a plant-specific machinery (Duncan et al., 2013; Murcha et al., 2014a; Murcha et al., 2014b). In addition to that, multiplication of the genes encoding components of the protein import machinery in several cases is the cause of more divergence and complexity of the mitochondrial import apparatus in plants.

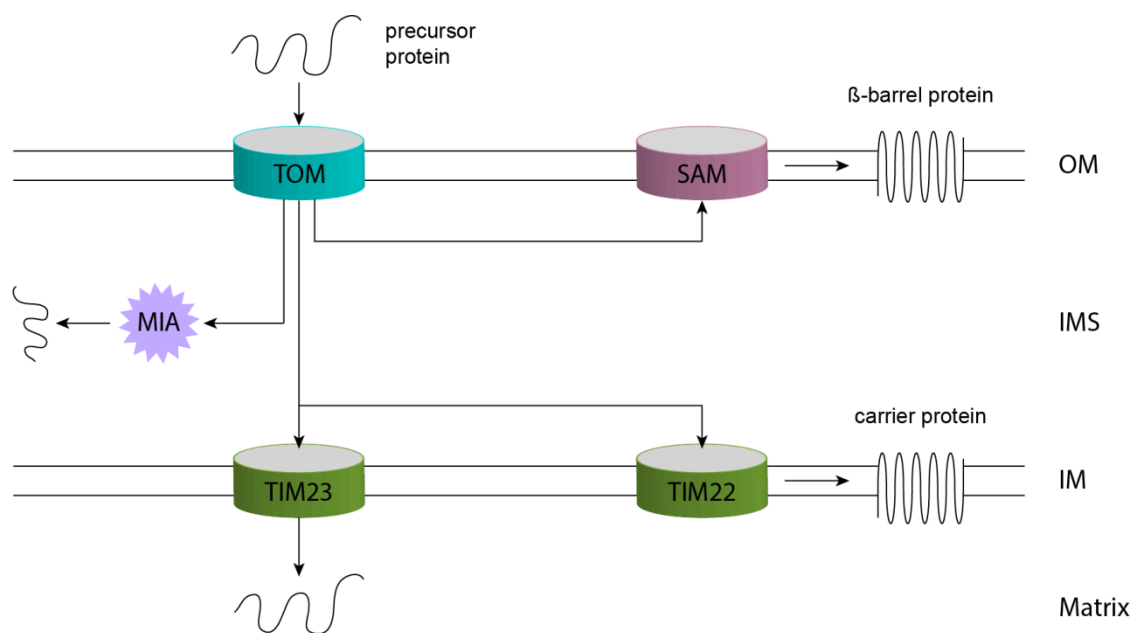


**Fig. 1 The mitochondrial protein import machinery**

All mitochondria-targeted precursor proteins pass through the TOM complex and are then delivered to the SAM, TIM23, TIM22 or MIA complexes. TOM - Translocase of the Outer membrane of Mitochondria, SAM - Sorting and Assembly Machinery of the outer membrane, TIM - Translocase of the Inner membrane of Mitochondria, MIA - Mitochondrial Intermembrane space Assembly machinery, OM - outer membrane, IMS - intermembrane space.

The TOM complex from yeast is a multisubunit protein import machinery containing a central channel, a central receptor and small Toms of mostly unknown function, together also known as the general insertion pore (GIP) complex (Milenkovic et al., 2007; Chacinska et al., 2009; Dudek et al., 2013). The GIP complex comprises the general insertion pore, Tom40, the small Tom proteins - Tom5, 6 and 7 - and the central receptor Tom22. There are two other receptors Tom20 and Tom70, that are loosely associated with the GIP complex and are functioning as the primary receptors for incoming precursor



proteins though they differ from each other on the basis of substrate specificity (Abe et al., 2000; Saitoh et al., 2007; Brix et al., 1997; Wu et al., 2006). Tom20 interacts with precursors that contain N-terminal cleavable presequences while Tom70 recognizes those with internal non-cleavable targeting signals. After being bound to the primary receptors, the presequences are transferred to the secondary receptor Tom22 which then delivers the peptides to the central translocation pore Tom40 (Kiebler et al., 1993; van Wilpe et al., 1999). However, it should be noted that this process is debated since other studies have shown that Tom20 and Tom22 can bind to presequences simultaneously instead of successively (Shiota et al., 2011). Tom22 was also shown to act as a receptor on the intermembrane space face for further transfer of presequences from TOM to the TIM23 complex as soon as they emerge from the Tom40 pore (van Wilpe et al., 1999; Moczko et al., 1997).

Yeast Tom20 is a type-II transmembrane protein that possesses a very short N-terminal region exposed to the intermembrane space, a single  $\alpha$ -helical transmembrane domain and a large C-terminal domain protruding into the cytosol. The large cytosolic part of the protein acts as the receptor domain, through which the protein interacts directly with the target sequences of mitochondrial precursor proteins (Perry et al., 2008; Moczko et al., 1994). NMR spectroscopic analysis of the cytosolic domain of rat Tom20 revealed that the receptor domain is comprised of five helices (Abe et al., 2000). A single tetratricopeptide repeat (TPR) motif is formed by the first two helices and together with the third helix they form a groove having a centrally located hydrophobic patch that enables the receptor to bind presequences. This study has also unraveled the chemical nature of this interaction, showing that the interaction between Tom20 and the presequences is hydrophobic in nature; the hydrophobic face of the amphiphilic presequence peptide interacts with the hydrophobic groove of the receptor while its hydrophilic face is exposed to the aqueous surface (Abe et al., 2000). Studies on yeasts revealed that a mild solubilization treatment is enough to make the Tom20 and Tom70 detached from the 400kDa GIP complex and appeared in lower molecular weight sub-complexes. This experiment suggested that Tom20 and Tom70 are not tightly associated with the GIP complex (Dekker et al., 1998). In addition to that, neither of these peripheral receptors is required for GIP complex formation and principal function, since in absence of Tom20 or Tom70 the GIP complex is still present and mitochondria are competent to import precursor proteins. Though Tom20

insertion into the outer membrane does not require Tom20 or Tom22, the cytosolic receptor domain of Tom22 is essential to stabilize the assembly of Tom20 into the TOM40 complex (Yamano et al., 2008).

In case of fungi and animals, the N-terminal region of Tom22 is exposed to the cytosol and the C-terminal region to the intermembrane space (Lithgow et al., 1994; Cousino R. et al., 1998). The cytosolic N-terminus consists of a *cis* receptor domains and a short amino acid stretch that serves as the targeting signal for Tom22 to mitochondria. The cytosol residing *cis*-receptor domain of Tom22 is able to bind presequences of incoming mitochondrial precursor proteins specifically and acts as a docking site for the peripheral receptors Tom70 and Tom20 (Brix et al., 1997; Kiebler et al., 1993; van Wilpe et al., 1999). From yeasts it is known that the *cis* receptor domain is essential for viability as shown from a study where a truncated construct of Tom22 lacking the first 65 amino acids cannot rescue the lethal phenotype of a  $\Delta tom22$  yeast strain (Cousino R. et al., 1998). The membrane spanning domain of Tom22 is responsible for interacting with the TOM complex and is essential for the assembly of the large 400 kDa GIP complex. The 400 kDa GIP complex contains four to six molecules of Tom40, three to six molecules of Tom22 and probably two to four copies of each of the three small Tom proteins (Dekker et al., 1998). Truncated versions of Tom22 lacking this domain are unable to assemble the GIP complex and therefore the 400 kDa complex dissociates into smaller 100 kDa complexes. This 100 kDa sub-complex most likely contains a single channel made up of a Tom40 dimer as well as all the small Tom proteins and this sub-complex is still able to import proteins. Neither the cytosolic domain nor the intermembrane space domain of Tom22 is required to maintain stability of the 400kDa GIP complex (van Wilpe et al., 1999). The C-terminal part of Tom22 that protrudes into the intermembrane space is called *trans*-receptor domain. It binds presequences of the precursor proteins once they are translocated through the Tom40 pore and transfers them to the TIM23 complex (Moczko et al., 1997; Waegemann et al., 2014). Yeast mitochondria containing Tom22 lacking this *trans*-receptor domain show impaired import of proteins with N-terminal presequence (Moczko et al., 1997). The *cis* and *trans* receptor domains of fungal and mammalian Tom22 contain clusters of acidic amino acid residues. This suggests that contact with the presequences occurs through electrostatic interactions (Bolliger et al., 1995) since the presequences generally form amphiphillic helices with one side containing positively charged amino acids whereas the

other side is hydrophobic in nature. *In vitro* protein import analysis of different precursor proteins into yeast mitochondria lacking the cytosolic receptor domain of Tom20 or Tom22 revealed that these two receptors show specificities to similar kind of substrates indicating that both of these receptors are involved in the same pathway of targeting signal recognition in protein translocation into mitochondria (Yamano et al., 2008). This evidence supports the hypothesis that the opposite sides of an amphiphilic helix formed by the same presequence is recognized by Tom20 and Tom22 simultaneously; while Tom20 recognizes the hydrophobic side, the Tom22 interacts with the positively charged hydrophilic side of the amphiphilic helix (Abe et al., 2000; Brix et al., 1999). Recently, a study in yeasts showed that the cytosolic domain of Tom22 can interact with Tom20 most likely through a region rich in acidic residues around the amino acids 44-52, named as acidic Tom20-interacting region (Shiota et al., 2011). It was further shown that this acidic Tom20-interacting region of Tom22 is also responsible for binding presequences. Furthermore, this study revealed that the cytosolic domain of Tom20 interacts with Tom22 most likely via the region around the first  $\alpha$ -helix. This Tom22-interacting domain is a part of the hydrophobic groove that constitutes the binding site of presequences in rat Tom20. This study further revealed that the cytosolic domains of Tom20 and Tom22 dissociate from each other in presence of mitochondrial presequences indicating that there is a possible competition between Tom22 and the presequences to interact with Tom20.

### **1.1.2 Protein Translocation into Plant Mitochondria**

In plants, orthologs for most of the above mentioned translocation components have been identified and are believed to take up similar functions as in yeasts and mammals. However, there are significant amount of dissimilarities compared to yeasts and mammals and thus the plant import apparatus appears as a unique system. The outer membrane translocation pore TOM40 is well conserved and has been shown to be essential for plant viability. Arabidopsis has two TOM40 isoforms, TOM40-1 and TOM40-2, with TOM40-1 being the higher expressed one and Arabidopsis plants lacking this isoform are lethal (Lister et al., 2004; Baker et al., 1990). TOM40 has a  $\beta$ -barrel structure and is deeply integrated in the outer membrane. Though no Tom22 ortholog has been found in plants, a truncated form of Tom22, called TOM9, is present (Macasev et al., 2000; Macasev et al.,

2004). By contrast, sequence and structure analyses did not find any direct orthologs or protein with similar structure for Tom70 and Tom20 in plants. However, a 23 kDa protein, named TOM20, has been identified which appears to be functionally similar to the yeast Tom20 (Jänsch et al., 1998; Werhahn et al., 2001; Heins et al., 1996). Tom70 might be completely missing in plants, but a novel outer membrane component called OM64 that is unique to plants could represent a candidate to take over the function of Tom70 as a receptor.

### ***TOM20***

Though Tom20 from yeasts and plants display no significant similarity in their primary sequences and not even in their orientation, yeast and plant Tom20 are functionally equivalent. Therefore, it is believed that those two proteins have originated from two independent genetic ancestors (Perry et al., 2006). Studies on TOM20 through NMR spectroscopic analysis revealed that the large cytosolic domain of TOM20 has seven antiparallel  $\alpha$ -helices. Four of these helices -  $\alpha_2$ ,  $\alpha_3$ ,  $\alpha_4$  and  $\alpha_5$  - form two TPR motifs (Lister et al., 2007; Perry et al., 2006; Rimmer et al., 2011). These TPR motifs contain 43-44 AA residues instead of the 34 AA residues as found in yeast and mammal Tom20 (Lamb et al., 1995). The two TPR motifs of TOM20 are flanked by three other helices:  $\alpha_1$  on one side and  $\alpha_6$  and  $\alpha_7$  on the other side and together they form a groove. This groove contains a unique bidentate binding site to bind presequences that have two hydrophobic patches separated by a distance of around 20°A. Leu12, Phe13, Ile16 and Trp79 of TOM20 comprise the first hydrophobic patch, whereas the second patch is formed by Phe90, Leu91, Leu135 and Ala139 (Rimmer et al., 2011). In case of plants, the presequences of the mitochondrial precursor proteins usually have at least two receptor binding domains, each of which is able to interact with both presequence binding sites of TOM20. As in yeasts and mammals, these interactions are hydrophobic in nature and it has been suggested that the involvement of both interaction sites is necessary for the most efficient recognition of presequence by the receptor. Three different isoforms of TOM20 have been identified in Arabidopsis, called TOM20.2, TOM20.3 and TOM20.4 (according to the chromosome on which they are located), and all of them seem to act as receptors for precursor proteins (Lister et al., 2007). In yeasts, when either Tom20 or Tom70 was depleted, it resulted in severe growth defects and impaired protein import into mitochondria. Moreover, the absence of both receptors at the same time was lethal

(Ramage et al., 1993). Depletion of all three TOM20 isoforms in Arabidopsis showed only a minor impairment in the protein import ability and the plants show slight delay in flowering time (Lister et al., 2007).

In yeasts, Tom20 is not an integral part of the TOM complex but plant TOM20 is tightly associated with the complex. The protein has been shown to migrate with the TOM complex on blue native (BN) PAGE even after solubilization of mitochondria with strong anionic detergents (Lister et al., 2007). In addition, the TOM complex in plants can be formed with only one TOM20 isoform since in all TOM20 double knockout plants a protein complex of a similar apparent molecular mass as in wild type was detected. This indicates that the integrity of the TOM complex is not disrupted as long as one TOM20 isoform remains. Interestingly, TOM20 has also been found in a second complex with higher molecular weight, which is present in wild type but is found more prominently in *tom20-3/tom20-4* double knockout plants (Lister et al., 2007). Despite being integral part of the TOM complex as well as the major presequence receptor of the TOM complex, mitochondria isolated from *tom20-2/tom20-3/tom20-4* tripple knock-out plants are import competent (Lister et al., 2007). Therefore, it is clear that the import of precursor proteins does not depend on TOM20 at least *in vitro*. It cannot be excluded that the absence of TOM20 can be compensated by another import component such as AtOM64, since the later was found upregulated in absence of TOM20 (Duncan et al., 2013).

### **OM64**

OM64 has been suggested to substitute Tom70 in plants. Arabidopsis mutants lacking OM64, showed similar phenotypic effects as the *tom20-2/tom20-3/tom20-4* tripple knock-out. A minor defect of the import of some precursors has been reported and the plants do not show any severe growth phenotype. However, generation and analysis of a quadruple knock-out line in Arabidopsis lacking OM64 and all three isoforms of TOM20 showed that these plants are embryo lethal (Duncan et al., 2013). From those results it can be concluded that both in yeasts and plants, either of these two receptors Tom20/Tom70 or TOM20/OM64, respectively, is required to recognize the presequences and deliver the precursor proteins to the GIP.

### **TOM9**

Plants contain a truncated form of yeast Tom22, which in line with its molecular mass, is called TOM9 (Macasev et al., 2000; Macasev et al., 2004). TOM9 has a single pass transmembrane domain which is homologous to that of Tom22 as well as an IMS localized *trans* receptor domain of similar size to Tom22. This *trans* receptor domain of TOM9 is not conserved on a sequence level but is functionally homologous to that of Tom22. This was verified by a chimeric construct composed of the cytosolic and transmembrane domain of Tom22 and the IMS domain from TOM9. This chimeric protein could complement the protein import and growth defects of a yeast strain lacking the endogenous Tom22 protein (Macasev et al., 2000). The cytosolic domain of TOM9 is much shorter compared to Tom22 and in particular has lost the acidic residue rich domain which in yeasts is believed to bind precursors and is hence called *cis* receptor domain (Macasev et al., 2004). This suggests that TOM9 is not likely to act as an electrostatic receptor for mitochondrial presequences. Indeed, when studied *in vitro* by NMR spectroscopy the cytosolic domain of TOM9 failed to bind presequences directly (Rimmer et al., 2011). However, TOM9 has been shown to bind TOM20 and the interaction between TOM9 and TOM20 is affected by the presence of presequences suggesting that TOM9 and presequences compete with each other for the same binding site within TOM20 (Rimmer et al., 2011). In a proposed model, the hydrophobic presequence-binding site of TOM20 is normally occupied by the cytosolic domain of TOM9, which is displaced by the presequences of incoming mitochondrial precursors. Binding of presequences to TOM20 increases the concentration of precursor proteins close to the GIP and thus facilitating their further transfer through the TOM complex (Rimmer et al., 2011). This model does not fully explain the necessity for TOM9 binding to TOM20 but the altered properties of TOM9 might be an adaptive change in plants upon the evolvement of a novel organelle, the plastid. Inability of chloroplast presequences to compete with TOM9 binding to TOM20 would ensure selectivity in mitochondrial protein targeting.

## **1.2 Aim of this study**

The aim of this study was to investigate calcium signalling in plant endosymbiotic organelles with a special focus on calcium/CaM regulation of mitochondrial protein import. The specific goals of the present study were

- to identify novel mitochondrial CaM-binding proteins, to analyse their CaM binding properties and to unravel the impact of CaM binding to these proteins within the context of their specific function
- to provide an in-depth characterisation of the new mitochondrial CaM targets by biochemical studies and by generation and analysis of loss-of-function mutants
- to investigate the basis for chloroplast calcium-dependent phosphorylation by identification of the corresponding kinase

## 2 Materials

### 2.1 Chemicals

All chemicals used were of the highest quality available and obtained from known manufacturers.

**Table 1** - Special chemicals/materials used in this study

Name	Company
Calmodulin agarose	Sigma-Aldrich GmbH, Germany
n-Dodecyl $\beta$ -D-maltoside	
Pig brain calmodulin	Enzo Life Sciences, Germany
Synthetic TOM9.2 peptide	Eurogentec, Germany
1-Ethyl-3-[3-Dimethylaminopropyl]Carbodiimid Hydrochlorid (EDC)	Pierce, Germany
Sulfo-N-Hydroxysulfosuccinimide (Sulfo-NHS)	
Dithiobis(succinimidylpropionate) (Lomant's Reagent)	Thermo Scientific Pierce, Germany
ATTO 520	ATTO-TEC GmbH, Germany
standard treated glass capillaries (K002 Monolith NT.115)	Nano Temper, Germany
Dexamethasone	Sigma-aldrich GmbH, Germany
Oligonucleotides	Eurofins MWG Operon, Germany
Complete protease inhibitor cocktail	Roche, Germany
Phosphatase inhibitor Phospho-Stop (EDTA Free)	
Immobilon PVDF membrane	Milipore, Germany
Ni-NTA agarose	Quiagen, Germany
Strep-Tactin Sepharose	IBA, Germany
Amylose resin	New England Biolabs, Germany
Chitin beads	



## 2.2 Enzymes and kits

**Table 2** - Enzymes and kits used in this study

Name	Company
DNA polymerases	New England Biolabs, Germany
DNA restriction enzymes	Fermentas, Germany
Phusion polymerase	New England Biolabs, Germany
Taq polymerase	Genaxxon, Germany
pENTR/D-TOPO	Invitrogen, Germany
LR Clonase II	Invitrogen, Germany
Nucleobond Plasmid DNA purification	Macherey-Nagel, Germany
Plant RNeasy kit	Qiagen, Germany
RNase H Minus, Point Mutant	Promega
TNT-Coupled Reticulocyte Lysate System	Promega

## 2.3 Molecular weight and size markers

**Table 3** - Molecular weight and size markers used in this study

Name	Company	Purpose
peqGOLD Protein-Marker I	Peqlab, Germany	SDS PAGE protein size marker
PageRuler Prestained Protein Ladder Plus	Fermentas, Germany	SDS PAGE protein size marker
HMW native marker kit	GE Healthcare	BN PAGE marker
GeneRuler 1kb DNA Ladder Plus	Fermentas, Germany	DNA size marker for agarose gels

## 2.4 Plasmid DNA vectors

**Table 4** - List of vectors used in this study

Vector	Feature	Company
pMALc-5x	Protein expression plasmid	New England Biolabs, Germany
pTwin1		
pET21b		Stratagene, USA
pET21d		
pENTR/D-TOPO	Entry vector for Gateway system	Invitrogen, Germany
pOpOff2(Hyg)	Plant transformation vector	Wiepolska et al., 2005
pBIN saGFP 1-10		kind gift from Dr. Simon Lander Stael, University of Vienna
pBIN saGFP 11		

## 2.5 Bacteria strains

**Table 5** – List of bacteria strains used in this study

Organism	Strain	Purpose	Company/Reference
<i>E. coli</i>	DH5 $\alpha$	Amplification of DNA plasmid /cloning	Stratagene, USA
	DB 3.1 (ccdb survival)		
	TOP10		Invitrogen, Germany
	BL21 Codon Plus (DE3)-RIPL	Protein expression	Stratagene, USA
	NEB Express		NEB, Germany
	ER2566		
<i>A. tumefaciens</i>	LBA1334	Plant transformation	Diaz et al., 1989
	GV3101		Van Larebeke et al., 1974

## 2.6 Oligonucleotides

All oligonucleotides used in this study can be found in Appendix I.

## 2.7 List of constructs

**Table.6** – Constructs used in this study

Constructs	AGI code	Plasmid	Purpose	Author
TOM9.2	At5g43970	pOpOFF2(hyg)	generation of stable transgenic line	self made
TOM9.2	At5g43970 FL	pMALc5x	protein expression	self made
TOM9.2	At5g43070	pMALc5x	protein expression	self made
TOM9.2-CD	At5g43970	pMALc5x- StrepII	protein expression	self made
TOM9.2-ΔCD	At5g43970	pMALc5x- StrepII	protein expression	self made
TOM9.2Δ27-47	At5g43070	pMALc5x- StrepII	protein expression	self made
TOM20.3-CD	At3g27080	pMALc5x- StrepII	protein expression	self made
TOM9.1	At1g04070	pMALc5x	protein expression	self made
CaS-C	At5g23060	pTWIN1	protein expression	gift from S. Stael
CaS-C 373 <sub>s/a</sub>	At5g23060	pTWIN1	protein expression	self made
CaS-C 378 <sub>s/a</sub>	At5g23060	pTWIN1	protein expression	self made
CaS-C 380 <sub>t/v</sub>	At5g23060	pTWIN1	protein expression	self made
CaS-C 373 <sub>s/a</sub> +378 <sub>s/a</sub>	At5g23060	pTWIN1	protein expression	self made
CaS-C 373 <sub>s/a</sub> +380 <sub>s/a</sub>	At5g23060	pTWIN1	protein expression	self made
CaS-C-373 <sub>s/a</sub> +378 <sub>s/a</sub> +380 <sub>t/v</sub>	At5g23060	pTWIN1	protein expression	self made
TOM9.2	At5g43970	pET21b	protein expression /in vitro translation	self made
TOM20.3- FL_StrepII	At3g27080	pET21b- StrepII	in vitro translation	self made

TIM8	At5g50810	pGEM7Z	in vitro translation	gift from J. Whelan
TIM23.3	At3g04800	pGEM7Z	in vitro translation	gift from J. Whelan
TOM40	At3g20000	pSP65	in vitro translation	gift from J. Whelan
mtGST	At5g42150	pF3A	in vitro translation	gift from S. Schwenkert
TRX	AT2G41680	pBIN-saGFP1-10C	Protein localization	Gift from M. Fuchs
TRX	AT2G41680	pBIN-saGFP11C	Protein localization	Gift from M. Fuchs
SNRK2.2	At3g50500	pBIN-saGFP11C	Protein localization	self made

## 2.8 Accession numbers

**Table 7** – Accession numbers of proteins used in experimental studies

Gene name	organism	Gene Bank accession/AGI
RISP 2	<i>Arabidopsis thaliana</i>	At5g13440
TOM9.2	<i>Arabidopsis thaliana</i>	At5g43970
TOM9.1	<i>Arabidopsis thaliana</i>	At1g04070
TOM20.3	<i>Arabidopsis thaliana</i>	At3g27080
CaS	<i>Arabidopsis thaliana</i>	At5g23060
SNRK2.2	<i>Arabidopsis thaliana</i>	At3g50500
TAK1	<i>Arabidopsis thaliana</i>	At4g02360

**Table 8** – Accession numbers of proteins used in alignment

<b>name</b>	<b>organism</b>	<b>accession number</b>
HsTom22	<i>Homo sapiens</i>	NP_064628.1
ScTom22	<i>Saccharomyces cerevisiae</i>	NP_014268.1
NcTom22	<i>Neurospora crassa</i>	CAF05975.1
AtTOM9.2	<i>Arabidopsis thaliana</i>	NP_199210.1
AtTOM9.1	<i>Arabidopsis thaliana</i>	NP_563699.1
TcTOM9	<i>Theobroma cacao</i>	XP_007050174.1
PtTOM9	<i>Populus trichocarpa</i>	XP_002301850.1
GmTOM9L1	<i>Glycine max</i>	XP_003542441.1
VvTOM9L1	<i>Vitis vinifera</i>	XP_002272982.1
MdTOM9L1	<i>Malus domestica</i>	XP_008372389.1
OsTOM9	<i>Oryza sativa</i>	EAZ21626.1
ZmTOM9	<i>Zea mays</i>	NP_001241795.1
SmTOM9	<i>Selaginella moellendorffii</i>	EFJ35283.1
PpTOM9	<i>Physcomitrella patens</i>	XP_001755556.1
OtTOM9	<i>Ostreococcus tauri</i>	XP_003078090.1

## 2.9 Radioisotopes

Radioactive elements [ $\gamma$ - $^{32}\text{P}$ ] ATP (3000 Ci/mmol) and EXPRESS [ $^{35}\text{S}$ ]-Methionine/Cysteine mix (1175 Ci/mmol) were obtained from Perkin Elmer LAS (Rodgau, Germany).

## 2.10 Antibodies

$\alpha$ -TOM9.2 polyclonal antibody was generated by Pineda Antibody-Service (Berlin, Germany) in rabbit using purified recombinant TOM9-Hisx6 as antigen. Polyclonal antibodies against TOM20.2, OM64 (outer membrane protein of mitochondria 64) and HSP70 (heat shock protein 70) were kind gifts from Dr. Serena Schwenkert and  $\alpha$ -TOM40 (Translocase of Outer membrane of Mitochondria 40) antibody was generous gift from Dr.

Chris Carrie, LMU Munich. Antisera raised against SHMT (serine hydroxymethyltransferase), AOX (alternative oxidase), COXII (cytochrome c oxidase subunit II), GDCH (glycine decarboxylase complex prototein H), IDH (isocitrate dehydrogenase) antibodies were obtained commercially (Agrisera, Vännäs, Sweden). Antibodies against TIM17, VDAC and Porin were obtained as kind gifts from Prof. James Whelan, La Trobe University, Australia and Prof. Jürgen Soll, LMU Munich.

## 2.11 Plant material and growth conditions

If not otherwise stated all experiments were performed using *Arabidopsis thaliana*, ecotype Columbia. Mutant plants refer to dexamethasone induced *TOM9.2* RNAi knock-down plants generated on *Arabidopsis thaliana*, ecotype Columbia back ground

Mitochondria were either isolated from wild type *Arabidopsis* plants were grown on commercially available soil under an 8 h photoperiod at  $100 \mu\text{mol m}^{-2} \text{s}^{-1}$  white fluorescent light and  $22^\circ\text{C}$  for 4 weeks or from mutant and wild type plants grown for 14 days in liquid media containing  $\frac{1}{2}$  Murashige & Skoog (MS), 1% sucrose and 0.05% MES, pH 5.7 with or without, 20  $\mu\text{M}$  Dexametasone (Dex) (in DMSO) under a 16 h photoperiod at light on an orbital shaker at 80 rpm. Phenotypic analysis, microarray analysis and quantitative real-time PCR were performed using plants grown on  $\frac{1}{2}$  MS agar media containing either 20  $\mu\text{M}$  Dex (in DMSO) or DMSO as solvent control under a 16 h photoperiod at  $100 \mu\text{mol m}^{-2} \text{s}^{-1}$  white fluorescent light and  $22^\circ\text{C}$  for as long as indicated for each experiment. Hypocotyl length measurement was performed using plants grown under light fluence rates of 0, 0.3, 1.0, 30 or 77  $\mu\text{mol m}^{-2} \text{s}^{-1}$  of white fluorescent light at  $22^\circ\text{C}$  with a 16 h photoperiod.

For chloroplast isolation wild type *Arabidopsis* (Col-0) were grown on commercially available soil for six weeks under an 8h long photoperiod at  $100 \mu\text{mol m}^{-2} \text{s}^{-1}$  white fluorescent light and  $22^\circ\text{C}$ .

## 3 Methods

### 3.1 Nucleic acid methods

#### 3.1.1 General nucleic acid methods

Protocols described in Sambrook (1989) were used for standard molecular biological methods, such as amplification of DNA by polymerase chain reaction (PCR), agarose gel electrophoresis, detection of DNA, determination of DNA concentration, growing conditions of bacteria and bacterial transformation. Isolation of RNA was performed using Plant RNeasy kit (Quiagen, Hilden, Germany) as per manufacturer's manual. Restriction digestion and ligation of DNA fragments were performed using enzymes from Life Technologies (Darmstadt, Germany) as stated in the manufacturer's instructions. Plasmids were isolated by alkaline lysis with SDS (Sambrook, 1989). Manufacturer's instructions were also followed to purify PCR products and DNA fragments from agarose gels using DNA purification kits (Macherey-Nagel, Düren, Germany).

#### 3.1.2 Molecular cloning and construction of expression plasmids

Promega M-MLV reverse Transcriptase, RNase H Minus, Point Mutant was used to generate cDNA from Arabidopsis leaves according to the manufacturer's instructions. The coding sequence of full length *TOM9.2* (bp 1-297) was amplified by PCR (all primer sequences are provided in appendix I). Sequences for NdeI and EcoRI restriction sites were included in the forward and reverse primers, respectively to install the specified restriction sites in the PCR product in order to facilitate directional cloning into pMALc5x (NEB, Germany) with an N-terminal MBP tag. Sequence for StrepII tag was inserted at the 3' end of the gene by including the sequence in the reverse primer to get an additional C-terminal StrepII tag to facilitate protein purification. The cytosolic domain of *TOM9.2* (*TOM9.2-CD*) was constructed by amplifying the sequence comprising bps 1-156. A variant lacking the cytosolic domain (*TOM9.2-ΔCD*) was constructed by amplifying bps 157-297 and *TOM9.2-ΔCaMBD* (corresponding to *TOM9.2* lacking CaM binding domain) was constructed by overlap extension amplification of bps 1-78 and bps 142-297. Coding region corresponding to full length *TOM9.1* was cloned with an N-terminal MBP tag into pMALc5x plasmid. In a similar fashion the cDNA sequence of the cytosolic domain of *TOM20*, (*At3g27080*, *TOM20-CD*) (Perry AJ, 2005) was amplified from bp 1-435 and inserted directionally into pMALc5x; a C-

terminal StrepII tag was introduced as described above. Full length TOM9 was also cloned into pET21b which provides a C-terminal 6xHistidine tag using NdeI and NotI restriction sites in the forward and reverse primers respectively.

CaS (calcium sensor) lacking the N-terminal amino acids were cloned into pTWIN1 in frame with the N-terminal intein tag. Point mutations at position S<sub>373</sub>, S<sub>378</sub> and T<sub>380</sub> in the CaS sequence were generated by PCR-based site-directed mutagenesis on the pTWIN1-CaS plasmid. Double and triple point mutations were created by above mentioned method using single point mutated and double point-mutated constructs respectively as templates.

### 3.1.3 Construction of plasmids to generate transgenic plants

The full length coding region of *TOM9.2* (bps 1-297) was first cloned into the Gateway entry vector pENTR-D-TOPO (Invitrogen, Germany) and thereafter was introduced into pOpOff2(Hyg) (Wielopolska et al., 2005) by Gateway recombination (LR ClonaseII, Invitrogen). The resulting vector pOpOff2(Hyg)-*TOM9.2* was used to stably transform *Arabidopsis* by floral dipping (Clough et al., 1998) to generate dexamethasone (Dex) inducible knock-down plants.

## 3.2 Protein methods

### 3.2.1 General protein methods

Proteins were separated by SDS-PAGE according to Laemmli (1970). Polyacrylamide gels were stained by Coomassie Brilliant Blue R250 (Sambrook J, 1989) or by silver staining as described in (Blum et al., 1987). Protein concentration of extracts or purified recombinant proteins was determined by using the Coomassie Bradford protein assay kit (Life Technologies, Darmstadt, Germany) according to manufacture instructions. Chlorophyll concentration was determined as described by Arnon (1949). Chloroform-methanol precipitation of proteins was performed following the protocol described by Wessel and Flügge (1984). Transfer of proteins onto PVDF membranes was performed according to the semi-dry blot method (Khyse-Andersen 1984). Radiolabeled proteins were detected by exposure to phosphorimager screens analysed on a Typhoon Trio (GE Healthcare) or by exposure to X-ray film.



### 3.2.2 Purification of mitochondria

Enriched mitochondria fractions were isolated as described previously (Millar et al., 2007) either from rosette leaves of 4 weeks old soil grown *Arabidopsis* plants or from whole plants grown for 14 days in liquid culture. Plant material was ground thoroughly in grinding buffer [0.3 M Sucrose, 25 mM Tetrasodium pyrophosphate, 2 mM EDTA, 10 mM  $\text{KH}_2\text{PO}_4$ , 1% PVP-40, 1% (w/v) BSA, 20 mM ascorbate, pH 7.5] into a homogenous suspension and filtered through four layers of gauze. The extract was centrifuged at 2,450 g for 5 min at 4°C to remove cell debris and larger organelles. The supernatant was centrifuged at 17,400 g for 20 min at 4°C to pellet down mitochondria and thylakoids. The organelle pellets were resuspended in washing buffer [0.3 M Sucrose, 10 mM TES pH 7.5, 0.1% (w/v) BSA] and centrifuged again at 2,450 g for 5 min at 4°C to remove any remaining chloroplasts. The supernatant was transferred to new tubes and centrifuged at 17,400 g for 20 min at 4°C to pellet down mitochondria, which were then resuspended in washing buffer and loaded onto PVP-40 gradients [zero to 4.4% PVP in 28% Percoll in washing buffer] and centrifuged at 40,000 g for 40 min at 4°C without brake. The thylakoid fraction was discarded. Mitochondria were collected, washed two times in washing buffer and pelleted at 31,000 g for 15 min at 4°C. Aliquots of mitochondria pellet were either used immediately or frozen in liquid  $\text{N}_2$  and stored at -80°C until use.

### 3.2.3 Purification of stromal extracts from *Arabidopsis*

Leaves of 6-7 weeks old *Arabidopsis* plants were used to isolate chloroplasts as described by Seigneurin-Berny et al. (2008). Chloroplasts were disrupted by suspension in lysis buffer [20 mM Tricine/NaOH pH 7.6, 20 mM NaCl, 10% (v/v) glycerol, 1 mM DTT] supplemented with protease inhibitor (Roche, EDTA free). The suspension was incubated on ice for 15 min and then centrifuged at 60,000 g for 10 min to separate the soluble stromal proteins from membranes. The membranes were washed again in the same supernatant and centrifugation was repeated as mentioned before. Afterwards the extract was concentrated using Amicon Ultra centrifugal units (10 kDa cut off, GE Healthcare). All the above mentioned procedures were carried out on ice or at 4°C.

### 3.2.4 Expression and purification of recombinant proteins

All MBP-, Strep- or His-tagged proteins were heterologously expressed in BL21 Codon Plus (DE3)-RIPL *E. coli* cells and purified under native conditions. TOM9 with a C-terminal 6x-Histidine tag was purified using Ni-NTA superflow (Qiagen) and provided to Pineda antibody service, Germany to generate polyclonal antibody in rabbit. Strep-tagged proteins were purified using Strep-tactin agarose (IBA, Germany) as per manufacturer's protocol. MBP-tagged TOM9.1 and MBP (expressed using the pMALc-5x plasmid without insert) were purified using Amylose resin (NEB, Germany) as indicated by the provider.

N-terminally Intein-tagged proteins were expressed in ER2566 *E. coli* cells and purification of tag-less proteins was performed using the IMPACT-pTWIN protein purification system (NEB, Germany) according to the manufacturer's instructions.

### 3.2.5 Affinity chromatography on CaM-agarose

Purified mitochondria pellets corresponding to about 3 mg wet weight were incubated in 200  $\mu$ l resuspension buffer (20 mM Tris-HCl, pH 7.5, 150 mM NaCl, 1% n-Dodecyl  $\beta$ -D-maltoside) for 30 min on ice to extract membrane proteins. Insolubilized components were centrifuged down at 50,000 g for 20 min and discarded. The supernatant, containing soluble proteins as well as extracted membrane proteins was collected, diluted 10-fold in binding buffer (20 mM Tris-HCl, pH 7.5, 150 mM NaCl, 0.1 mM CaCl<sub>2</sub>) and incubated with 100  $\mu$ l pre-washed slurry of CaM-agarose, having a ligand concentration of 10 mg/ml (Sigma-Aldrich, Germany) for 4-h at constant slow rotation. The flow through was collected afterwards and the beads were washed three times with five column volumes of wash buffer (20 mM Tris-HCl, pH 7.5, 500 mM NaCl and 0.1 mM CaCl<sub>2</sub>). Proteins that specifically bound to the ligands were eluted using elution buffer containing either an excess of 20  $\mu$ M of commercially available pig brain calmodulin (Enzo Life Sciences, Germany) in binding buffer or using 5 mM EDTA/EGTA in place of calcium in the binding buffer. All the above mentioned steps were carried out at 4<sup>0</sup>C.

### 3.2.6 Bioinformatical analyses

Predictions of potential CaM-binding regions were performed using the tool provided in the calmodulin target database (<http://calcium.uhnres.utoronto.ca/ctdb/ctdb/home.html>). Helical wheel projections were performed using the online program provided on <http://rzlab.ucr.edu/scripts/wheel/wheel.cgi>. Multiple sequence alignments were made using the program Clustal X 2.0 (Thompson et al., 1997). A comparison of gene expression between both TOM9 paralogs was carried out with the program implemented in Geninvestigator (<https://geneinvestigator.com/gv/plant.jsp>). The ImageJ programme was used to measure hypocotyl length of Arabidopsis seedlings.

### 3.2.7 Chemical cross-linking using EDC or DSP

Interaction of TOM9 with CaM was assayed by chemical cross-linking using the 0 Å cross-linker EDC (1-Ethyl-3-[3-dimethylaminopropyl]carbodiimide hydrochloride) (Arazi et al., 1995). Cross-linking assays were performed in a total volume of 30 µl with approximately 3 µg of purified recombinant protein and 5 µg of pig brain calmodulin in cross-linking buffer (50 mM Hepes-KOH, pH 7.5, 50 mM NaCl and 0.1% n-Dodecyl β-D-maltoside) with either 0.1 mM CaCl<sub>2</sub> or 5 mM EDTA/EGTA. The reaction mix was incubated on ice for 45 min before addition of 2 mM EDC and 5 mM S-NHS (Sulfo-N-hydroxysulfosuccinimide). Reactions were carried out at 21<sup>0</sup>C for 30 min and stopped by adding SDS-PAGE sample buffer. Purified MBP was used as a control instead of TOM9 variants. All samples were resolved on SDS-PAGE followed by visualization by silver staining (Blum et al., 1987). To analyse the interaction between peptide and CaM by cross-linking assays, a synthetic peptide comprising AAs 31-51 of TOM9 was obtained from Eurogentec (Cologne, Germany) and reconstituted in cross-linking buffer. Unless otherwise stated, 900 pmol peptide was used in combination with 300 pmol pig brain CaM per reaction. In control experiments, CaM was replaced by equivalent amounts of BSA (Applichem GmbH, Germany).

Cross-linking assays with 100 µM DSP (100 % in DMSSO) instead of EDC and S-HNS were performed as stated above. In some experiments a three molar excess of CaM was added to the reaction. As control CaM was replaced by BSA. Equal amount of DMSO was added as solvent control for DSP.

### 3.2.8 Co-immunoprecipitation

Co-Immunoprecipitation experiments were carried out using proteins extracts from purified Arabidopsis mitochondria. Mitochondria corresponding to 2 mg wet weight were resuspended in 200  $\mu$ l of Co-IP buffer comprising of 50 mM Hepes pH 7.5, 50 mM NaCl and supplemented with 1% n-Dodecyl  $\beta$ -D-maltoside (Applichem GmbH, Germany) and incubated for 30 min on ice. The soluble extract was collected by centrifugation at 61,000 g for 10 min. The supernatant was diluted 10 fold with Co-IP buffer without n-Dodecyl  $\beta$ -D-maltoside to achieve detergent concentration below 0.1% and divided into two equal parts; 5  $\mu$ l of  $\alpha$ -TOM20.2 antibody and 5  $\mu$ l of pre-immune serum were added to the each part, respectively, and both were incubated for 1 hr at 4°C in a vertical rotor. 25  $\mu$ l of Protein A plus Agarose (Pierce, Germany) beads were pre-equilibrated in Co-IP buffer containing 0.01% chicken egg albumin (Sigma-Aldrich, Germany), added to each of the reactions and incubated further for 2 hrs under the same conditions. Beads were transferred into a column, the flow through was collected and the beads were washed 3 times with 500  $\mu$ l of Co-IP buffer containing 0.1% n-Dodecyl  $\beta$ -D-maltoside. Bound proteins were eluted by heating the beads at 96°C in SDS-PAGE sample buffer.

### 3.2.9 Microscale Thermophoresis (MST)

Purified recombinant TOM20-CD corresponding to 10 nmol was labelled in 500  $\mu$ l reaction volume with the fluorescence dye ATTO-520 NHS-Ester (ATTO-TEC, Germany) according to the manufacturer's instruction. Unreacted dye was removed and the labelled protein brought into MST buffer (50 mM Hepes-KOH pH 7.5, 50 mM NaCl, 0.1mM CaCl<sub>2</sub>, 0.05% Tween-20) using a PD-10 column (GE Healthcare) Unlabelled purified TOM9-CD ranging from 1.83-60,000 nM in MST buffer was used to titrate 100 nM of labelled TOM20-CD. Potential aggregates were removed by centrifuging all protein stocks at 18,000 g for 10 min prior to use. Standard treated glass capillaries (K002 Monolith NT.115) were used to soak the protein mixture. MST was performed in a Monolith NT.115 instrument (Nano Temper, Munich, Germany) as described earlier (Schweiger et al., 2013). Data analysis was performed using the Monolith software. Furthermore, 67 nM of labelled TOM20-CD and 10  $\mu$ M of TOM9-CD were mixed and CaM was used to titrate this protein mixture with a concentration ranging from 2-100,000 nM in presence of either 0.1 mM CaCl<sub>2</sub> or 5 mM EGTA/EDTA. As a control BSA was used instead of CaM.

### 3.2.10 Blue Native PAGE

Mitochondria corresponding to 25 µg wet weight were solubilized by resuspending in 20 mM Tris/HCl pH 7.4, 0.1 mM EDTA, 50 mM NaCl, 10% (w/v) glycerol and 5 g/g tissue (w/w) digitonin followed by incubating on ice for 30 min. Insolubilized components were pelleted down by centrifuging at 100,000 g for 15 min at 4°C. BN sample buffer (100 mM BisTris, pH 7.0, 750 mM ε-aminocaproic acid, 5% (w/v) Coomassie G250) was added to the supernatant and the protein complexes were resolved on a 5-16 % continuous Blue Native acrylamide gel as described previously (Schägger and Jagow, 1991; Jänsch et al., 1998). Proteins were either visualized by Coomassie Blue staining or blotted onto PVDF membrane and immunodetected with α-TOM40, α-TOM20, α-TOM9, α-TIM17 and α-COXII antibodies using the ECL detection system. Complex-I activity staining was performed as described earlier (Sabar et al., 2005).

### 3.2.11 *In vitro* protein import into *Arabidopsis thaliana* mitochondria

Import competent mitochondria were purified from wild type *Arabidopsis* plants grown in liquid culture as described in chapter 3.2.2. <sup>35</sup>S-labelled precursor protein was synthesized using TNT-Coupled Reticulocyte Lysate System (Promega) following manufacturer's instruction. *In vitro* protein import into mitochondria was carried out as described previously (Lister et al., 2007). In short, about 100 µg of purified mitochondria were mixed with 4 µl of radio-labelled precursor in case of TOM40 and 8 µl in the other cases (to equalize protein content in the assay) in a 200 µl reaction with addition of 100 µM CaCl<sub>2</sub> either with or without 10 µM CaM. Import reactions were carried out for 20 minutes at 25°C. After washing of the mitochondria to remove non-imported proteins, half of the mitochondria were re-isolated and analyzed directly. The other half was treated either with 100 mM Na<sub>2</sub>CO<sub>3</sub> at 4°C for 30 minutes followed by isolation of the membrane fraction by centrifugation at 52,000 rpm or with 0.1 µg/µl of the protease thermolysin (Sigma, München, Germany). All samples were subsequently resolved on SDS-PAGE and the results visualized by exposing on phosphorimager screens using the Typhoon Trio (GE Healthcare).

### 3.2.12 Fractionation of Arabidopsis stroma proteins by FPLC

500 µl of stromal extract (see 3.2.3) were loaded onto a pre-equilibrated size exclusion column, HiLoad 16/600 Superdex 200, preparation grade (GE Healthcare) and separated using an Äkta protein purification system (GE Healthcare) using the lysis buffer described in section 3.2.3. Fractions of 1 ml each were collected and aliquots of 5 fractions were pooled together for *in vitro* phosphorylation assay using recombinant CaS protein as substrate by (see 3.2.13). Active fractions in which the phosphorylation of CaS protein was detected, were pooled together from 3-4 successive runs and further separated by anion exchange column chromatography on a Mono-Q 5/50 GL (GE Healthcare) in the above buffer using a linear NaCl-gradient ranging between 5-20% in a 25 ml volume. Fractions of 250 µl were collected and aliquots of three samples were pooled together for phosphorylation assays. Active fractions were analyzed individually on silver-stained SDS-PAGE and specific proteins from these fractions were identified by LC-MS/MS at the Protein analysis Unit, Medical School, LMU Munich.

### 3.2.13 In vitro phosphorylation assays of recombinant proteins

In vitro phosphorylation assays were carried out using recombinant purified CaS protein (see 3.2.4), corresponding to 500-1000 ng and catalytically amounts (50–100 ng) of Arabidopsis stromal extract or isolated fractions from FPLC based purification (see 3.2.12.). All reactions were performed at RT for 20 min in a total volume of 25 µl kinase buffer (equal to lysis buffer as described in section 3.2.3 containing additionally 4 mM MgCl<sub>2</sub>) with 2 µM of ATP and 0.1 µCi/ µl of <sup>32</sup>P-γ-ATP supplemented with either 4 mM CaCl<sub>2</sub> or 5 mM EGTA. Assays were stopped by addition of SDS-sample buffer and proteins were resolved on SDS-PAGE and visualised by Coomassie staining. Radiolabeled proteins were detected by exposing on phosphoimager screen and analysed on a Typhoon Trio (GE Healthcare).

## 3.3 Plant methods

### 3.3.1 Generation of transgenic plants

*Arabidopsis thaliana* Col-0 plants were transformed by pOpOff2(Hyg)-*TOM9.2* using Agrobacteria GV3101 mediated transformation by floral dip method (Clough and Bent, 1998). Positive transformants were selected on ½ MS-agar plates containing 30 µg/ml Hygromycin (Harrison et al., 2006). Offspring from T2 progeny were re-screened on selection

media to identify lines with single insertions. Homozygous lines were identified from selected lines at the T3 generation and further propagated. For induction of RNAi, plants were treated with Dex as indicated for each experiment.

### 3.3.2 Phenotypic analysis of mutant plants

To analyse the early flowering phenotype, seeds were sown on  $\frac{1}{2}$  MS-plates with or without 20  $\mu$ M Dex and allowed to grow vertically. Plants were monitored until bolting started and visible leaves were counted. 4-5 days after the onset of bolting, plants were transferred to soil and photographs were taken after three more days of growth. To compare hypocotyl length in wild type vs. knock-down lines, seedlings were grown for four days horizontally on  $\frac{1}{2}$  MS-plates under different light conditions as indicated either with or without Dex. Photographs were taken after laying the seedlings on separate plates. Hypocotyl length was measured from the photographs for twenty seedlings among the major size groups using ImageJ software.

### 3.3.3 Microarray analysis

Microarray analysis was performed in collaboration with Dr. Katrin Philippar, LMU, Munich. Dex induced and non-induced RNAi plants of two independent lines were grown (see 2.11 for plant growth condition) and rosette leaves of appr. 18 days old plants were harvested when the induced RNAi plants started bolting. Harvesting of plant material was performed at the end of photoperiod since floral regulatory genes show highest expression during this particular time of the day (Paula Suarez-Lopez and Hitoshi Onouchi, 2001; Valverde et al., 2004; Wahl et al., 2013). Total RNA was isolated using Plant RNeasy kit (Qiagen) as per the manufacturer's protocol. A pool of 15 plants was used for each RNA sample to minimize biological variation. Three independently grown and harvested samples were used in each case (n=3).

200 ng of RNA from each sample was processed and hybridized to Affymetrix GeneChip *Arabidopsis* ATH1 Genome Arrays using the Affymetrix 3'-IVT Express and Hybridisation Wash and Stain kits (Affymetrix, High Wycombe, UK) as per manufacturer's instructions. Raw signal intensity values (CEL files) were computed from the scanned array images using the Affymetrix GeneChip Command Console 3.0. Robin software was used for quality check and normalization and to process the raw intensity values (Lohse et al., 2010), using default

settings as described previously (Duy et al., 2011). Background correction across all arrays (between-array method) was accomplished by the robust multiarray average normalization method (Irizarry et al., 2003). Differential gene expression of +Dex (n = 5) vs -Dex (n = 6) samples was statistically analyzed using the linear model-based approach developed by Smyth et al (2004). The resulting *P* values were corrected following nestedF procedure for multiple testing, applying a significance threshold of 0.05 in combination with the Benjamini and Hochberg false-discovery rate control (Benjamini and Hochberg, 1995).

### 3.3.4 Quantitative real-time PCR

Quantitative real-time PCR (qPCR) was performed in collaboration with the group of Dr. Gabriel Schaaf, University of Tuebingen. To perform qPCR, cDNA was prepared from 1 µg of the same RNA used for microarray analysis following manufacturer's instruction (Roboklon, AMV Reverse Transcriptase Native). qPCR was carried out using the SYBR Green reaction mix (Bioline, Sensimix SYBR No-ROX kit) in a Bio-Rad CFX384 real time system. The reference gene was PP2AA3 (At2g26820). Data were analysed using the Bio-Rad CFX Manager 2.0 (admin) system.

### 3.3.5 Self-assembly GFP assay

Green fluorescent protein (GFP) has 11 β-sheets in total and when all the β-sheets are together, only the GFP fluorescence is observed. This protein can be splitted into two parts, one containing the first 10 β-sheets (saGFP1-10) while the second part having the 11<sup>th</sup> β-sheet (saGFP11). If they are expressed in the same cellular compartment, they can assemble together and give fluorescence. Modified pBIN19 binary vector was used to transiently transform Tobacco (Bevan 1984). Here, gene of interest was cloned under 35S promoter with a C-terminal saGFP11, whereas chloroplast stroma localized nadph-dependent thioredoxin reductase c (TRX) was cloned with a C-terminal saGFP1-10. *Agrobacterium tumefaciens* LBA1334 was transformed with pBIN19-35S::saGFP1-10C or pBIN19-35S::saGFP11C constructs via electroporation. Transformed agrobacteria were grown overnight in LB medium supplemented with 50 mg/ml kanamycin in 5 ml culture volume. Cells were harvested by centrifugation and resuspended in Agromix containing 10 mM MES pH 6.0, 10 mM MgCl<sub>2</sub> and 200 µM Acetosyringone so that the final OD<sub>600</sub> was 1.0. After 2 h incubation



at 30°C the cell suspensions were mixed accordingly and was used to co-infiltrate leaves of 3-4 weeks old tobacco plants (*Nicotiana benthamiana*). Infiltrated leaves with transiently co-expressed proteins of interest were harvested after 48 h and used for protoplast isolation as described previously by Koop et al. (1996). Subcellular localization of the proteins was analysed by confocal laser scanning microscopy using a TCS-SP5 (Leica Microsystems, Germany) and the Leica LAS AF software.

### **3.4 Bacteria methods**

#### **3.4.1 Preparation of chemical-competent *E. coli***

Chemically-competent *E. coli* were generated as described previously by Inoue et al. (1990) with slight modifications. A pre-culture was prepared by inoculating 3-5 independent *E. coli* colonies into 100ml LB media containing 20 mM MgSO<sub>4</sub> and incubating at RT with shaking overnight. The OD of the pre-culture was measured and an amount was added to 600 ml fresh LB media containing 20 mM MgSO<sub>4</sub> so that the OD<sub>600</sub> was 0.2. The culture was incubated further under shaking at RT until an OD<sub>600</sub> of 0.5 was reached. Cells were centrifuged down at 700 g for 10 min at 4°C and resuspended in 50 ml ice cold TB buffer (10 mM CaCl<sub>2</sub>, 10 mM PIPES/NaOH pH 6.7, 15 mM KCl, 55 mM MnCl<sub>2</sub>). The cells were pelleted again by centrifugation at 400 g for 10 min at 4°C and resuspended in ice cold TB buffer containing 7% DMSO. The suspension was incubated on ice for additional 30 min, divided into aliquots and frozen rapidly using liquid nitrogen.

#### **3.4.2 Preparation of electro-competent Agrobacteria**

50 ml overnight cultures of Agrobacteria were prepared and inoculated into 600 ml LB followed by incubating at 30°C under vigorous shaking for 1.5 days until an OD<sub>600</sub> of 1.5-2 was obtained. The cells were cooled down on ice for 10 min before the suspension was centrifuged for 15 min at 6,000 g at 4°C to pellet down the cells. After discarding the supernatant, the pellet was resuspended in 50 ml of 1 mM HEPES/NaOH pH 7.0. Cells were again collected by centrifugation at 4,000 g and 4°C for 15 min and resuspended in 1 mM HEPES/NaOH pH 7.0. This washing step was repeated twice. The cell pellet was finally resuspended in 4-6 ml 10 % glycerol. Aliquots were prepared and frozen in liquid nitrogen followed by storing at -80°C.

## 4 Results

Though it is well known that mitochondria are able to sequester cellular calcium (cf. Slater and Cleland, 1953), till date very little is known about the pathways controlled by calcium signaling within mitochondria. In recent studies calmodulin (CaM) regulation of mitochondrial protein import has been demonstrated (Kuhn et al. 2009) and a CaM-like protein (CML) has been shown to be localized in mitochondria (Chigri et al., 2012). Taken together, these results evidence that mitochondria are indeed part of the cellular calcium signalling network, however, the basis of calcium/CaM regulation of mitochondrial processes is little understood.

### 4.1 Isolation of CaM-binding proteins from plant mitochondria

To identify potential novel CaM-regulated proteins, mitochondria isolated and purified from *Arabidopsis* leaves were solubilised using non-ionic detergent and the whole protein extract was used for affinity chromatography on CaM-agarose in the presence of calcium. Upon removal of unbound proteins by washing the CaM-agarose beads extensively with wash buffer, protein specifically bound to the CaM-ligand were eluted competitively with elution buffer containing an excess of free pig brain CaM. Calcium concentration was kept constant throughout the experiment. Analysis of the fractions by SDS-PAGE followed by silver-staining revealed a number of proteins in the eluate fraction, two of which were successfully identified by LC-MS/MS. One of them appeared at around 30 kDa, whereas another one was found in the size range of about 10 kDa size (Fig. 2). These proteins do not appear in the elution, when calcium is replaced with EDTA/EGTA calcium (data not shown) from the binding, wash and elution buffers. Though there were several protein bands observed in the elution, only the two most promising bands were sequenced and identified. The binding of these proteins to the CaM-agarose beads in the presence of calcium and the fact that they could be eluted with an excess of CaM in presence of calcium indicates that the interaction between CaM and these candidates is specific and calcium-dependent and that they present bonafide CaM targets.

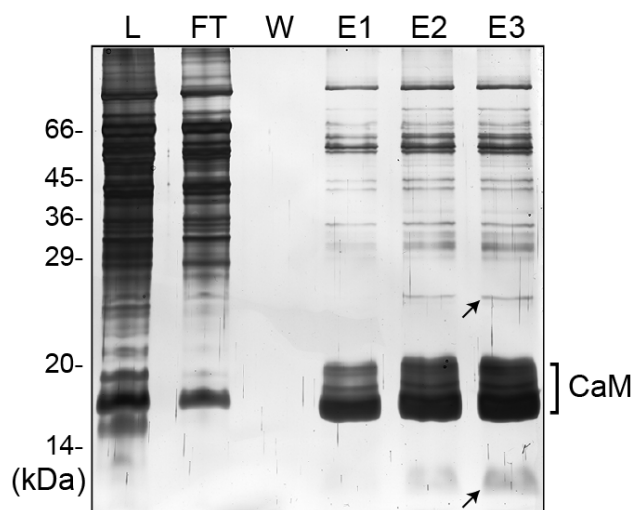


**Fig. 2 CaM-agarose affinity chromatography of Arabidopsis mitochondrial proteins**

Mitochondrial proteins were extracted using non-ionic detergent and loaded (L) onto CaM-agarose beads in presence of calcium. After collecting the flow through (FT), the slurry was washed (W) several times to remove non-specifically bound proteins. CaM-interacting proteins were eluted (E) using an excess of free pig brain CaM. Calcium concentrations were kept constant through all steps. Bands marked with arrows indicate proteins that were identified through LC-MS/MS.

#### 4.1.1 Identification of CaM binding proteins by mass spectrometry

LC-MS/MS analysis of both proteins isolated by CaM- agarose chromatography (see above) was performed at the Center for Protein Analytics, LMU-Munich. The 30 kDa protein band was identified as the Ubiquinol-cytochrome C reductase iron-sulfur subunit, also called RISP, which is the core component of complex III of the mitochondrial electron transport chain. Fifteen peptides were identified which could be matched to At5g13430 and/or At5g13440 (RISP1 and RISP2 respectively) since Arabidopsis contains two isoforms that are highly similar (Fig. 3A). Four peptides were identified from the 10 kDa protein that can be matched exclusively to TOM9.2 (At5g43970), which is a well-known component of the translocon at the outer membrane of mitochondria (TOM complex) of Arabidopsis (Macasev et al., 2000; Werhahn et al., 2003)(Fig. 3B). The protein is an ortholog of yeast Tom22, however, in plants it lacks most of the cytosolic domain and therefore is much smaller in size (Macasev et al., 2000).

**A At5g13440 sequence coverage**

```

1 MLRVAGRRLF SVSQRSTAT SFVLSRDHTL SDGGNSSAS RSVPSADLSS
51 FNSYHRSVIR GFASQVITQG NEIGFGSEVP ATVEAVKTPN SKIVYDDHNNH
101 ERYPPGDPSK RAFAYFVLSG GRFVYASVLR LLVLKLIVSM SASKDVLALA
151 SLEVDLGSIE PGTTVTVKWR GKPVFIRRRRT EDDIKLANSV DVGSLRDPQE
201 DSVRVKNPEW LIVVGVCTHL GCIPLNAGD YGGWFCPCHG SHYDISGRIR
251 KGPAPYNLEV PTYSFLEENK LLIG

```

**B At5g43970 sequence coverage**

```

1 MAAKRIGAGK SGGDPNILA RISNSEIVSQ GRRAGDAVE VSKKLLRSTG
51 KAAWIAGTTF LILVVPLIIE MDREAQINEI ELQQASLLGA PPSPMQRGL

```

**Fig. 3 Identification of CaM binding proteins**

Specifically binding proteins from the CaM eluate were analysed by LC-MS/MS method.

**A.** The 30 kDa protein was identified as the Rieske Iron Sulphur Protein-1 or 2. The amino acid sequence of the isoform 2 is shown and residues that were identified are labelled in red.

**B.** The 10 kDa protein was identified as TOM9.2 and region identified by LC-MS/MS are labelled in red. Details of the LC-MS/MS analysis can be found in appendix III.

Subsequently, TOM9.2, RISP1 and RISP2 were cloned and recombinantly expressed in *E.coli*. For the two RISPs several trials using different vectors and expression lines were made to purify the recombinant protein. However, none of them were successful and further analysis was therefore abolished and all further studies were made exclusively on TOM9.2.

**4.2 Confirmation of TOM9.2 binding to CaM**

In order to confirm that TOM9.2 is indeed a CaM binding protein, pull down assay on CaM-agarose were performed with purified mitochondria as described above (see section 4.1), however, bound proteins were eluted by replacing calcium with EGTA/EDTA and the results were analysed by western blot analysis. To that end, all samples were resolved in SDS-PAGE, the proteins were blotted onto PVDF membranes and immunodecorated with either  $\alpha$ -TOM9.2 or  $\alpha$ -SHMT (serine hydroxymethyltransferase) as a control. Both proteins could be detected in the load and the flow-through but upon elution with EGTA/EDTA only TOM9.2

could be detected highly enriched in the eluate while no reaction with the SHMT antibody was visible (Fig. 4). These results strongly support the identification of TOM9.2 as a protein that interacts with CaM specifically and in a calcium-dependent manner.

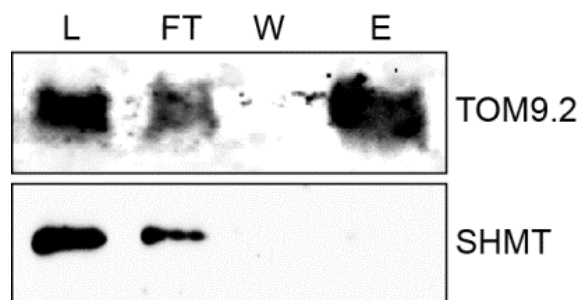


**Fig. 4 Pull-down of endogenous TOM9.2 by CaM**

Mitochondrial protein extract was prepared using non-ionic detergent and loaded onto CaM-agarose beads (L) in presence of calcium. Flow through (FT) was collected afterwards and the slurry was washed (W) several times to remove non-specifically bound proteins. CaM-binding proteins were eluted (E) by chelating out calcium from the buffer using EGTA/EDTA. Samples were analysed on SDS-PAGE followed by immunodetection with TOM9.2 and SHMT antibodies.

As further confirmation, a pull-down assay on CaM-agarose using recombinant MBP-tagged TOM9.2 was performed (Fig. 5). Despite the presence of a single membrane helix in the full-length TOM9.2 (see Fig. 10), the MBP-tagged protein could be expressed in a soluble form and was partially purified by chromatography on amylose resin before it was applied to the CaM-agarose in the presence and absence of calcium (Fig. 5). Even though several other proteins were still present in the partial purified protein fraction (Fig. 5, L), only TOM9.2 was found in the eluate fraction in the presence of calcium (Fig. 5; upper panel). TOM9.2 did not bind to CaM-agarose in the absence of calcium (Fig. 5, middle panel) nor could MBP alone indicating that the MBP-tag does not promote CaM binding (Fig. 5; lower panel). These data further confirm the specific calcium-dependent binding of TOM9.2 to CaM.

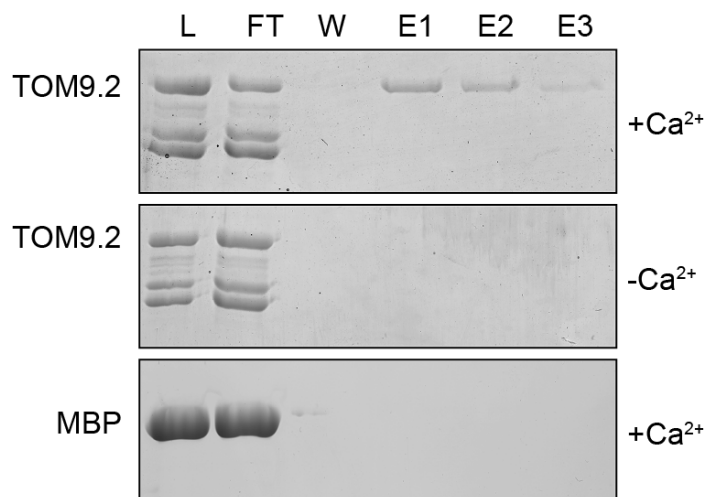


**Fig. 5 Pull-down assay on CaM-agarose using recombinant proteins**

Partially purified recombinant MBP-tagged TOM9.2 or MBP alone were loaded (L) onto CaM agarose beads. After collecting the flow through (FT), beads were washed thoroughly (W) and proteins bound specifically to the beads were eluted using excess of CaM. The assay was done either in presence (upper panel) or in absence (middle panel) of calcium. As a negative control, MBP alone was only used in the presence of calcium (bottom panel).

### 4.3 TOM9.2 binds to CaM at its cytosolic domain

To identify which domain is particularly responsible for CaM binding, cross-linking experiments were performed using the 0 Å cross-linker EDC/NHS, which had been successfully employed previously for interaction studies on CaM and its targets (Arazi et al., 1995). In contrast to CaM-agarose chromatography, this method allows an easy and comparable analysis of different proteins and protein variants under various conditions in a single experiment. All TOM9.2 variants used in this experiment contained both an N-terminal MBP and a C-terminal Strep-tag and were purified by Strep-Tactin agarose. All protein variants were soluble even those containing the membrane-spanning domain. Initial cross-linking assays were carried out with the full-length TOM9.2 proteins and with commercially available pig brain CaM in either the presence or absence of calcium (Fig. 6A, upper most panel) and all reactions were analysed by SDS-PAGE and silver staining.

No cross-link product between TOM9.2 and CaM was visible without cross-linker (Fig. 6A; lanes 1, 3, 5 and 7), nor could any cross-link product be detected when calcium was absent from the reaction mixture (Fig. 6A; lanes 5 - 8). However, a novel protein band appeared at the expected size of a TOM9.2/CaM cross-link product exclusively in the presence of CaM,

calcium and EDC/NHS together with TOM9.2 (Fig. 6A, upper panel, lane 4). The same experiment was repeated with MBP alone instead of TOM9.2 showing no cross-link product in any case (Fig. 6A, lower most panel). This result shows that calcium-dependent interaction of TOM9.2 with CaM can also be observed by cross-linking.

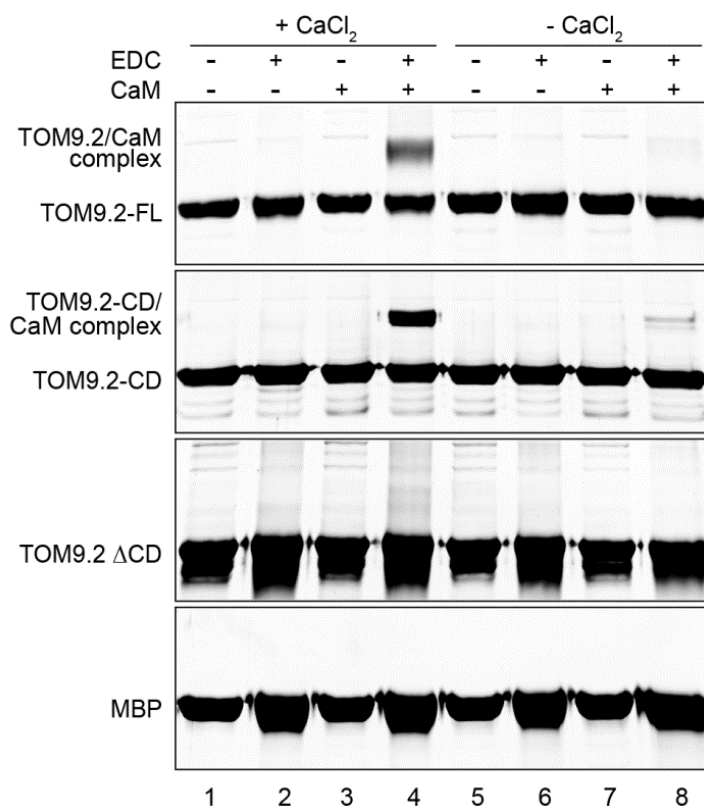


**Fig. 6 Cross-linking assays with CaM**

Cross-linking assays were performed between CaM and TOM9.2-FL (full-length TOM9.2), TOM9.2-CD (TOM9 cytosolic domain), TOM9.2-ΔCD (TOM9 without the cytosolic domain) and MBP either with or without calcium using the 0-Å cross-linker EDC/NHS. MBP was included as an additional negative control.

TOM9.2 is a small basic protein containing a single membrane spanning helix (TM-domain) comprising about 17 amino acids (AAs), through which it is anchored in the outer mitochondrial membrane (Macasev et al., 2004). The N-terminal cytosolic domain is about 52 AAs long, whereas the C-terminal intermembrane space domain (trans-receptor domain) is only about 30 AAs long (Macasev et al., 2004). To reveal which of these domains is responsible for CaM-binding, additional cross-linking experiments were performed with TOM9.2 variants including only the cytosolic domain from AA 1-52 (TOM9.2-CD) or excluding the cytosolic domain and thus ranging from AA 53-99 (TOM9.2-ΔCD). As with the

full length protein, a clear cross-link product of the correct size could be observed in case of TOM9.2-CD in the presence of EDC/NHS, CaM and calcium (Fig. 6, second panel, lane 4), while no cross-link product appeared when the experiment was done with TOM9.2-ΔCD (Fig. 6A, third panel lane 4), suggesting that the CaM-binding domain (CaMBD) of TOM9.2 is situated on its cytosolic domain.

#### 4.3.1 In silico identification of a potential CaMBD of TOM9.2

The TOM9.2 sequence was analysed in silico using the web-based program that is part of the CaM Target database ([http://calcium.uhnres.utoronto.ca/ctdb/pub\\_pages/search/index.htm](http://calcium.uhnres.utoronto.ca/ctdb/pub_pages/search/index.htm)). It showed a high propensity for CaM binding between AAs 27 and 51 of the TOM9.2 sequence (Fig. 7A). Normalized scores (0-9) are shown beneath the respective residues where 9 represents the highest probable score. The criteria used for these numbering are as indicated in the program.

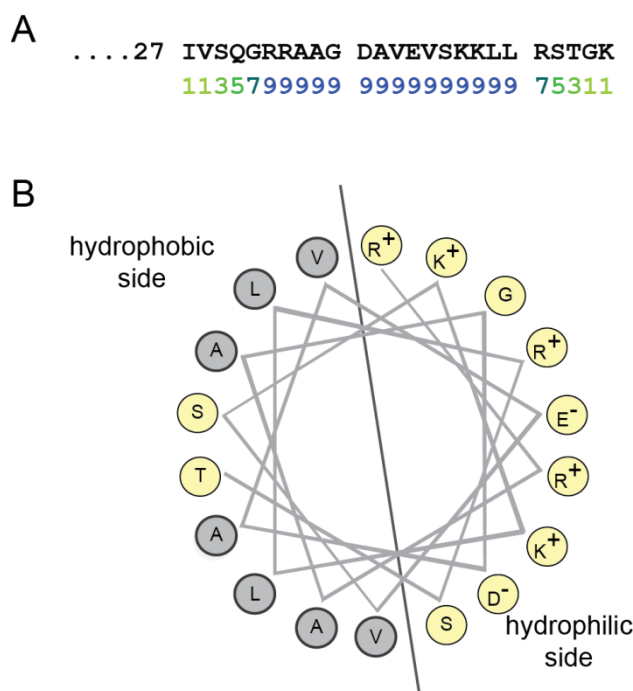


**Fig. 7 Prediction and analysis of the TOM9.2 CaMBD**

**A.** A CaMBD search analysis using the tool provided on the CaM target database (<http://calcium.uhnres.utoronto.ca/ctdb/ctdb/sequence.html>) predicted a potential binding site between AAs 27 and 51 of TOM9.2.

**B.** A helical wheel projection (<http://rzlab.ucr.edu/scripts/wheel/wheel.cgi>) showed the formation of amphiphilic helix between AA 32-49 of the TOM9.2 sequence. Hydrophobic residues are indicated in grey. Positively charged AAs are indicated by “+”, whereas negatively charged AAs are indicated by “-”.



A helical wheel analysis was performed (<http://rzlab.ucr.edu/scripts/wheel/wheel.cgi>) using the sequence of this region (Fig. 7B). This analysis showed that a basic amphiphilic helix with a net charge of +3 can be formed in the region between Arg-32 and Thr-49 of TOM9.2 (Fig. 7B), which is a typical feature involved in CaM binding (O'Neil and DeGrado, 1990).

### 4.3.2 Experimental confirmation of the CaMBD

To confirm if the predicted region between Arg-32 and Thr-49 of TOM9.2 is indeed a functional CaMBD, a protein variant lacking this region (TOM9.2- $\Delta$ CaMBD) was used in comparative cross-linking assay with the previously analysed variants (Fig. 8A).

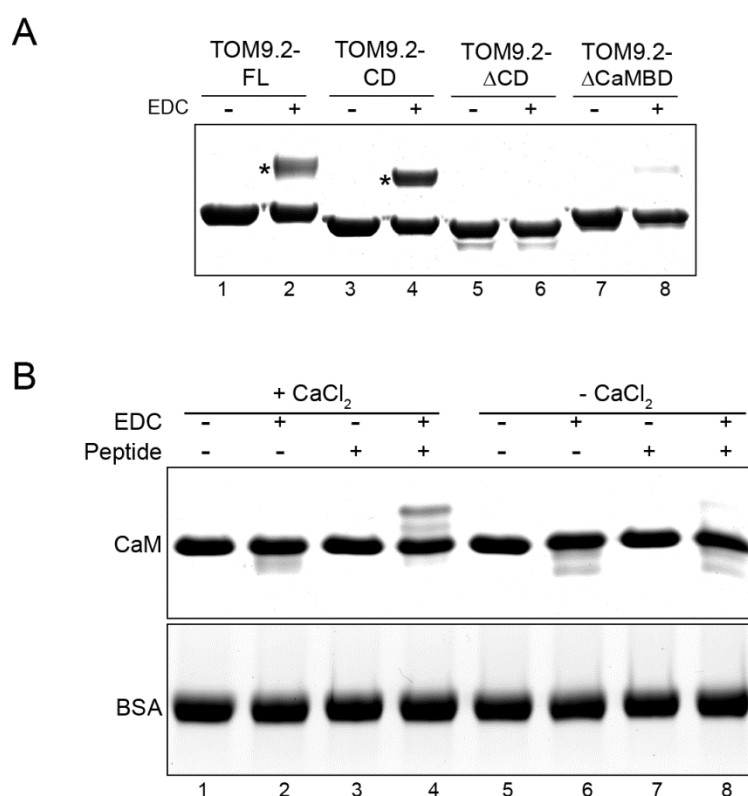


**Fig. 8 The predicted CaMBD of TOM9.2 mediates interaction with CaM**

**A.** Cross-linking assays between CaM and different recombinant TOM9.2 variants in the presence of calcium. TOM9.2-FL (full-length TOM9.2), TOM9.2-CD (TOM9 cytosolic domain), TOM9.2- $\Delta$ CD (TOM9 without the cytosolic domain) and TOM9.2- $\Delta$ CaMBD (TOM9.2 without the potential CaMBD) using the cross-linker EDC/NHS. All reactions were performed in the presence of calcium and were analysed by SDS-PAGE and Coomassie staining.

**B.** SDS-PAGE analysis of cross-linking assays with CaM and a peptide comprising the potential CaMBD of TOM9.2 (G31-K51) either in presence or in absence of calcium (upper panel). Cross-link product between peptide and CaM is indicated with Asterisk. In a control reaction CaM was replaced by BSA (lower panel). Proteins were visualized by Coomassie staining.

In contrast to full length protein (TOM9.2-FL) and the cytosolic domain alone (TOM9.2-CD), a nearly complete loss of cross-link product is observed for TOM9.2 $\Delta$ CaMBD (Fig. 8A). To corroborate this result, a peptide comprising the amino acids 31-51 of TOM9.2 was synthesized and used in cross-linking assays (Fig. 8B). The peptide can clearly interact with CaM when calcium is provided in the reaction (Fig. 8B, upper panel, lane 4) but not in the absence of calcium (Fig. 8B, upper panel, lane 8). No cross-link product was detected when the peptide was allowed to react with BSA instead of CaM (Fig. 8B, lower panel).

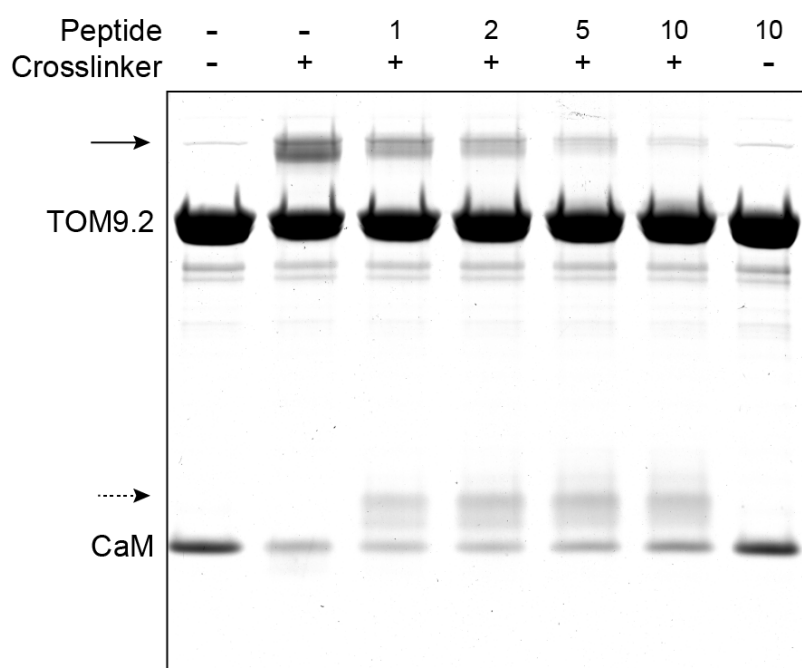


**Fig. 9 CaMBD-peptide competes with TOM9.2 for binding to CaM**

SDS-PAGE analysis of cross-linking assays between full-length TOM9.2 and CaM in the presence of increasing amounts of CaMBD-peptide. The molar ratio of peptide: TOM9.2 in the assay is indicated. Proteins were visualized by Coomassie staining. The cross-link product between TOM9.2-FL and CaM is indicated by solid arrow, whereas the dotted arrow represents the cross-link product between peptide and CaM.

To also elucidate if this peptide can compete with full length TOM9.2 for binding to CaM, cross-linking reactions were performed in which increasing molar ratios of peptide relative to TOM9.2 was added to the reactions. In these assays a clear correlation between a reduction in the TOM9.2/CaM cross-linking product and a respective increase in the peptide/CaM cross-linking product was observed (Fig. 9). Taken together these results strongly suggest that

---

TOM9.2 is a CaM interacting partner with its CaMBD located on its cytosolic domain just before the start of the TM-domain.

#### **4.4 The TOM9 CaMBD is conserved among dicots**

Tom22 is essential in yeasts and the protein is conserved between yeast and mammal. It might thus have been expected that the protein is also conserved in plants. However, all the plant orthologs of Tom22 are much smaller, showing similarity only in the transmembrane and intermembrane space domain but lacking the acidic rich cytosolic-receptor domain (Werhan et al., 2003). It has been proposed that Tom22 acts as presequence receptor via this *cis*-receptor domain and consequently the actual role of the plant orthologs, where this receptor domain is missing, is not really understood. An alignment of several plant TOM9 proteins with Tom22 from yeasts and mammals (Fig. 10) confirmed that the transmembrane region is reasonably conserved, while the cytosolic domain is not only smaller but even in the residual part displays much greater diversity. The predicted CaMBD of TOM9 is not found in Tom22 and is furthermore truncated in the monocots (Fig. 10). By contrast, this domain is reasonably conserved in all dicot sequences and in all cases contains at least two previously described CaM binding motifs (Rhoads and Friedberg, 1997). Taken together, these results suggest that only TOM9 from dicotyledonous plants are CaM-binding proteins.

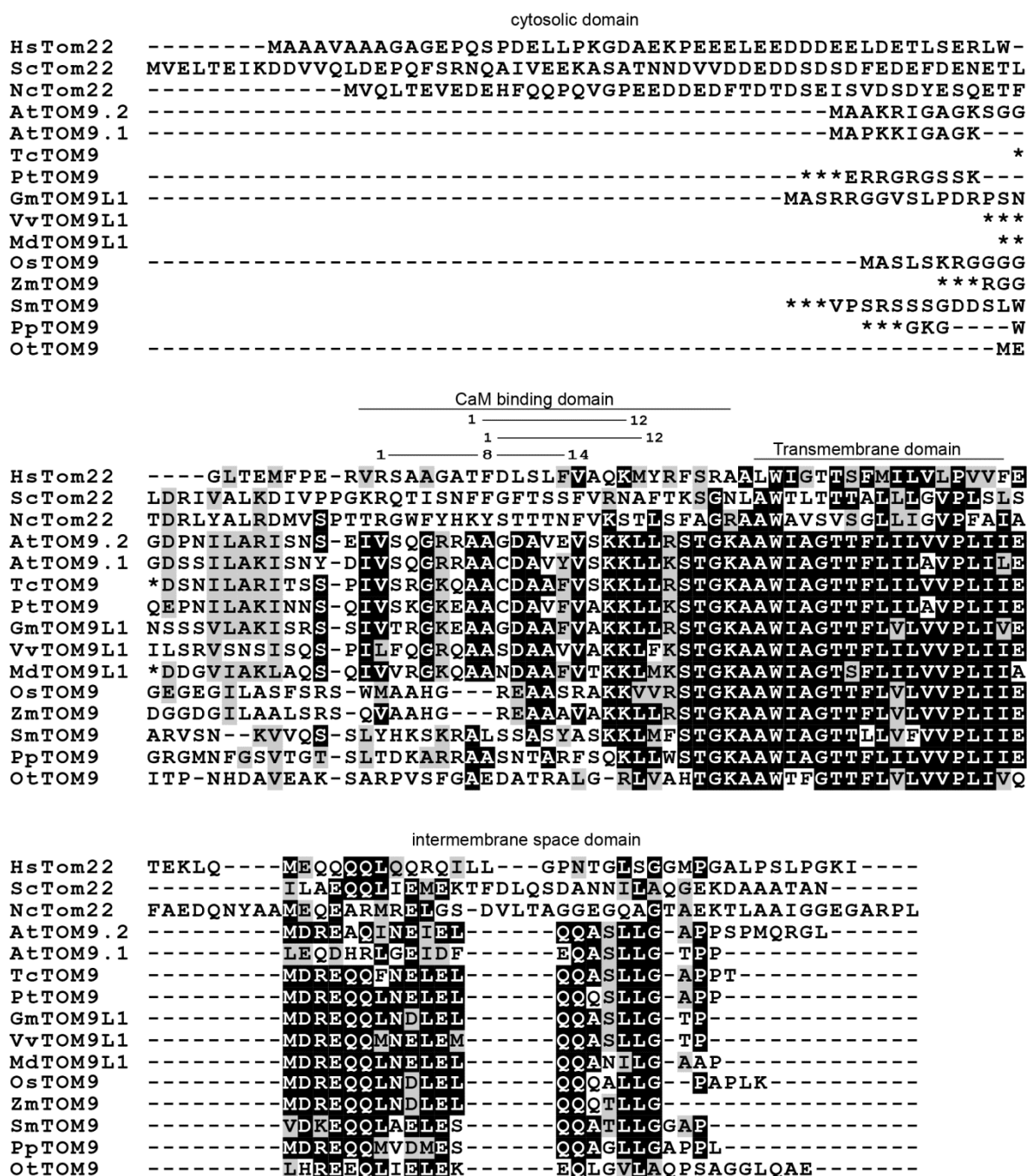


**Fig. 10** The TOM9 CaMBD is conserved among dicots

Multiple sequence alignment of TOM9/Tom22 proteins from different non-plants as well as higher and lower plants was performed using Clustal X.2. Identical and conserved residues are marked with black and grey boxes, respectively. The position of the CaMBD of TOM9.2 from Arabidopsis (AtTOM9.2) along with the predicted CaM binding motifs is indicated. ‘‘L’’ stands for -like protein as indicated in the NCBI database (<http://www.ncbi.nlm.nih.gov/>). Hs- *Homo sapiens*; Sc- *Saccharomyces cerevisiae*; Nc- *Neurospora crassa*; At- *Arabidopsis thaliana*; Tc- *Theobroma cacao*; Pt- *Populus trichocarpa*; Gm- *Glycine max*; Vv- *Vitis vinifera*; Md- *Malus domestica*; Os- *Oryza sativa*; Zm- *Zea mays*; Sm- *Selaginella moellendorffii*; Pp- *Physcomitrella patens*; Ot- *Ostreococcus tauri*.

#### 4.4.1 AtTOM9.1 can also interact with CaM

In the model plant *Arabidopsis*, there is a second isoform of TOM9, which is named TOM9.1 (Fig. 10). Both isoforms show high sequence similarity to each other especially in the N-terminal cytosolic part as well as the trans-membrane domain (Fig. 10). The sequence alignment also indicates that the predicted CaM-binding motifs are conserved in this isoform and the CaM-binding property of TOM9.1 was thus tested *in vitro*. Crosslinking assays with EDC/SHC showed that recombinant MBP-tagged TOM9.1 could interact with pig brain CaM in a calcium-dependent manner (Fig. 11, upper panel, lane 4). As shown before, no cross-linking product could be detected when TOM9.1 was replaced with MBP. This result confirms that TOM9.1 can interact with CaM in the same fashion as TOM9.2.

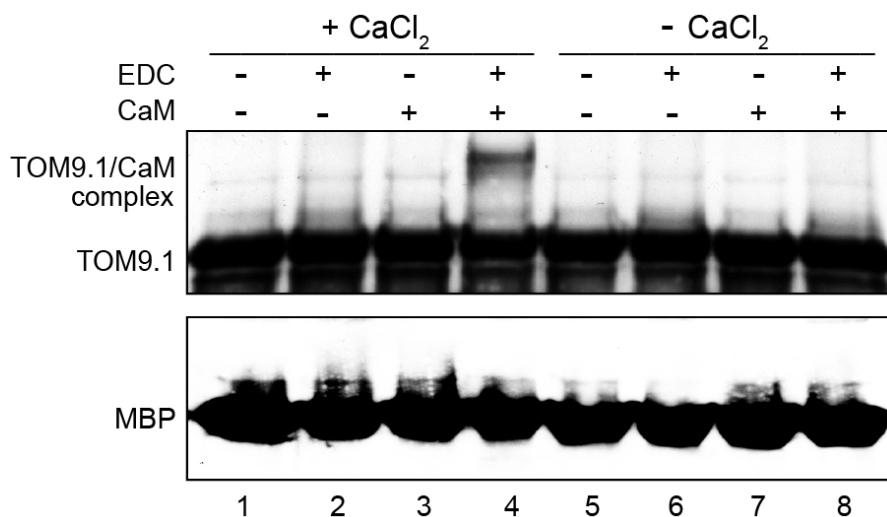


**Fig. 11 TOM9.1 interacts with CaM *in vitro***

Cross-linking experiment was performed between recombinant MBP-tagged TOM9.1 and pig brain CaM using 0 A° cross-linker, EDC/SHC either in presence (+CaCl<sub>2</sub>) or in absence (-CaCl<sub>2</sub>) of calcium (upper panel). Reactions were analysed on SDS-PAGE followed by western blotting and immunodetection using an MBP antibody. Recombinant MBP was used as negative control (lower panel).

#### 4.5 CaM-binding to TOM9.2 affects its interaction with TOM20

It was shown previously by NMR spectroscopy that TOM9.1 can interact with another component of the TOM complex, TOM20, on the cytosolic surface of mitochondria (Rimmer et al., 2011). Present findings suggest that TOM9.2 interaction with CaM also takes place on the cytosolic surface. Moreover, the binding sites for CaM and TOM20 within the cytosolic domain of TOM9.2 overlap with each other, hence suggesting a probable competition between TOM20 and CaM for interaction with TOM9. To elucidate this possibility, cross-link experiment were performed between TOM9.2-CD and the cytosolic domain of TOM20 (TOM20-CD) (Perry et al., 2005) using the 12Å cross-linker DSP, which was previously employed successfully to show interaction between yeast Tom22 and yeast Tom20 (Mayer et al., 1995). A clear cross-link product of the expected size could be observed illustrating the suitability of this set-up to analyse TOM9/TOM20 interaction (Fig. 12A). More importantly, cross-linking of TOM9.2 and TOM20 was inhibited in presence of a 3 molar excess of CaM, while no inhibition was observed in presence of an equivalent amount of BSA (Fig. 12B). This result provides initial indication that CaM might interfere in the interaction between TOM20 and TOM9.

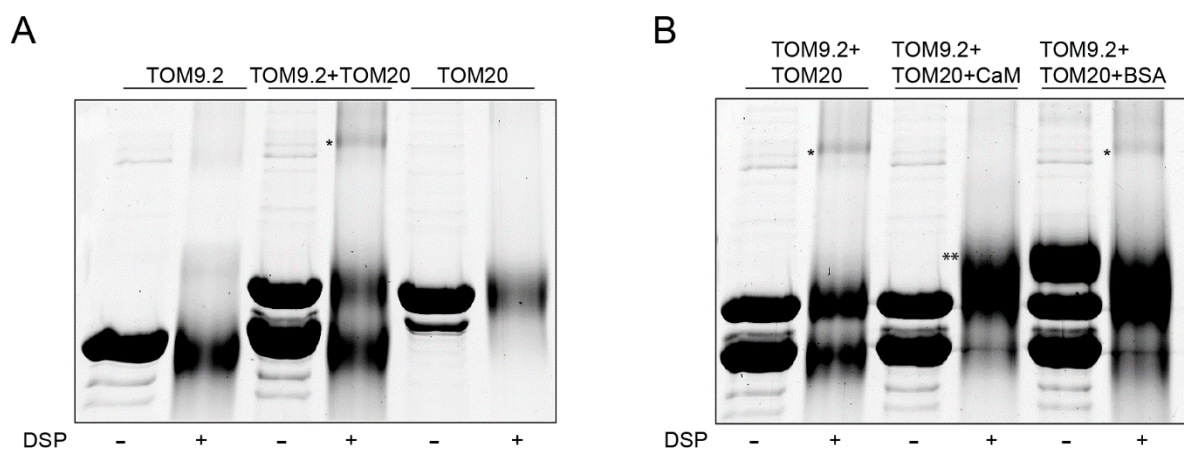


**Fig. 12 Influence of CaM on the interaction between TOM9 and TOM20**

**A.** Cross-linking assays were performed with recombinant TOM9.2-CD and and TOM20-CD using DSP as cross-linker in presence of calcium. Asterisk denotes the TOM9/TOM20 cross-link product.

**B.** Cross-linking assays were performed with recombinant TOM9.2-CD and TOM20-CD in the presence of a 3 molar excess of either CaM or BSA. The TOM9.2-CD/TOM20-CD cross-link product is indicated by (\*). A putative cross-link product between TOM-CD and CaM is denoted by (\*\*).

To further substantiate this finding and better quantify the the interaction between the two TOM subunits, Micro Scale Thermophoresis (MST) was performed. In this method one fluorescently labelled molecule is allowed to interact with an unlabelled molecule and upon interaction the hydration shells of the interacting partners change, hence showing a change in their mobility under micro-temperature gradient. This change in thermophoretic movement can be measured for the labelled molecule and from these data the kinetic parameters of the interaction can be derived.

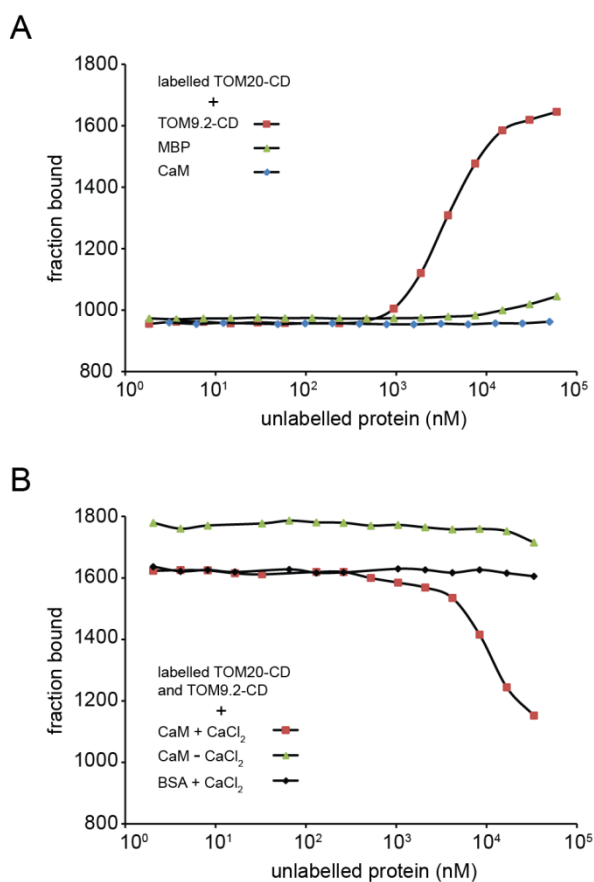


**Fig. 13 MST analysis of the interaction between TOM9.2, TOM20 and CaM**

**A.** Fluorescently labelled cytosolic domain of TOM20 (TOM20-CD) corresponding to 100 nM was titrated with unlabelled TOM9.2-CD (red squares), CaM (blue diamonds) or MBP (green triangles). Experiments were repeated several times and one representative data set is shown.

**B.** Constant amounts of labelled TOM20-CD (67 nM) and unlabelled TOM9.2-CD (10 μM) were titrated with unlabelled CaM in the presence of calcium (red squares) or in absence of calcium (green triangles). Unlabelled BSA (black diamonds) in the presence of calcium was used as a control.

TOM20-CD was fluorescently labelled with Atto-520 ester and 100 nM of the labelled protein was titrated with unlabelled TOM9.2-CD. MST measurement revealed a clear change in thermophoretic movement confirming the interaction between these two components (Fig. 13A). The experiment was repeated several times and an affinity constant ( $K_D$ ) of  $4.9 \pm 0.23 \mu\text{M}$  could be derived from the results. As a control, unlabelled MBP was used instead of TOM9.2-CD and no change in thermophoresis was observed indicating that there is no interaction with TOM20-CD. Thermophoresis was also measured between labelled TOM20-CD and unlabelled CaM but did not reveal any interaction between these proteins (Fig. 13A).

To determine if there is any effect of CaM on the interaction between TOM9.2 and TOM20, MST was performed using constant concentrations of labelled TOM20-CD and unlabelled TOM9.2-CD in presence of an increasing concentration of unlabelled CaM. Addition of CaM resulted in a clear reduction in thermophoresis when calcium was present in the reaction (Fig. 13B). Three molar excess of CaM compared to TOM9.2 was able to reduce the interaction between TOM9.2 and TOM20 in terms of thermophoresis by 80%. When the same experiment was repeated in absence of calcium or using BSA instead of CaM in combination with calcium, no change in the thermophoresis was observed. Taken together, these results show that CaM interferes with the interaction between TOM9.2 and TOM20, which might be due to overlapping binding sites of CaM and TOM20 in TOM9.

#### **4.5.1 TOM9 interacts with TOM20 *in vivo***

To corroborate the interaction of TOM9 and TOM20 *in vivo*, co-immunoprecipitation (Co-IP) was performed using purified mitochondrial proteins. After solubilisation with non-ionic detergent, the mitochondrial protein extract was incubated with TOM20 antiserum. Protein A agarose beads were used to trap TOM20 antibody together with TOM20 proteins bound to the antibody as well as any interaction partner of TOM20 from within the mitochondrial extract. Proteins bound to the Protein A agarose beads were analysed on SDS-PAGE and western blot after extracting the proteins by heating the beads in presence of SDS. The TOM20 antibody was used to ensure that TOM20 itself was successfully precipitated by the antibody (Fig. 14).



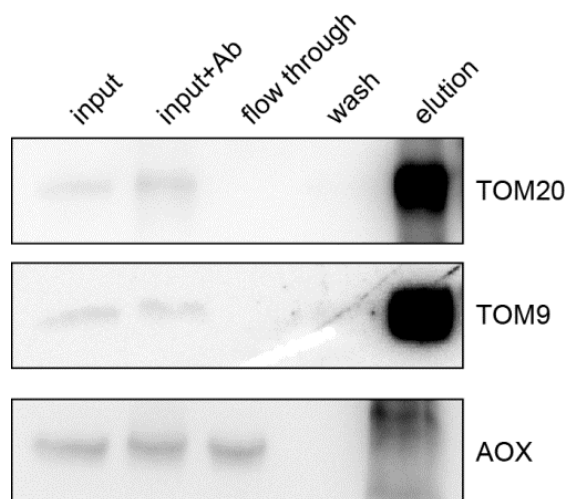


**Fig. 14 Co-immunoprecipitation of TOM9.2 along with TOM20**

After solubilisation with non-ionic detergent mitochondrial proteins (input) were incubated first with TOM20.2 antibody (input+Ab) and afterwards with protein A plus agarose beads. The flow through was collected and after washing the beads thoroughly (wash), bound proteins were eluted (elution) by heating the beads in SDS sample buffer. Samples were resolved on SDS-PAGE followed by immunodetection using TOM20.2, TOM9.2 and AOX antibodies.

Probing the fraction with the TOM9 antibody showed that TOM9 was precipitated along with TOM20 confirming that the two proteins also interact *in vivo*. By contrast, AOX, a protein of the matrix could not be identified in the elution (Fig. 14).

#### 4.6 Role of CaM for the targeting of TOM9 to mitochondria

Earlier studies on Tom22 from rat suggested that a positively charged hydrophobic domain close to the TM domain is responsible for its targeting into mitochondria (Nakamura et al., 2004). Since TOM9 binds to CaM through a positively charged amphiphilic domain close to the membrane spanning domain, it was important to more closely elucidate the role of this region in terms of mitochondrial targeting of TOM9. To that end, *in vitro* import assays with <sup>35</sup>S-Met labelled full length TOM9.2 (TOM9.2-FL) and TOM9.2 lacking the CaM binding domain (TOM9.2-ΔCaMBD) into purified mitochondria were performed (Fig. 15). To differentiate between surface bound protein and properly inserted protein, half of the mitochondria were subsequently treated with sodium carbonate to remove all surface-bound precursor proteins leaving only integral membrane proteins in the pellet. Under standard reaction conditions a considerable amount of radio-labelled TOM9.2-FL was found associated

with the mitochondria and upon carbonate extraction a significant portion of the protein remained in the membrane fraction, indicating that TOM9.2-FL was successfully inserted into the mitochondrial membrane (Fig. 15, left panel). When TOM9.2- $\Delta$ CaMBD was tested under the same standard import conditions, only very little protein associated with the mitochondria and no insertion into the membrane could be observed (Fig. 15, right panel). These results indicate that this particular domain plays a role for the targeting of TOM9 to the outer membrane of mitochondria.

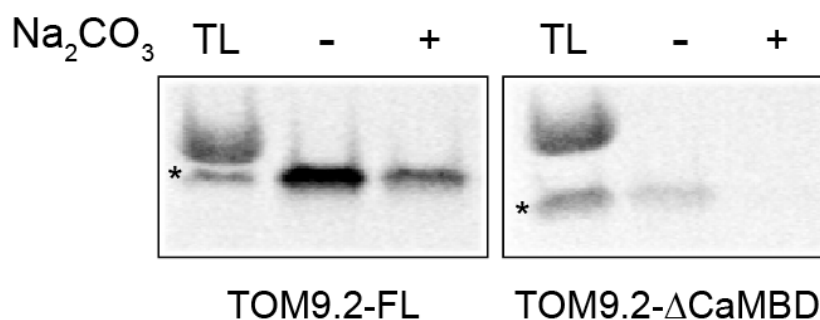


**Fig. 15 The CaMBD of TOM9 is crucial for its targeting to mitochondria**

In vitro import of radio-labelled full length TOM9.2 (TOM9.2-FL) and TOM9.2 lacking the CaM binding domain (TOM9.2 $\Delta$ CaMBD) into isolated mitochondria was performed. To distinguish between surface bound and inserted proteins, half of the reaction was extracted with sodium carbonate (+) while the other half remained untreated (-). TL: 1/10<sup>th</sup> of the translation product used in each assay. ‘\*’ represents translated products of interests. All reactions were analyzed by SDS-PAGE and autoradiography.

Next, the effect of exogenous CaM on TOM9.2 import was tested by adding pig brain CaM in a range of 1-10  $\mu$ M to a standard import reaction (Fig. 16). While up to 1  $\mu$ M CaM had no significant effect on insertion of TOM9.2 into the mitochondrial membrane, the amount of successfully inserted TOM9.2 decreased substantially with higher CaM concentrations. This suggests that CaM can negatively regulate TOM9 insertion into the mitochondrial membrane and the inhibitory CaM concentration lies between 1-2.5  $\mu$ M (Fig. 16).

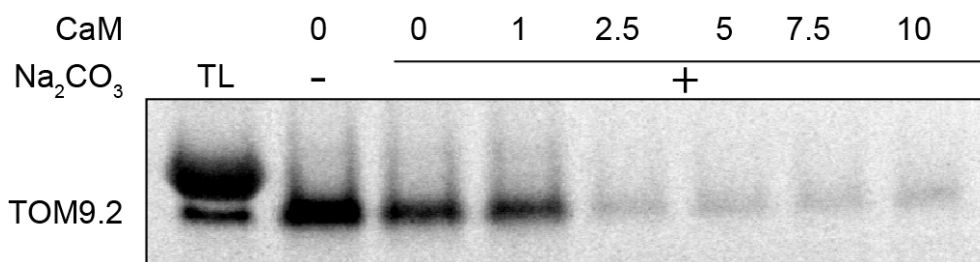


**Fig. 16 CaM inhibits TOM9.2 targeting into mitochondria**

<sup>35</sup>S-Met labelled TOM9.2-FL was imported into purified Arabidopsis mitochondria in presence of increasing amounts of CaM in the reactions. After carbonate extraction, reactions were analyzed by SDS-PAGE and autoradiography.

Since CaM affects the interaction of TOM9.2 with TOM20 and in yeast the proteins work together to facilitate the import of other mitochondrial proteins, the effect of CaM in mitochondrial import was further tested on several other nuclear encoded mitochondrial proteins. As before, radioactively labelled precursor proteins were imported into purified Arabidopsis mitochondria. For the integral outer membrane proteins TOM9.2, TOM20 and TOM40 extraction with carbonate was used to distinguish between insertion and surface binding. In order to assess import of the inter membrane space protein TIM8 and the matrix protein mtGST, mitochondria were treated with thermolysin to remove all precursors bound to the mitochondrial surface. In this case, only fully imported proteins are protected from the protease. All experiments were performed either in absence (-) or in presence (+) of 10 μM pig brain CaM (Fig. 17).

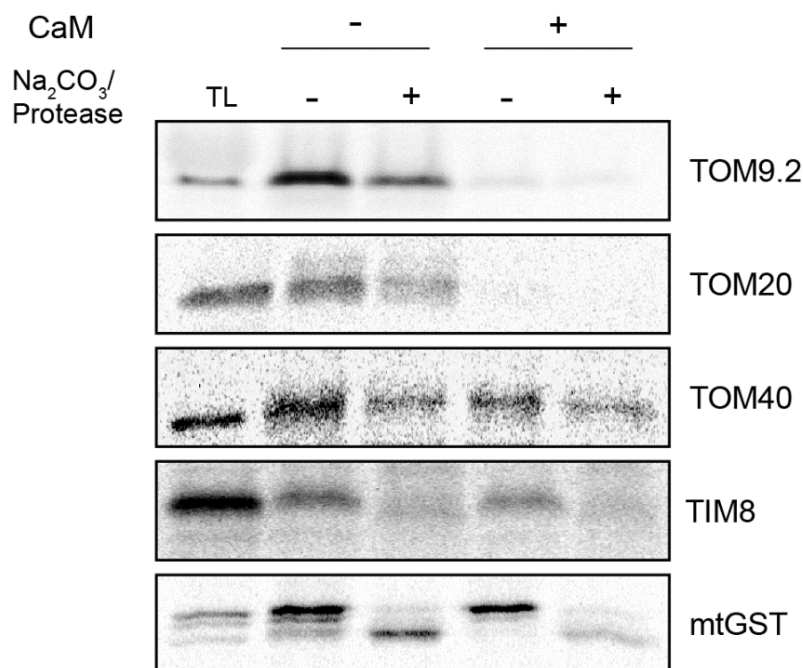


**Fig. 17 Effect of CaM on mitochondrial protein import**

<sup>35</sup>S-Met labelled mitochondrial precursor proteins were imported into purified mitochondria in absence (-) or in presence of 10  $\mu$ M CaM (+). To distinguish between surface bound and imported proteins, half of the reaction was either extracted with sodium carbonate (in case of TOM9.2, TOM20 and TOM40) or by protease protection assay (TIM8 and mtGST) while the other half remained untreated (-). TL: 1/10<sup>th</sup> of the translation product used in each assay.

No large difference was observed in case of TOM40, TIM8 and mtGST protein either with regard to the association with the import machinery not for the import/insertion of these proteins. By contrast, binding as well as membrane insertion were drastically reduced for both TOM9 and TOM20 in the presence of CaM (Fig. 17). These results indicate that also insertion of TOM20 is affected by CaM, however, this might be due to an indirect effect on TOM9.

#### 4.7 Screening for T-DNA insertion lines in the *TOM9.2* gene locus

The functional role of TOM9.2 in plants is not very well understood. One way to address the function of a protein *in vivo* is the analysis of plant lines with a loss of *TOM9.2* expression. A search for *TOM9.2* T-DNA insertion lines was performed at <http://signal.salk.edu/cgi-bin/tdnaexpress> (Alonso et al., 2003). No line containing a T-DNA insertion within the gene locus could be found. However, three lines (SALK\_095668.47.30.x, SALK\_059740.46.20.x,

SALK\_059639.52.30.x) for which the given sequence supposedly matched within the 5'-UTR of At5g43970 were listed. Seeds for all lines were obtained from NASC and screened for T-DNA insertions via PCR-genotyping but unfortunately no plants containing the suggested T-DNA were found. Another line (WiscDsLoxHs023\_01B) was obtained commercially where the sequence given also matched with the 5'-UTR of At5g43970 and this line was found to be positive for the insertion (Fig. 18A). However, when purified mitochondria from these plants were analyzed by immunodetection with the TOM9.2 antibody, no significant loss in the amount of TOM9.2 protein could be detected (Fig. 18B), indicating that the T-DNA insertion has no effect on *TOM9.2* gene expression.

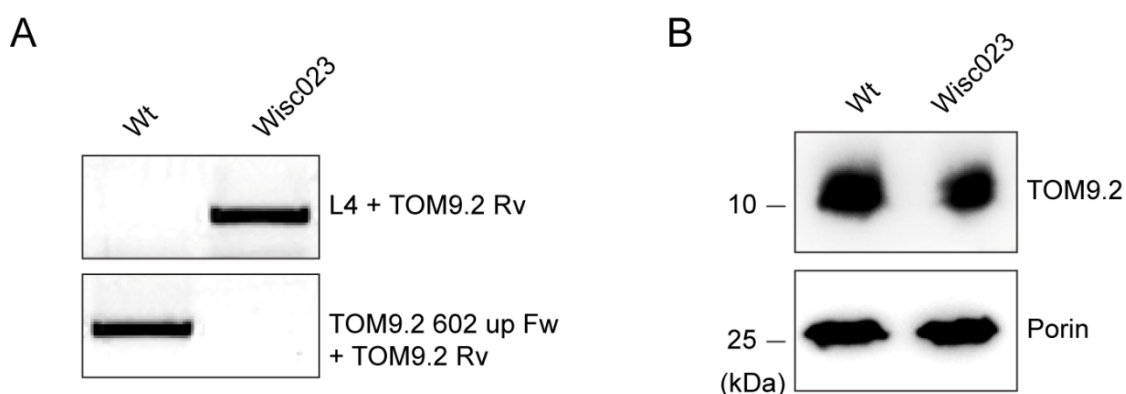


**Fig. 18 Analysis of the WiscDsLoxHs023\_01B T-DNA insertion line**

**A.** Genomic DNA was isolated from wild type (Wt) and WiscDsLoxHs023\_01B plants (Wisc023) and PCR was performed using either left border primer (L4) and gene specific reverse primer (TOM9.2 Rv) or gene specific forward (TOM9.2 02 up Fw) and reverse primer.

**B.** Protein extracts from purified mitochondria isolated from wild type (Wt) and t-DNA insertion line (Wisc023) were analysed by immunoblotting using either TOM9.2 or Porin antibodies.

In order to confirm that the protein detected in the T-DNA insertion line is indeed TOM9.2 and not TOM9.1, specificity of the TOM9.2 antibody was tested using recombinant MBP-tagged TOM9.1 and TOM9.2 protein (Fig. 19). Serial dilutions were made for purified protein from both isoforms as well as MBP alone as negative control to confirm that the tag itself is not recognized by the antibody.

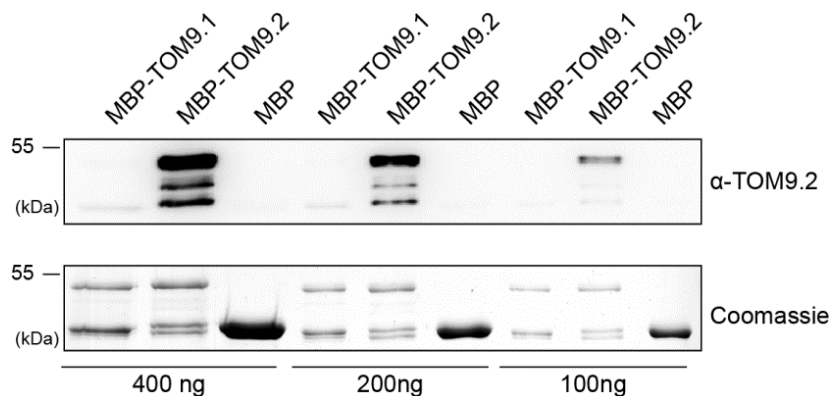


**Fig. 19 TOM9.2 antibody is specific to TOM9.2 protein.**

Recombinantly generated MBP-tagged TOM9.1 and TOM9.2 proteins were diluted serially and resolved on SDS-PAGE followed by either western blotting and immunodetection by TOM9.2 antibody (upper panel) or visualization of proteins after staining with Coomassie brilliant blue. Recombinant MBP was used as control.

Western blot analysis clearly shows the specificity of the antibody raised against TOM9.2 since neither TOM9.1 nor the MBP tag is recognized (for details how the antibody was raised, see section 2.10).

#### 4.8 Generation of *TOM9.2* knock-down plants RNA silencing

In lieu of a T-DNA insertion line, the next step was to create *TOM9.2* knock-down lines. For this purpose, wild-type *A.thaliana*, var Col-0 was transformed with pOpOFF-2(Hyg)-*TOM9.2* via Agrobacteria-mediated transformation and two independent knock-down lines (kd-5-10 and kd-6-12) were identified and further propagated (for details, see 3.3.1). Plants were grown on media without sucrose either containing Dex (+Dex) or same amount of solvent DMSO (-Dex). Both RNAi lines grew well, even upon induction of silencing with Dex. To confirm if these RNAi lines are really knock-down for *TOM9.2* expression, plant extracts were prepared and proteins were analysed by immune-decoration using the TOM9.2 antibody (Fig. 20). A porin antibody was used as control to show that equal amounts of mitochondria were loaded in each lane. It is clearly visible that the knock-down lines when not induced, express TOM9.2 at the same level as in wild type (Fig. 20, upper panel). However, upon induction with Dex, no TOM9.2 can be detected in either mutant line indicating that *TOM9.2* is efficiently silenced by the RNAi induction. Since the plants are viable both on medium without sucrose as well as on soil (see below), these results also imply that TOM9.2 is not essential for plant growth.

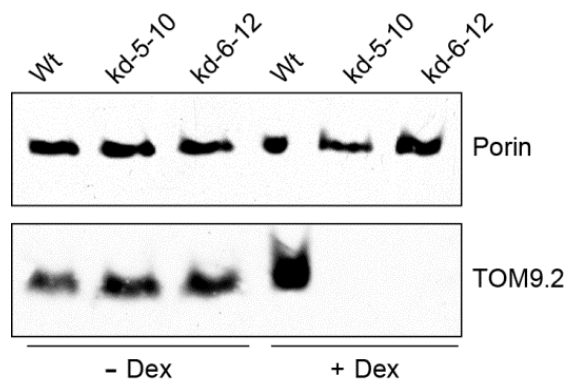


**Fig. 20 Western blot analysis of *TOM9.2* knock-down plants**

Protein extracts were prepared from Dex treated (+Dex) or non-treated (-Dex) plate grown plants from wild type (Wt) and two independent *TOM9.2* knock-down lines (kd-5-10 and kd-6-12). Proteins after precipitating with chloroform-methanol, were resolved on SDS-PAGE followed by immunoblotting using *TOM9.2* and Porin antibodies.

#### 4.8.1 *TOM9* knock-down plants exhibit several phenotypes

scTOM22 is an essential protein (Baker et al., 1990; Lithgow et al., 1994; Hoenlinger et al., 1995). By contrast, the experiments so far have shown that the loss of *TOM9.2* is not lethal. However, the RNAi silenced plants do exhibit several phenotypic anomalies. When grown in liquid culture, the plants are yellowish compared to wild type and slightly smaller (Fig. 21). No differences in root growth could be observed (data not shown).

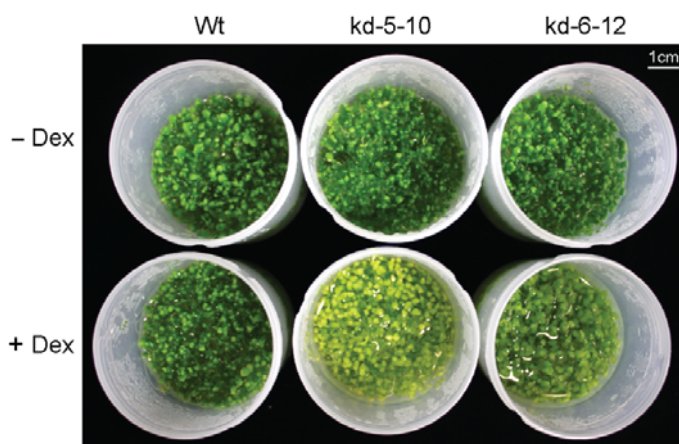


**Fig. 21 *TOM9.2* knock-down plants grown in liquid culture**

*TOM9.2* knock-down plants were grown with or without dexamethasone (+/- Dex) treatment along with wild type control. Shown are plants that had been grown for 14 days in liquid culture.

Another phenotypic alteration could be observed for plants grown on plates. A difference in the hypocotyl length was observed between plants grown on  $\frac{1}{2}$  MS plate containing either Dex or no Dex at 16 hours light under a wide range of low light intensity for four days. The induced knock-down plants showed significantly shorter hypocotyls in comparison with wild type or non-induced mutants (Fig. 22A and B). No difference was observed under higher light intensities ( $> 100 \mu\text{mol m}^{-2} \text{s}^{-1}$ ) and but the difference persisted in the whole range from 0 to about  $30 \mu\text{mol m}^{-2} \text{s}^{-1}$ .

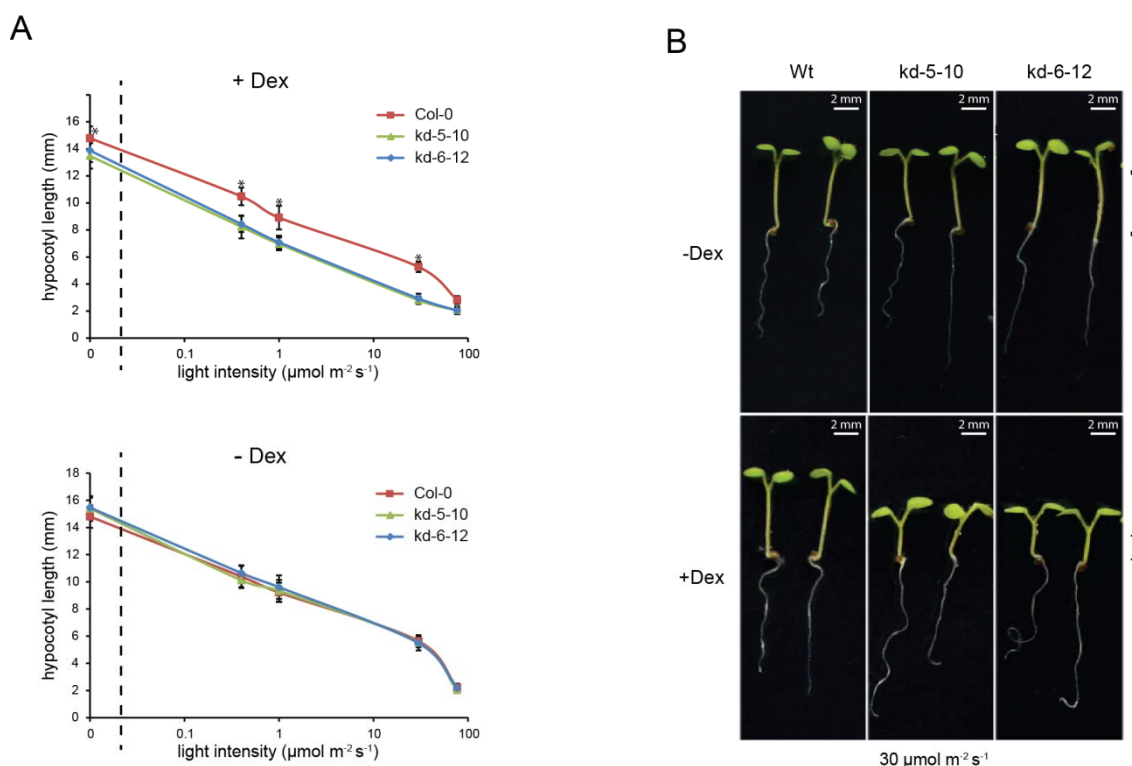


**Fig. 22 TOM9.2 knock-down plants have shorter hypocotyls**

**A.** Seeds from Wild type (Wt) and *TOM9.2* knock-down lines (kd) were sown on solid media containing either Dex (+Dex) or solvent control (-Dex) and grown for 4 days under white light of variable fluence rates. Hypocotyl length was measured for several plants ( $n=20$ ). The data presented here are in logarithmic scale separated from the origin (0,0) by a vertical dotted line. Students T-tests were performed and data point with a  $p$  value  $<0.001$  are denoted by asterisks.

**B.** A representative picture of 4 days old seedlings grown under  $30 \mu\text{mol m}^{-2} \text{s}^{-1}$  are shown. Scale as indicated by bars. Hypocotyl length of the mutant that was considered for the analysis is marked with square brackets.



Furthermore, when the plants were grown on solid media containing Dex, *TOM9.2* knock-down plants flower earlier compared to wild type or untreated plants (Fig. 23A). The early flowering became even more visible when the plants were transferred to soil allowed to grow for a few more days since the plate limit extensive plant growth.

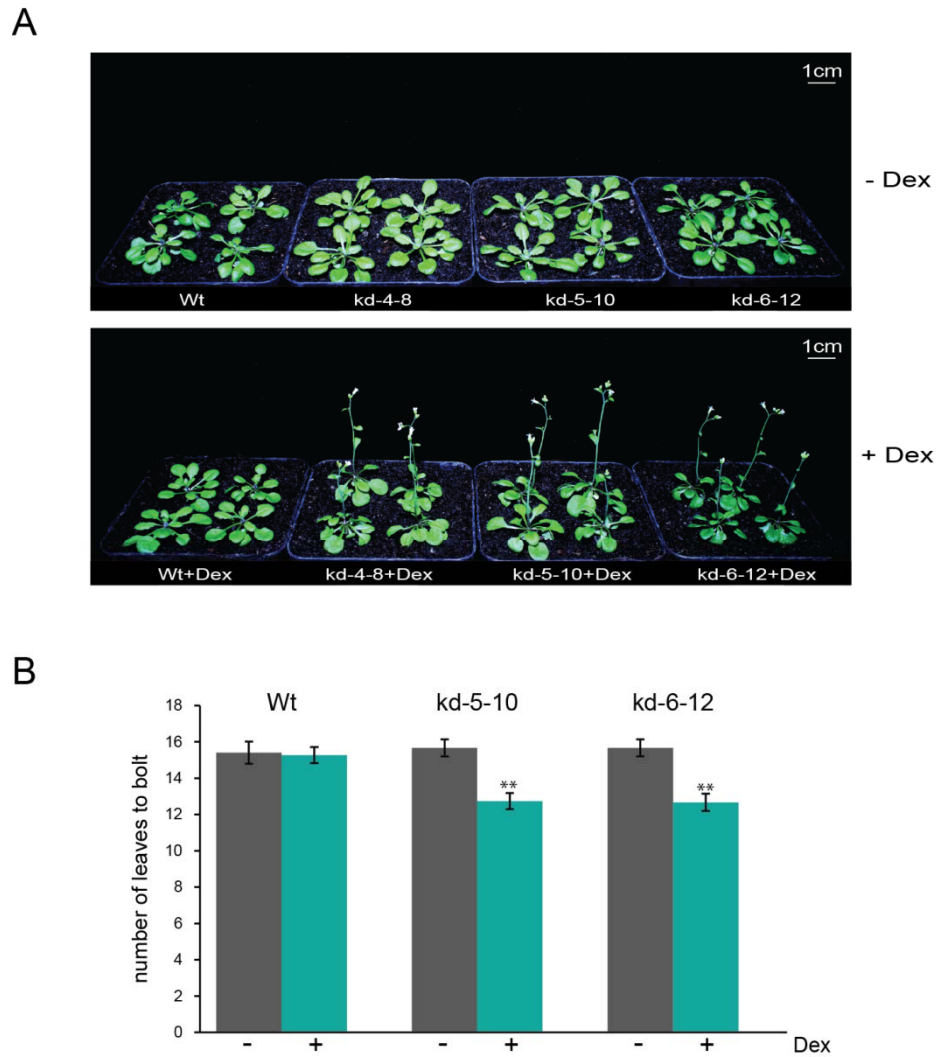


**Fig. 23 *TOM9.2* knock-down plants flower earlier than wild type**

**A.** Seeds from wild type (Wt) and two independent *TOM9.2* knock-down lines (kd) were sown on plates containing either Dex (+Dex) or solvent control (-Dex) and grown for 20 days under long day condition. They were then transferred to soil and grown further for 3 days under same condition before the photographs were taken.

**B.** Leaves from the above mentioned plants were counted at the day when the bolting was first visible. Data represent the mean of 15 different individuals. Students T-Test was performed and data with a *P* value <0.001 are indicated by asterisks.

A closer look at these plants revealed that the early flowering is caused by bolting at an earlier developmental stage, as seen by counting the number of leaves at the time of bolting (Fig. 23B). While the wild type and the untreated plants bolt at stage later than 1.14 (when 14 leaves are longer than 1 mm), the Dex treated mutant lines bolt before they reach stage 1.12 (when 12 leaves are longer than 1 mm) (Boyes et al., 2001).

#### **4.9 *TOM9.2* knock-down plants have up-regulated expression of genes related to floral development**

Since a near absence of *TOM9.2* results in several phenotypic abnormalities, especially early flowering, global gene expression changes between Dex-induced and non-induced RNAi plants were analysed by DNA micro array (ATH1 GeneChip) performed in collaboration with Dr. Katrin Philippar, Botany, LMU-Munich. Rosette leaves were harvested from induced and non-induced RNAi plants at the time when the inflorescence bud of the mutant plants was first visible just at the end of the photoperiod since floral regulatory genes are highest expressed at this time of the day (Suarez-Lopez et al., 2001; Valverde et al., 2004; Wahl et al., 2013). In total, 147 genes were found to be significantly up-regulated and 73 to be down-regulated when DNA microarray data were compared between induced and non-induced plants of the two independent RNAi lines used for the previous analyses (Fig. 24 and appendix II). Overall, the number of up-regulated genes was double of the down-regulated genes revealing a stronger effect on induction of gene expression also mirrored by the fact that the intensity of up-regulation was generally higher (see appendix II). First, the authenticity of *TOM9* RNAi lines was confirmed by the significant down-regulation of *TOM9.2* transcripts in both the RNAi lines (2.2-fold down-regulation, see Table 2). The genes with significantly altered expression level were further categorized according to the TAIR10 genome release (<https://www.arabidopsis.org/>). Major changes were observed in candidates involved in regulation of transcription (category 27 in Fig. 24), in particular transcription factors (25 up-; 9 down-regulated). Moreover, 11 transcripts for genes encoding phosphatases or kinases were up-regulated (8 genes belonging to the functional category associated with protein modification, 3 kinase genes having signalling functions) indicating that signalling processes through protein phosphorylation and/or dephosphorylation are induced. The candidate with the strongest induction fell in this category with 13-fold up-regulation. This gene, *At3g05640*, encodes a protein phosphatase, which has recently been shown to be involved in promoting inflorescence stem growth in Arabidopsis (Sugimoto et al., 2014).

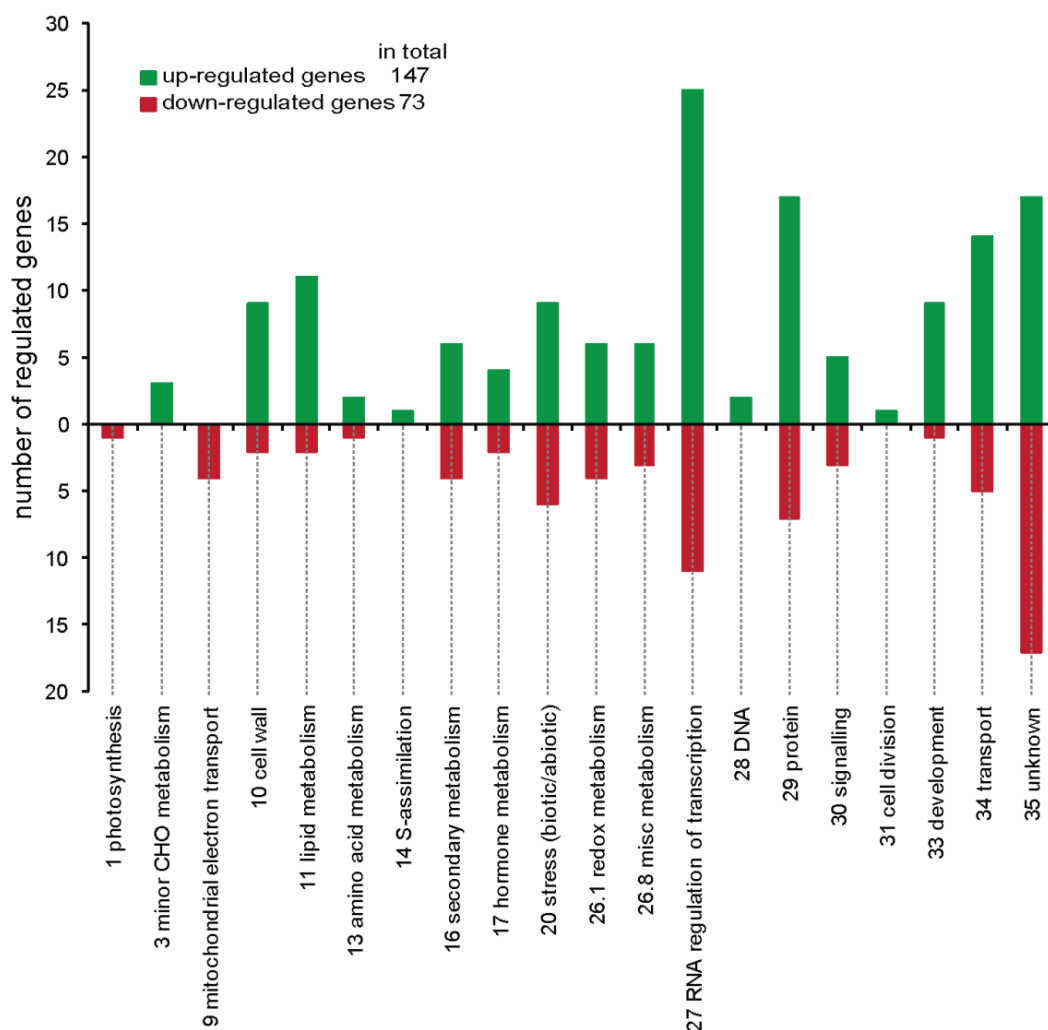


**Fig. 24 Differential gene expression in *TOM9.2* RNAi plants**

DNA microarray analysis (ATH1 GeneChip) was performed with induced and non-induced *TOM9.2* RNAi plants from two independent lines (kd-5-10 and kd-6-12). Gene expression pattern between induced (+Dex,  $n = 5$ ) and non-induced (-Dex,  $n = 6$ ) was compared and analysed. Differentially regulated genes ( $P$  value  $\leq 0.05$ ) were tabulated into functional categories according to TAIR10. Presented functional categories are as indicated. Green and red bars present numbers of up- and down-regulated genes of each functional category, respectively. Mean signal intensities and fold changes along with other information are provided in the appendix II.

The next major change observed on the transcript level was for genes involved in transport processes (14 up-, 5 down-regulated). Among specific sugars and metabolite transport related genes, 7 candidates were found to be up-regulated, whereas 2 were down-regulated. Among

developmental genes, that are member of MtN21-like transporter family, 6 were found to be associated with membrane transport (5 up-, 1 down-regulated). Furthermore, 3 genes with increased (including the Ca<sup>2+</sup>-transporter CAX1) and 3 candidates with decreased expression were found that are associated with Ca/CaM-dependent functions (Appendix II). Genes related to carbohydrate metabolism were found to be only up-regulated. Interestingly, no major changes were observed in transcript abundance for most genes encoding mitochondrial proteins. Exceptions obviously included *TOM9.2* but also four down-regulated genes that code for components of the complex V of the mitochondrial respiratory chain: *At2g07698*, *At2g07741*, *At2g07671* and *At2g07707*.

**Table 1** Differential expression of flowering related genes in *TOM9.2* RNAi lines

The average scaled signals of several selected genes involved in flowering are given for non-induced (-Dex) and induced plants (+Dex) along with the fold change (FCH) and respective *p* values. *SEP*, *SEPALLATA*; *SPL4*, *SQUAMOSA-PROMOTER BINDING PROTEIN-LIKE*; *PI*, *PISTILLATA*; *FT*, *FLOWERING LOCUS T*; *AGL8*, *AGAMOUS-LIKE 8*; *AP3*, *APETALA 3*

Gene	AGI	-Dex	+Dex	FCH	<i>p</i> value
<i>FT</i>	At1g65480	301.08	571.29	1.90	0.0025
<i>SPL4</i>	At1g53160	113.71	217.78	1.92	0.0013
<i>AGL8</i>	At5g60910	227.91	306.85	1.35	0.1278
<i>SEP1</i>	At5g15800	32.18	43.56	1.35	0.0209
<i>SEP2</i>	At3g02310	21.39	30.99	1.45	0.0221
<i>SEP3</i>	At1g24260	27.22	40.87	1.50	0.0106
<i>PI</i>	At5g20240	23.81	34.29	1.44	0.0013
<i>AP3</i>	At3g54340	24.87	31.10	1.25	0.0558

More interestingly with regard to the early flowering phenotype is the fact that a total of 14 genes involved in flower/meristem development were found to be induced in *TOM9.2* knock-down lines (Table 1). Up-regulated flower development genes include transcription factors such as *SEPALLATA* (*SEP 1, 2, 3*; Teper-Bamnolker and Samach, 2005), *SQUAMOSA-PROMOTER BINDING PROTEIN-LIKE* (*SPL4/FTM6*; Yang et al., 2008), and *PISTILLATA* (*PI*; Krizek and Meyerowitz, 1996), as well as the promoter of flowering, *FLOWERING LOCUS T* (*FT*; Samach et al., 2000; Turck et al., 2008) and its antagonist *TERMINAL FLOWER 1* (*TFL1*; Shannon and Meeks-Wagner, 1991).

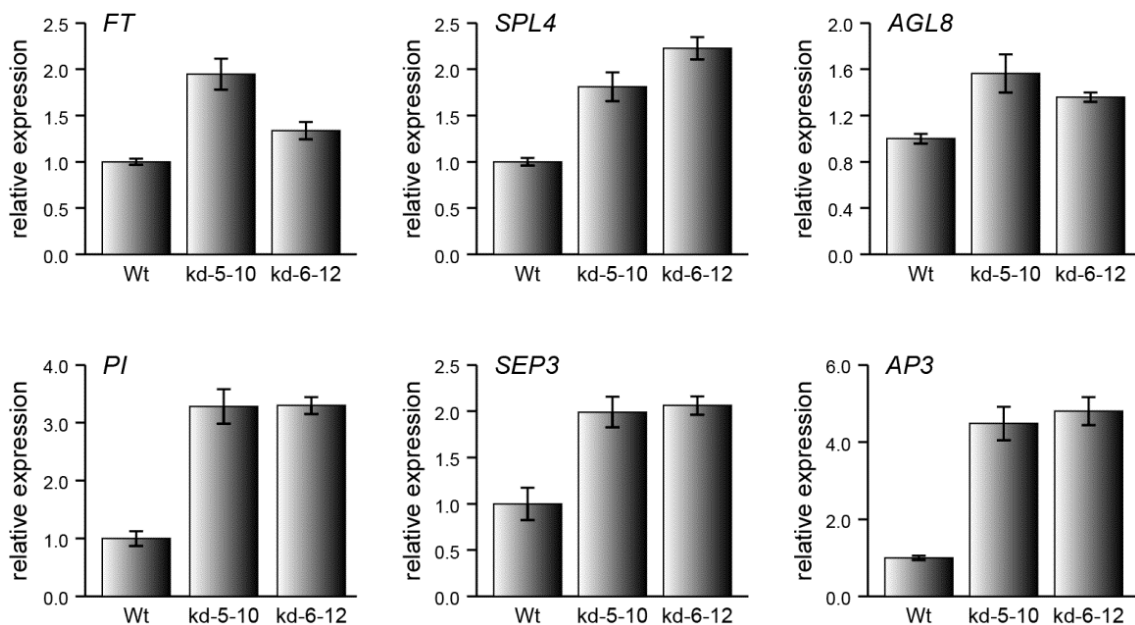


**Fig. 25 Flowering regulatory genes are up-regulated in *TOM9.2* RNAi plants**

Quantitative real-time PCR analysis of the relative expression of flowering related genes. Wild type (Wt) was set to 1. *PP2AA3* was used as reference gene. Error bar represents SEM of triplicate reactions. *FT*, *FLOWERING LOCUS T*; *SPL4*, *SQUAMOSA-PROMOTER BINDING PROTEIN-LIKE*; *AGL8*, *AGAMOUS-LIKE 8*; *PI*, *PISTILLATA*; *SEP3*, *SEPALLATA 3*; *AP3*, *APETALA 3*

In order to confirm the alteration in the expression of flowering related genes, quantitative real-time PCR was performed for several candidates in collaboration with the group of Dr. Gabriel Schaaf, University of Tübingen (Fig. 25). Two other genes, *AGAMOUS-LIKE 8* (*AGL8/FUL*; Ferrandiz et al., 2000) and *APETALA 3* (*AP3*; Krizek and Meyerowitz, 1996)

were also included in the qPCR analysis even though they were not significantly upregulated on the basis of the selected  $P$  value of 0.05 in the DNA microarray analysis (Table 1 and Appendix II). However, there  $P$  values for AGL8 and AP3 were 0.12 and 0.055 respectively and both genes are known to regulate flowering. In all cases the qPCR showed a clear up-regulation of these genes thus corroborating the micro-array data as well as providing a basis for the visible early flowering of the *TOM9.2* knock-down plants.

Though *TOM9.2* was found to be clearly down-regulated, no other mitochondrial protein import component showed altered gene expression level (Table 2 and Appendix II).

**Table 2** Differential expression of TOM complex subunits in *TOM9.2* RNAi lines

The average scaled signals of several selected genes encoding components the TOM complex in non-induced plants (-Dex) and induced plants (+Dex) are presented along with the fold change (FCH) and respective  $p$  values.

Gene	AGI	-Dex	+Dex	FCH	$p$ value
<i>TOM9.2</i>	At5g43970	499.57	224.24	0.45	<0.0001
<i>TOM9.1</i>	At1g04070	130.55	123.92	0.95	0.7947
<i>TOM20.1</i>	At3g27070	30.62	31.34	1.02	0.8029
<i>TOM20.2</i>	At1g27390	264.19	267.00	1.01	0.9380
<i>TOM20.3</i>	At3g27080	433.12	453.21	1.05	0.6809
<i>TOM20.4</i>	At5g40930	455.56	453.59	1.00	0.9744
<i>TOM40</i>	At3g20000	830.25	804.60	0.97	0.7916
<i>TOM5</i>	At5g08040	944.55	874.75	0.93	0.3446
<i>TOM6</i>	At1g49410	484.64	468.69	0.97	0.7554
<i>TOM7</i>	At5g41685	486.42	484.79	1.00	0.9778

In yeast, Tom22 plays the role of organizer of TOM complex by acting as a docking site for Tom20, thereby assembling it into the TOM complex (van Wilpe et al., 1999; Gerbeth et al., 2013). To analyse a potential function of TOM9 in TOM complex assembly in plants, mitochondria were purified from wild type and induced *TOM9.2* RNAi seedlings grown in liquid culture and protein content as well as complex assembly was analysed.

#### 4.10 *TOM9.2* knock-down plants display differential mitochondrial protein abundance

The abundance of several mitochondrial proteins from different sub-compartments was analysed using specific antibodies (Fig. 26). This analysis revealed that the alleged TOM9-interacting partner TOM20 is present but is reduced to about 50 % of the wt content despite the fact that the corresponding gene is not down-regulated (Table 2). The general import pore (GI) TOM40 also seems to be slightly reduced, however the observed difference is rather minor and lies within the error rate of the methods. In case of two outer membrane proteins not involved in protein import, VDAC (Voltage-dependent anion channel) and Porin, no significant changes were visible. OM64 (Mitochondrial Outer Membrane Protein 64), however, which is believed to be the functional homolog of yeast Tom70, was clearly up regulated (Fig. 26).

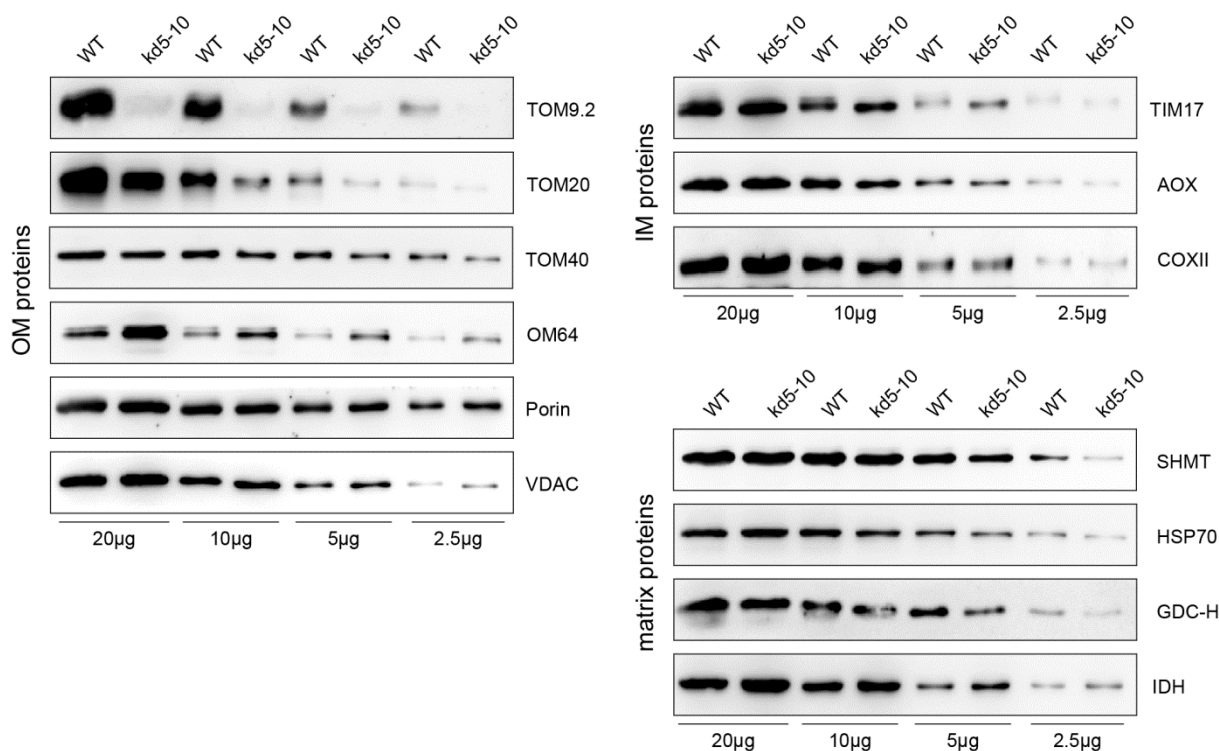


**Fig. 26 Western blot analysis of mitochondrial protein abundance in *TOM9.2* knock-down plants**

Mitochondria were purified from wild type and *TOM9.2* knock-down plants grown in liquid culture supplemented with Dex and serially diluted protein extracts were separated on SDS-PAGE and blotted onto PVDF membrane. Proteins were visualized by immunodecoration with antibodies against mitochondrial proteins from different sub-compartments (OM = outer membrane; IM = inner membrane).

Several proteins of the inner membrane or the matrix were also tested, including TIM17 (Translocase of Inner membrane of Mitochondria 17), COXII (cytochrome oxidase subunit II), AOX (Alternate Oxidase) SHMT (serine hydroxymethyltransferase), HSP70 (Heat shock protein 70), GDC-H (subunit H of the glycine dehydrogenase complex) and IDH (isocitrate dehydrogenase). From this whole set only TIM17 was found to be slightly increased.

#### **4. 11 *TOM9.2* knock-down plants show a reduction in assembled TOM and TIM23 complex**

Previous experiments on yeasts had shown that Tom22 is responsible for the organization of the TOM complex. In the absence of Tom22 the 400 kDa TOM complex dissociates into a 100 kDa sub-complex comprised of Tom40 and the smaller Tom subunits but lacking the receptors (van Wilpe et al., 1999). To elucidate if *TOM9.2* also plays a similar role in plants, digitonin solubilized mitochondrial protein complexes from wild type and *TOM9.2* knock-down plants were separated on a 5-16% BN-PAGE (see section 3.2.10). Proteins were blotted onto PVDF membrane and immune-decorated using antibodies directed against several TOM components (Fig. 27). This analysis revealed that, though a 400 kDa complex could be detected using *TOM9.2*, *TOM20* or *TOM40* antibodies, the amount of TOM complex was severely reduced in mitochondria from the *TOM9.2* knock-down plants (Fig. 27). Unlike yeasts, a smaller TOM complex could not be identified. To test whether the mitochondrial inner membrane translocase complex TIM23, which in yeasts is known to interact with Tom22, is present in these knock-down plants, immune-decoration was performed with an antibody against TIM17, which is an integral part of the TIM23 complex (sometimes also referred to as TIM23:17). Interestingly, also this complex was found to be severely reduced. To check the integrity of another mitochondrial complex not involved in protein import, complex IV of the respiratory chain, a COX-II antibody was used. While there might be a slight reduction in complex-IV content, the loss is far less severe compared to the TOM or the TIM23 complex.



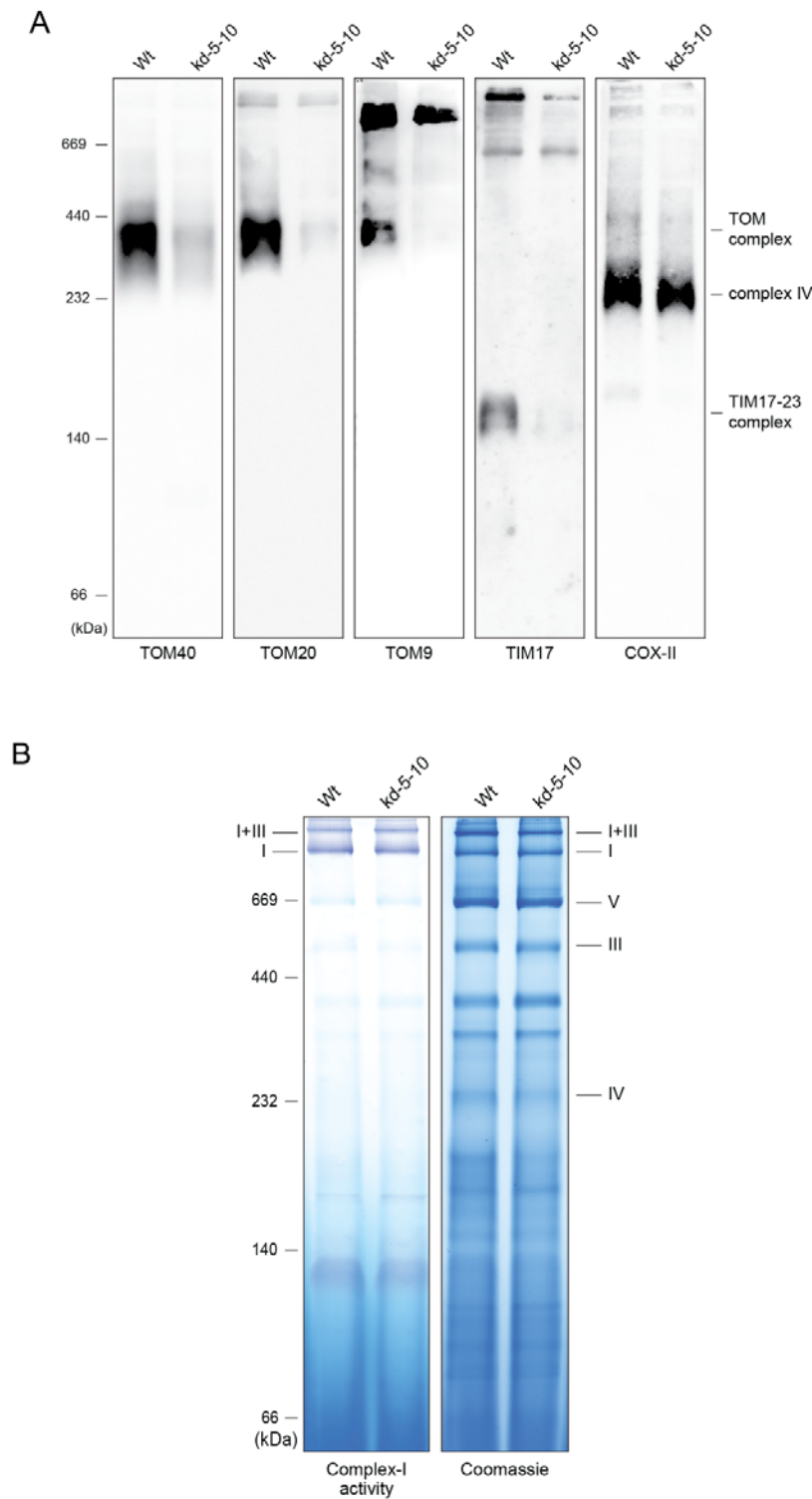


**Fig. 27 *TOM9.2* knock-down plants are deficient in TOM and TIM23 complexes**

**A.** BN-PAGE analysis of protein from wild type (Wt) and *TOM9.2* knock-down (kd-5-10) mitochondria. Proteins after solubilizing with digitonin were resolved on a 5-16% BN PAGE, blotted onto PDMF and immune-decorated with antibodies for detection of various protein complexes.

**B.** Identical loaded BN-PAGES were stained for Complex-I activity (left) or with Coomassie (right).

As a loading control, a BN-gel was also stained with Coomassie. All respiratory chain complexes are clearly visible and seem to be present in the mutant mitochondria at the same level as observed in wild type mitochondria (Fig. 27 B). Only exception is the complex-IV, which in accordance with the result obtained from western blot analysis is slightly reduced in the mutant plants. When activity of the respiratory chain complex I was analysed it was confirmed that the complex from mutant mitochondria is equally active as from wild type mitochondria (Fig. 27B).

#### 4.12 Mitochondria from *TOM9.2* knock-down plants are import competent

The severe reduction in the amount of TOM complex raised the question whether mitochondria from RNAi silenced plants are equally import competent as wild type mitochondria. Experiments performed on yeasts had shown that in absence of Tom22 from the TOM complex mitochondrial protein import was inhibited *in vitro* (van Wilpe et al., 1999). To analyse protein import competence, *in vitro* import was performed with mitochondria from wild type and mutant plants with several mitochondrial precursor proteins representing different sub-organellar locations, such as TOM40, TOM20 and TOM9, as well as TIM23 and mtGST (Fig. 28). For most of the proteins, no difference in import efficiency could be observed, indicated by similar amount of radioactive labelled protein observed in the untreated as well as the carbon extracted or thermolysin treated samples (Fig. 28).

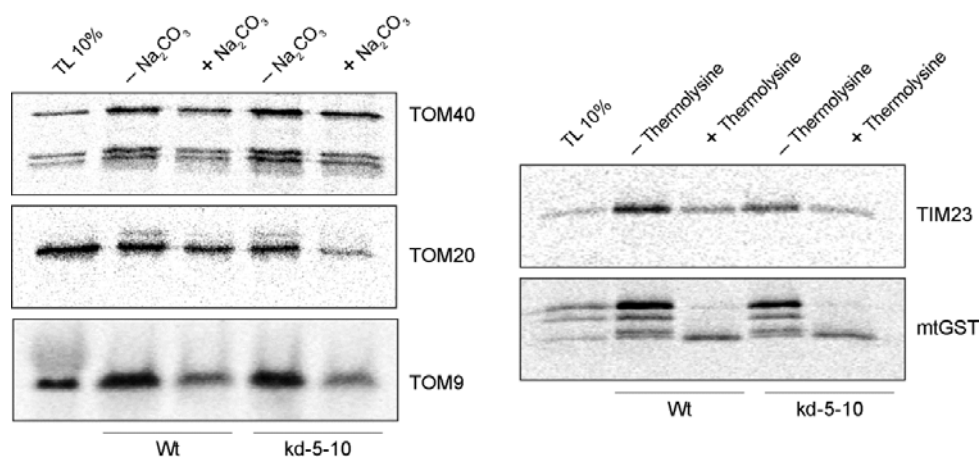


**Fig. 28 *TOM9.2* knock-down mitochondria can import proteins**

Mitochondria were purified from liquid cultured Dex-induced wild type (Wt) and *TOM9.2* knock-down plants (kd-5-10) and used to import radio-labelled different mitochondrial precursors. To analyze membrane insertion of TOM40, TOM20 and TOM9, carbonate extraction was performed. For TIM23 and mtGST, protease protection assay was carried out in order to analyze import.

In case of TOM9 and TOM20, a slight decrease in the carbonate extracted samples is visible for the mutant mitochondria, however, more detailed studies would be required to substantiate that finding. Since western blot analysis had shown that the total amount of TOM40, presumably present in its monomeric state, was not decreased drastically in the mutant plants (see 4.10), this import competency of the mutant mitochondria might result from the presence of unassembled TOM40 pores or residual assembled TOM complex. Viability of plants with complete knock-out for TIM23 has been reported recently (Wang et al., 2012), which indicates import competency of mitochondria with reduced level of TIM23. This could explain why the TOM9.2 knock-down plants also show no alteration in import of the matrix protein mGST even though the TIM23 complex is reduced

### **4.13 Calcium-dependent protein phosphorylation**

Calcium-dependent phosphorylation is well described in plants through calcium-dependent protein kinases (CDPKs) or CaM-dependent protein kinases (CaMKs). It has also been known for a while that several components of the photosystem are phosphorylated or dephosphorylated in order to get the active form. However, calcium-dependent phosphorylation was not reported in chloroplast until very recently (Stael et al., 2011) and very little is known about the role of this regulation in organelles. The set of targets identified in that publication included the Calcium Sensor protein (CaS), which has been known since some time for its low-affinity/high-capacity calcium binding promoted by its N-terminal, lumen-exposed part. It was further shown that CaS can induce changes in cytosolic  $\text{Ca}^{2+}$  concentration in guard cells, thereby regulating stomatal movements (Han et al., 2003). Phosphorylation of CaS was previously suggested to occur at stromal exposed Thr<sub>380</sub> promoted by thylakoid localized state transition kinase STN8 (Vainonen et al., 2008) and two other phosphorylation sites were reported at Ser<sub>373</sub> and Ser<sub>378</sub> (Reiland et al., 2009). However, no connection between calcium and these phosphorylation sites or the involvement of a specific calcium dependent kinase in phosphorylating CaS had been reported.

#### **4.13.1 Calcium-dependent phosphorylation site of CaS**

The the calcium-dependent phosphorylation occurs on the stromal-exposed C-terminal part of CaS (CaS-C) had been shown before using recombinant protein variants (Stael et al., 2011). In order to elucidate, whether calcium-dependent phosphorylation occurs on any of the

described phosphorylation sites, these positions were mutagenized to a similar but non-phosphorylatable amino acid residue (Ser>Ala; Thr>Val). After generation of recombinant proteins devoid of any tags, *in vitro* phosphorylation assays were performed in presence of  $^{32}$ P-labelled ATP using catalytical amounts of Arabidopsis stromal extract (for details see section 3.2.3). First of all it should be pointed out that, as described before, a clear increase in CaS phosphorylation can be observed in the presence of calcium (Fig. 29, Wt). Minor phosphorylation observed in the absence of calcium is equivalent to the signal observed in stroma alone without recombinant substrate under either conditions indicating that under the chosen conditions phosphorylation is strictly calcium-dependent. Interestingly, the experiment showed that mutation of Thr<sub>380</sub> to Val<sub>380</sub>, did not alter the quantity of phosphorylation compared to the wild type CaS (Fig. 29, compare Wt and 380<sub>t/v</sub>). This clearly confirms that this phosphorylation site is not dependent on a calcium-dependent stromal kinase. In other words, calcium-dependent phosphorylation of CaS does not occur at Thr<sub>380</sub>.

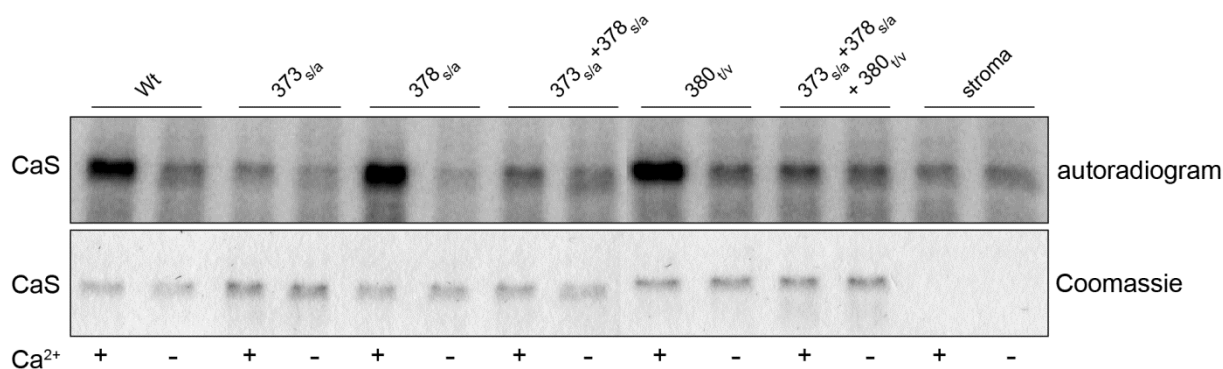


**Fig. 29 Ser<sub>373</sub> is the major calcium-dependent phosphorylation site of CaS**

*In vitro* kinase assays were performed with stromal extract using either wild type (Wt) or several mutagenized variants of CaS-C as substrate. Assays were performed in presence (+) or in absence of calcium (-) and as a control also without any addition of substrate (stroma). Reactions were resolved on SDS-PAGE and a Coomassie stain (lower panel) and the corresponding autoradiogram (upper panel) are shown.

In case of the two other previously described sites (Reiland et al., 2009), only the changing of Ser<sub>373</sub> to Ala resulted in a huge reduction in the phosphorylation in CaS-C (Fig. 29, compare Wt to 378<sub>s/a</sub> and 373<sub>s/a</sub>). This experiment was elaborated on by generating double (373<sub>s/a</sub> + 378<sub>s/a</sub>) and triple mutants (373<sub>s/a</sub> + 378<sub>s/a</sub> + 380<sub>t/v</sub>) followed by *in-vitro* kinase assay with the recombinant proteins (Fig. 29). In both the cases only a minor signal was detected which was

also detected in case of stroma alone (compare Fig. 29, stroma) and thus can be considered as background phosphorylation. Together, these results clearly show that among the described phosphorylation sites, only Ser<sub>373</sub> can be phosphorylated to a significant extent by stromal extract and exclusively in a calcium-dependent manner.

#### 4.13.2 Calcium dependency of CaS phosphorylation

In a next step, kinase assays were performed with varying concentration of calcium (Fig. 30). Since buffers are often contaminated with divalent cations, a total absence of calcium in the reaction was ensured by addition of the calcium chelator EGTA to the assay buffer. Indeed, the inclusion of EGTA removed most of the residual amounts of phosphorylation that could be observed in the sample without any additions (Fig. 30 compare (-) and EGTA). The minor phosphorylation observed in the EGTA control most likely result from the calcium-independent phosphorylation present in the stromal abstract (see Fig. 29, stroma).

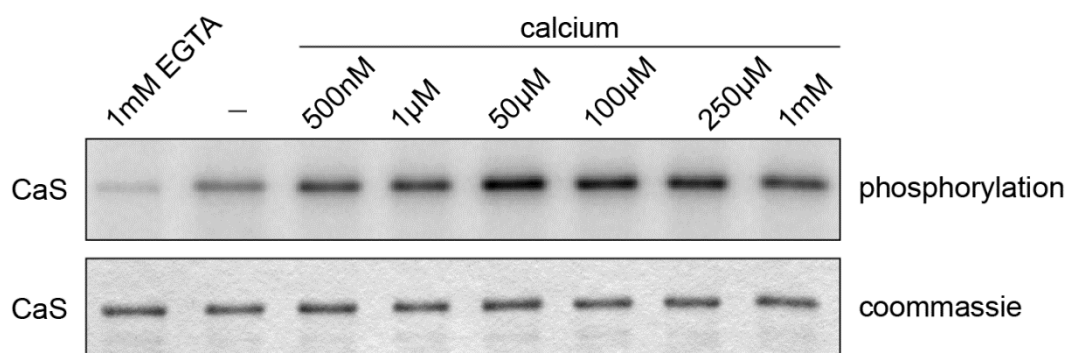


**Fig. 30 Calcium dependency of CaS-C phosphorylation**

In vitro kinase assays of recombinant wild type CaS-C using stromal extract either in absence of or in presence of calcium ranging in concentration from null (1 mM EGTA) to 1 mM. Reactions were resolved on SDS-PAGE and a Coomassie stain (lower panel) and the corresponding autoradiogram (upper panel) are shown.

The phosphorylation level steadily increased with increasing calcium concentration until saturation is reached at about 50  $\mu$ M (Fig. 30). The low concentration required for the activity of the kinase strongly supports the action of a true calcium-dependent kinase .

#### 4.14 Isolation of potential stromal calcium-dependent kinases

In a further step, it was attempted to identify the calcium-dependent kinase involved in the phosphorylation of CaS at Ser<sub>373</sub>. To that end, Arabidopsis stromal extracts were prepared as described in section 3.2.3 and used for column chromatographic purification.

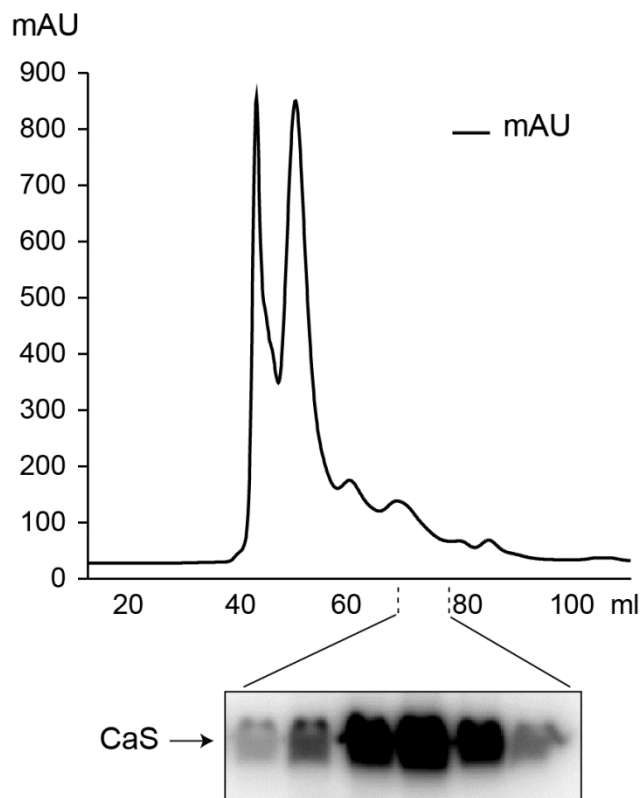


**Fig. 31 Size exclusion chromatography of Arabidopsis stromal extract**

Fractionation of Arabidopsis stromal extract on a Superdex200 HiLoad 16/600 size exclusion column. Absorbance at 280 nm is plotted on the Y-axis and elution volume (ml) on the X-axis. Fractions were tested for kinase activity using recombinant CaS in *in vitro* phosphorylation assays. The autoradiogram of the fractions between 69 – 77 ml showing highest levels of activity are shown below the graph.

Concentrated stromal extract was initially separated by size-exclusion chromatography using a prep grade Superdex200 HiLoad 16/600 column (Fig. 31; for details see section 3.2.12). Fractions of 1 ml were collected and aliquots of three successive fractions were combined to test for kinase activity with wild type CaS-C as substrate. Fractions with highest kinase activity were found between 69 - 77 ml (Fig. 31), which corresponds to the molecular mass of approximately 40 - 100 kDa. Active fractions from four successive runs were pooled and proteins were further fractionated on a Mono Q 5/50GL anion exchanger (Fig. 32; for details

see section 3.2.12). Fractions of 250  $\mu$ l were collected and again several fractions were pooled for initial kinase activity assays. In this case, two regions with high kinase activity were observed.

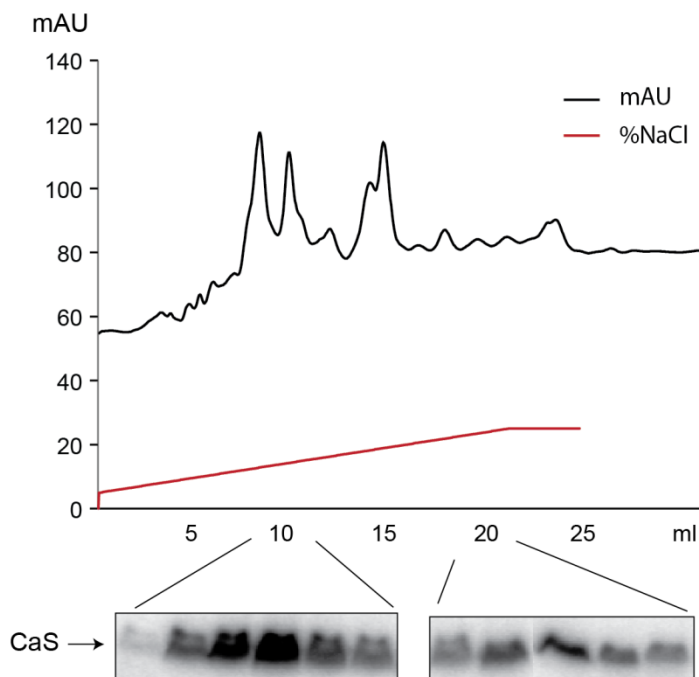


**Fig. 32 Anion-exchange chromatography of kinase-enriched fraction from SEC**

Active fractions from the Superdex200 chromatography were pooled and separated further on Mono Q 5/50 GL using a NaCl gradient of 5-25%. Absorbance at 280 nm is plotted on the Y-axis and elution volume (ml) on the X-axis. Fractions were tested for kinase activity using recombinant CaS as substrate. Fractions were tested for kinase activity using recombinant CaS in *in vitro* phosphorylation assays. The autoradiogram of the fractions 7.5 –12 ml and 18.25-22.25 ml showing highest levels of activity are shown below the graph.

Subsequently, fractions in the area of highest activity were analysed individually for enzymatic activity as well as separated on a SDS-PAGE followed by silver staining in order to identify unique protein bands enriched in the fractions with the highest kinase activity (Fig. 33). Protein bands marked with arrows were found to correspond well in their abundance to the observed kinase activity profile and were sequenced by LC-MS/MS at the Protein analysis Unit, Medical Faculty, LMU-Munich.

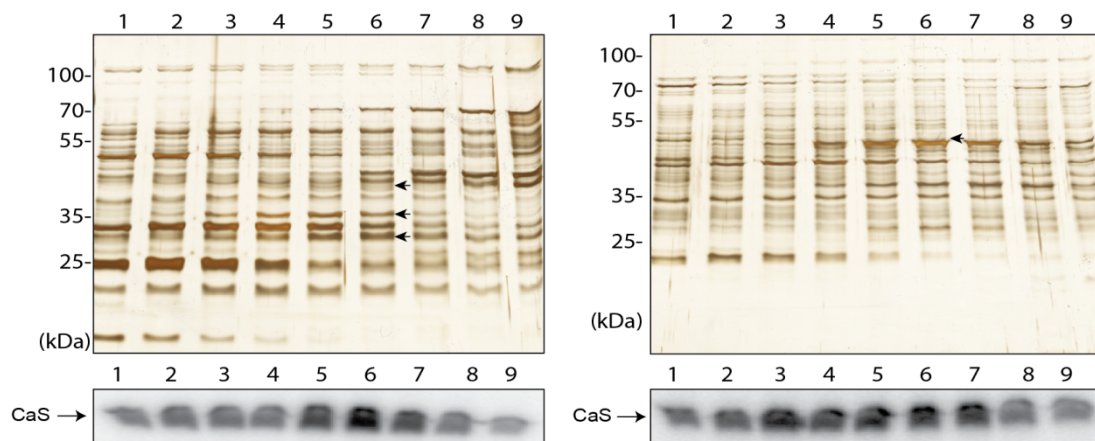


**Fig. 33 SDS-PAGE analysis of kinase enriched fractions from the Mono Q chromatography**

Fractions from the two active regions of the Mono Q chromatography (left, active peak I and right, active peak II) were resolved on SDS-PAGE followed by silver staining (A and B upper part). Individual fractions were analysed by kinase assay using CaS as substrate (A and B, lower part) and the corresponding autoradiograms between 9-11.25 ml (for peak I) and 19-21.25 ml (for peak II) are shown below the graph.

Mass spectrometric analysis of these protein bands revealed in total of five alleged kinases, namely Sucrose non-Fermenting-1 Related Kinase 2.2 (SNRK2.2), Leucine-rich repeat protein kinase like protein (LRRLK), Protein kinase family protein-1 (PKF-1), Thylakoid Associated Kinase 1 (TAK-1) and Protein kinase family protein-2 (PKF-2) (for details on the LC-MS/MS data see appendix III). Of these proteins, TAK-1, had been previously shown to be imported into chloroplast (Armbruster et al., 2009). For the other candidates, no experimental evidence for their localization exists.

#### 4.14.1 Analysis of subcellular localization of the identified kinases

After identification through LC-MS/MS, a self-assembly GFP (saGFP) system was used to confirm subcellular localization of the candidate kinases. In this system, one gene sequence is cloned N-terminally to the 1-10<sup>th</sup>  $\beta$ -sheets of GFP (saGFP1-10), while another gene sequence is cloned N-terminally to the missing part of the GFP, i.e. the 11<sup>th</sup>  $\beta$ -sheet (saGFP11). When a plant is co-transformed with both plasmids and the expressed fusion proteins are targeted into the same cellular compartment, the GFP can reassemble to a functional unit and fluorescence is visible. No direct protein-protein interaction is required (Sommer et al., 2011).



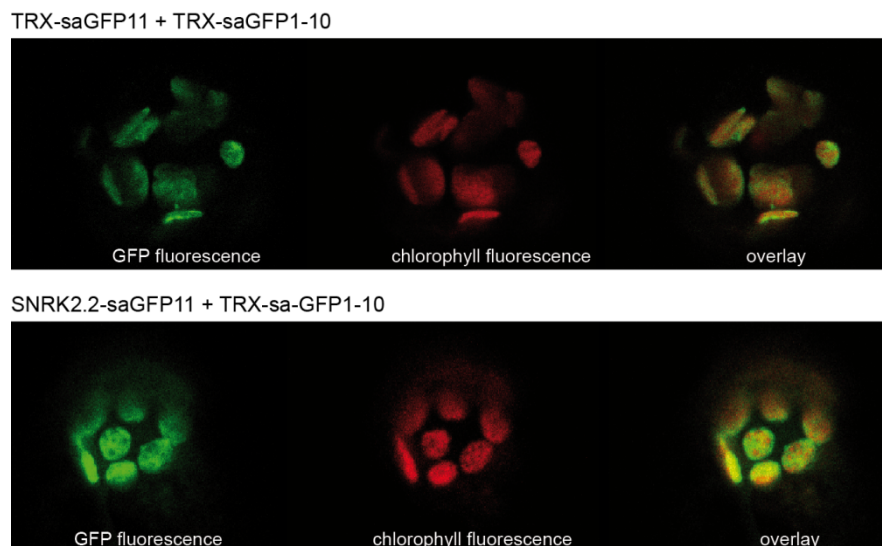


**Fig. 34 SNRK2.2 kinase is localized in chloroplasts**

Protoplasts isolated from tobacco leaves co-transformed with fusion proteins to the two parts of saGFP were visualised under confocal laser scanning microscope. Upper panel shows the co-transformation of the chloroplast marker protein nadph-dependent thioredoxin reductase c (TRX), whereas the lower panel shows the co-transformation of TRX and SNRK2.2 kinase. In both cases, a clear GFP signal is visible overlapping with the chlorophyll fluorescence.

The four candidates for which no localization had been previously established cloned N-terminally in frame with the smaller part of GFP (saGFP11) in a pBIN-saGFP system. As control protein, the chloroplast marker protein nadph-dependent thioredoxin reductase c (TRX) was fused N-terminally to both the larger part of GFP (saGFP1-10) as well as the 11<sup>th</sup>  $\beta$ -sheet in the same system. Tobacco mesophyll cells were co-transformed with various combinations of these constructs using *Agrobacterium* bacteria mediated transformation. Protoplasts were isolated from transformed leaf cells and GFP signals were visualised using laser confocal microscope. The control assay, comprising TRX-saGFP11 and TRX-saGFP1-10 showed a clear signal within the chloroplasts. From all candidates tested, only SNRK2.2 showed a clear chloroplastic localization (Fig. 34, while no chloroplast localization could be confirmed for the other three. Together with TAK, which had been previously shown to be imported into chloroplast (Armbruster et al., 2009) but was never shown to be involved in the calcium sensing, this leaves two potential candidates for a calcium-dependent kinase in chloroplasts. However, further studies, such as kinase assays with recombinant proteins are required for a definite identification.

## 5 Discussion

CaM acts as one of the principal calcium signalling mediators in the cell. Though multiple cases of cytosolic CaM-mediated signalling has been reported from higher organisms, its function in cellular organelles is not so well understood. Recently, a number of studies have been made to investigate the extension of the cellular calcium signalling network in organelles such as mitochondria and chloroplasts. These studies have identified a few mitochondria-localized CaM targets as well as a mitochondrial CaM-like protein (CML) (Bussemer et al., 2009; Chigri et al., 2012), which proves the presence of calcium signalling system in this organelle. Recent finding also provided evidences for a link between CaM and mitochondrial protein import (Kuhn et al., 2009; Aich et al., 2013). The present study was focused on the characterization of a novel mitochondrial CaM target TOM9, a component of the protein translocase complex of the outer membrane. Characterization was performed through biochemical analyses of the interaction between TOM9 and CaM and by analysis of the role of this interaction. Detailed analysis was carried out on loss-of-function mutant for TOM9 using transcriptomic and biochemical approaches and thereby elucidating the regulation of mitochondrial protein import machinery in plants.

### 5.1 The plant specific protein import system

Organelle protein import is a very important function that every higher organism has to perform. Genes of the original endosymbiont have been transferred to the nuclear genome in course of evolution. In order to maintain the organelle metabolic processes essential for cell viability it became thus necessary to import the required and now nuclear encoded proteins from the cytosol. In non-photosynthetic organisms, the situation is simpler since they only contain one type of double membrane bound organelles, the mitochondria. The scenario is more complicated with photosynthetic organisms, where chloroplasts also come into play. Plants had to develop a unique mitochondrial protein import system in order to distinguish between precursor proteins destined to mitochondria or chloroplasts. In addition to that, since plants are sessile organisms, they cannot escape from the day to day challenges of the harsh environment; instead they had to learn how to cope with these stressed conditions, e.g. by increased adaptability of cellular mechanisms, including the mitochondrial protein import system. The plant mitochondrial protein import machinery has several unique features, such

as structural and conformational alterations in composition as well as the lack and addition of some components (Duncan et al., 2013; Murcha et al., 2014). The yeast mitochondrial protein import apparatus is well studied, however, though several studies have been made on the plant translocase complexes, it is much less well understood. For example, a direct ortholog of yeast Tom20 is absent in plants; instead, a novel protein has been found in plants and named TOM20 that shows structural conservation to yeast Tom20 (Werhan et al., 2000). While the yeast Tom20 is N-terminally anchored into the outer mitochondrial membrane, the plant TOM20 is tail-anchored; even though, the two structures can be super-imposed and both were shown to function as primary receptor for incoming precursors (Rimmer et al., 2011). Furthermore, yeast Tom20 has been reported to be loosely associated with the TOM complex while in plants it has been shown to be an integral part of the complex. Another pre-sequence receptor from yeast, Tom70, is completely absent in plants. In this case, a novel protein called OM64 (mitochondrial outer membrane protein of 64 kDa) has been reported in plants, which is a direct homolog of chloroplast localised tetratricopeptide repeat protein TOC64-III (Chew et al., 2012) and is neither evolutionary nor structurally related to Tom70. Though it cannot bind to mitochondrial precursor proteins and has not been shown to associate with the TOM complex when studied on BN PAGE, its transient interaction with the TOM complex and acting as a secondary receptor under specific conditions cannot be ruled out (Lister et al., 2007; Murcha et al., 2014). By contrast, the principal pore forming complex Tom40 shows a high degree of conservation among all eukaryotes (Macasev et al., 2004) and has been described as essential for all organisms studied (Lister et al., 2004; Dekker et al., 1998). Though being present in two copies in *Arabidopsis*, only one isoform, TOM40.1, is predominant and the second isoform cannot complement TOM40.1 function.

The most prominent plant specific alteration observed for the TOM complex is the lack of Tom22, which in yeasts is believed to act as the principle precursor protein receptor (Hönliger et al., 1995; Bolliger et al., 1995; Mayer et al., 1995) while at the same time serving as the docking site for Tom20 and Tom70 (van Wilpe et al., 1999). In place of Tom22, a new protein called TOM9 has evolved through convergent evolution, which shows certain homology to yeast Tom22. It also contains a single transmembrane domain and the intermembrane space domain while not conserved on a sequence level can complement the corresponding domain of yeast Tom22 functionally (Macasev et al., 2004). By contrast, the N-terminal cytosolic domain is much shorter compared to Tom22 from non-plant organisms and lacks the acidic residue-rich domain. Those negatively charged residues of yeast Tom22 were believed to play an important role in presequence binding in yeast Tom22 (Kiebler et al.,

1993). Though later on it was shown that not the specific acidic residues, but the whole region is important for presequence recognition (Nargang et al., 1998). However, this truncation in the cytosolic domain causes TOM9 to lose its pre-sequence binding ability (Rimmer et al., 2011). Therefore, other functions for TOM9 have been discussed/suggested. Since plants contain chloroplasts in addition to mitochondria, it was presumed that this shortening of the cytosolic domain might be involved in the distinction between precursor proteins destined to mitochondria or chloroplasts (Murcia et al., 2014). However, no functional analysis of TOM9 had been presented so far.

## 5.2 Importance of TOM9 in the plant development

Generation and characterization of *TOM9.2* knock-down plants revealed that these plants are viable but if they experience then they flower earlier than wild type plants and show growth defects under sub-optimal growth conditions. Through DNA micro-array analysis, it was found that in line with the visible early flowering phenotype several genes related to flower development were indeed up-regulated (Wellmer et al., 2006; Irish, 2010). Confirmation of up-regulation of some candidates by qPCR analysis corroborated this finding. While 2.2 fold reduction was observed in case of *TOM9.2* in the affymetrix analysis, no transcriptional changes were observed in case of any other protein translocase component. Western blot analysis on purified mitochondria, however, revealed changes in the abundance of several mitochondrial proteins. Such lack of correlation between transcription and protein content was described previously for mitochondrial proteins (Lister et al., 2007, Law et al., 2012). This study also showed that lack of TOM9.2 proteins causes significant up-regulation of the OM64 protein, which is supposed to be another import receptor of plant mitochondria. This upregulation could be due to retrograde signalling under stressed condition as observed also in case of TOM20 knock-out plants (Lister et al., 2007). Micro-array analysis also showed an up-regulation of several stress-related genes (see appendix II) in the mutant plants which might be caused by mitochondrial dysfunction when mitochondrial protein import system is impaired.

Interestingly, shortening of hypocotyls as observed in the *TOM9.2* knock-down plants under sub-optimal light condition, was also observed in the TIM50 (Translocase of inner membrane mitochondria 50) knock-out plants. In yeasts, TIM50 is known to interact with the TOM9 homolog, Tom22, in the inter membrane space (Waegemann et al., 2014). Since the corresponding domain of TOM9 can complement the function of the Tom22 intermembrane

space domain function as found by yeast growth complementation assay (Macasev et al., 2004), a similar role of the TOM9 intermembrane space domain is anticipated, meaning that also TIM50 and TOM9 might interact. By contrast, a severe reduction in the TIM23 complex in the absence of a TOM component was never described before and thus this feature of the *TOM9.2* knock-down plants therefore validates a more detailed investigation in the future. A possible explanation could be that the TIM23 complex is stabilized through interaction with the TOM complex via TOM9 at the inter membrane space. The quantification of other protein import complexes such as SAM complex or TIM22 complex would be interesting but could not be performed in the present study due to lack of suitable antibodies.

Multiple sequence alignment of proteins from different non-plants as well as lower and higher plants revealed that several changes have been taken place in the domain structure of TOM9/Tom22 throughout evolution. Throughout all organisms analysed, the membrane spanning domain remains highly conserved (Fig. 10). In yeasts, this trans-membrane domain was shown to be essential for the TOM complex integrity (van Wilpe et al., 1999) and since it is highly conserved in all species studied, it can be presumed that it acts in a similar fashion in all organisms. The C-terminal part of the protein, i.e., the inter-membrane space domain, is functionally conserved at least between plants and yeast, as evidenced from a finding that a chimeric protein containing the cytosolic domain of yeast Tom22 and intermembrane space domain from Arabidopsis TOM9 could complement a *tom22.2* growth phenotype (Macasev et al., 2004). Besides being truncated in the plants compared to yeasts and mammals, the residual cytosolic domain is also not conserved among plants. The predicted CaMBD within the cytosolic domain is conserved only among dicots, but is interrupted among monocots and cannot be detected at all in the lower plants including green algae, mosses and ferns (Fig. 10). This might indicate a directed evolution of this protein in order to match the increasing adaptability to environmental stress in the higher land plants.

Like many the plant proteins, gene duplication has also occurred in case of TOM9 giving raise to two isoforms in Arabidopsis. In the present study CaM-binding could be confirmed for both the isoforms, TOM9.1 and TOM9.2 through *in vitro* cross-linking experiment, however, only TOM9.2 was identified in the eluate fraction of the affinity chromatography on CaM-agarose with purified mitochondria.

**Dataset:** 10 developmental stages (sample selection: AT-SAMPLES-3)  
2 genes (gene selection: AT-GENES-2)

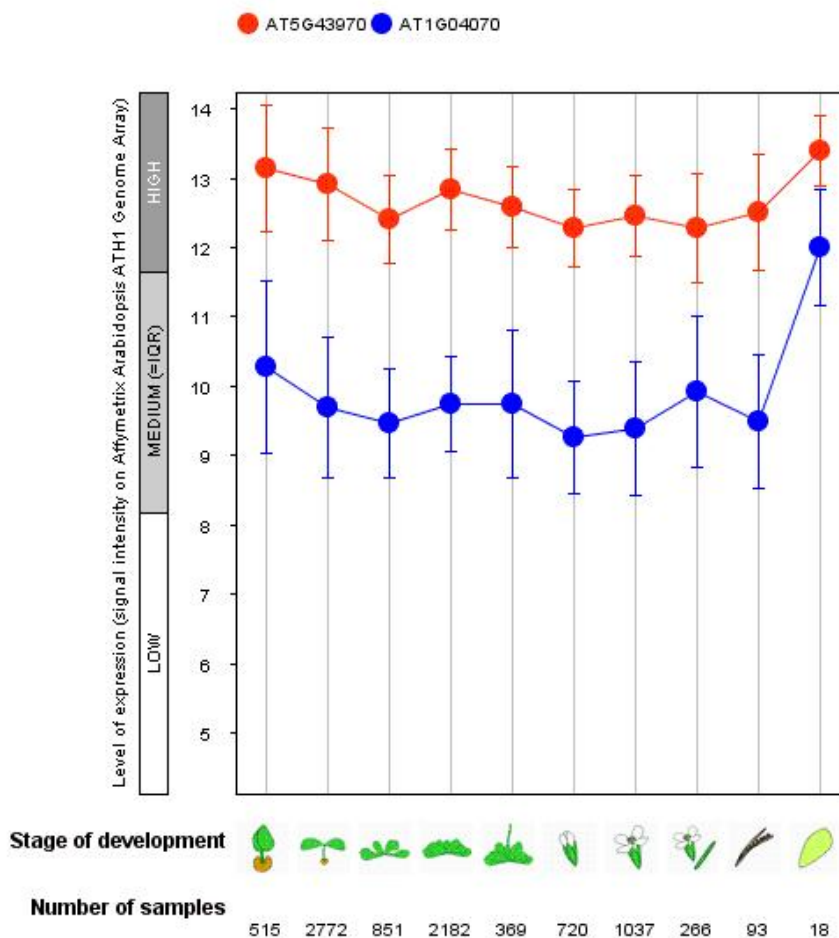


**Fig. 35 Gene expression profile of *TOM9.1* and *TOM9.2* from GENEVESTIGATOR**

Expression analysis of both *TOM9* isomers from *Arabidopsis thaliana* at different developmental stages using GENEVESTIGATOR program. A total of 10 stages are shown here. *TOM9.1* (At1g04070) is shown in blue, whereas the red data points indicate *TOM9.2* (At5g43970). Number of samples used in this analysis by the GENEVESTIGATOR is as indicated.

To know the expression pattern and levels of *TOM9.1* and *TOM9.2* genes, an analysis was performed using the GENEVESTIGATOR platform, which showed that while both the genes are expressed throughout the whole life cycle of *Arabidopsis*, the expression level of *TOM9.2* gene is significantly higher than of the *TOM9.1* gene (Fig. 35). This could explain why the mass-spectrometric analysis revealed only *TOM9.2*, while both the isoforms are CaM-interacting proteins.

## 5.2 Essentiality of TOM9 for the TOM complex organization

Mitochondrial proteins are mostly nuclear encoded and to enter into the mitochondria they all have to pass through the outer membrane localized translocase complex (TOM complex) also known as the general insertion pore (Alconada et al., 1995). Thus, the TOM complex can serve as the first regulatory check-point of mitochondrial protein import. Though it was long believed that the mitochondrial protein import mechanism is constitutive and does not need any regulation, recent studies have revealed that cellular metabolism, signalling, stress and pathogenesis of diseases are all connected to protein import and thereby affecting this process at multiple levels (Harbauer et al., 2014). An in-depth analysis of the viable *TOM9.2* knock-down plants revealed that these plants contain mitochondria largely lack the 400 kDa TOM complex, which indicates i) that TOM9.2 might have an essential function assembling the TOM complex and ii) unassembled TOM40 might be sufficient for proteins import under unrestricted conditions. While in yeast the absence of Tom22 causes dissociating of the 400 kDa TOM complex into a smaller 100 kDa complex containing only TOM40 and the small TOM proteins (van Wilpe et al., 1999), no smaller sized TOM complex can be detected in plants lacking TOM9.2. The presence of residual TOM complex could be due to the presence of the second isoform TOM9.1 in the *TOM9.2* knock-down plants, which could not be detected in the present study due to lack of an antibody (Fig. 17), but was found unchanged at transcript level by the affymetrix analysis (Table 1). However it is quite obvious that the phenotypic effects due to lack of TOM9.2 cannot be compensated by TOM9.1. The total amount of TOM40 proteins was found not to be changed significantly as was also observed in the TOM22 mutant in yeasts. Also, when studied *in vitro*, mitochondria from these mutants were able to import mitochondrial proteins. The surprising fact that in the absence of assembled TOM complex the ability to translocate proteins was not diminished could indicate that either un-assembled TOM40 channels are enough to import proteins under normal condition or an alternative means of protein translocation mechanism exists in plants. This fact can be correlated with the elevation in protein content of an alternative pre-sequence receptor OM64 (mitochondrial outer membrane protein of 64 kDa size) in the mutant mitochondria, which was also found elevated in the absence of the principal plant mitochondrial import receptor TOM20 (Lister et al., 2007). However, it cannot be excluded that this is an indirect effect of the reduction of TOM20 protein in the *TOM9.2* knock-down plants. The huge reduction in the amount of TOM20 proteins in the knock-down plants could also suggest that membrane insertion or stability of this principal receptor is directly dependent on TOM9.2. This correlates also well to former studies in yeasts showing that

---

Tom22 knock-out mutant were having a lower TOM20 protein content (van Wilpe et al., 1999). Since there was no change in *TOM20* transcript level, this reduction at the protein level might be related to stability of the protein or other post-translational events, however, the exact reason for this is yet to be investigated.

### **5.3 TOM9 as a CaM-binding protein**

TOM9.2 has been found during the screening for new mitochondrial CaM targets carried out in the present study and CaM binding could be confirmed by through in vitro cross-linking assay and pull down assays on CaM-agarose using purified mitochondria as well as recombinant TOM9.2 protein. In all cases the interaction was shown to be calcium dependent. Calcium is a very well known secondary messenger in eukaryotic cells which has been reported to be involved in a wide range of stress responses covering both abiotic and biotic stresses. Being one of the principal mediator of calcium signalling, CaM is directly involved in this system. Binding of TOM9 to CaM might therefore be a kind of stress-regulatory mechanism that plants acquired in the course of evolution to integrate the mitochondria into the cellular stress response system. Detailed analysis on recombinant TOM9.2 protein has revealed the presence of the CaM binding domain (CaMBD) of TOM9.2 on its cytosolic domain close to the start of the transmembrane domain. Cross-link assay using TOM9.2 lacking the predicted CaMBD showed huge reduction at the cross-link product corroborating this domain is the CaMBD. This finding could be confirmed by in vitro cross-linking assay with CaM using synthetic peptide consisting the predicted CaM binding sequence of TOM9.2 and not only that, this CaMBD peptide is shown to compete out the TOM9.2/CaM cross-link product. CaM binding to the cytosolic part of the protein indicates that the CaM-regulation of TOM9.2 takes place through a cytosolic CaM, depending on the cytosolic calcium state. Several CaM as well as CMLs are found in the cytosol of the cell allowing for a wide degree of differential regulation. However, it remains to be elucidated which of the many CaMs and CMLs interacts with TOM9.2. As observed from the alignment study, this cytosol localized CaMBD is highly conserved in the TOM9 ortholog and paralogs from dicotyledonous plants. This observation suggests that similar kind of regulation through CaM occurs at the cytosol in case of higher plants and indicates



#### 5.4 CaM regulation of mitochondrial protein import

A link between mitochondrial protein translocation and CaM has been reported may it be in lower eukaryotes or in plants. Previous results have shown that the addition of specific CaM inhibitor or depletion of calcium inhibits protein import into mitochondria in vitro (Kuhn et al., 2009). This results would implicate that CaM acts as a positive regulator of the process. This regulation was suggested to take place at the TIM complex and therefore either at the intermembrane space or in the matrix. Another study on *Leishmania* showed that import of a mitochondrial CaM binding protein is blocked when its CaM binding domain (CaMBD) was removed, which proposed a cytosolic interaction and again suggested a positive regulation by CaM (Aich and Saha, 2013). However, CaM binding to TOM9.2 on the cytosolic site and the negative affect of CaM on TOM9.2 membrane insertion would imply a role of CaM as negative regulator of the import process mediated from the cytosolic site. The contrasting nature of CaM regulation for mitochondrial protein translocation depending on target as well as sub-cellular location of the interaction is not unexpected, since the calcium dynamics of the cytosol varies from that of mitochondria (Logan and Knight, 2003). Also, different stimuli could require different affects on mitochondrial functions adns as already stated above, a large number of different CaM are present in the cytosol and at least one in the mitochondria that could be part of such a differential regulation system.

However, the situation is even more complex. It was shown in previous studies for TOM9.1 and Tom22 that they interact with another component of the TOM complex, TOM20, which in plants is believed to act as the principal receptor of the TOM complex (Rimmer et al., 2011). In the current study, an interaction between TOM9.2 and TOM20 could be confirmed by co-immunoprecipitation as well as by thermophoresis experiments. The affinity of this interaction could also be quantified through thermophoresis measurements. Through cross-linking and thermophoresis assays it could further be shown that CaM interferes with this interaction. A closer look at the binding sites of CaM and TOM20 to TOM9 revealed that these two binding sites overlap with each other, meaning that the interference of CaM in TOM9/TOM20 interaction might result from a potential competition between CaM and TOM20 for at the same site. Again, this might be an adaptive function in higher plants acquired through evolution to cope with stressed condition since the CaMBD on TOM9 is conserved only in higher plants. This result has to be considered in light of the intersting finding that a import of TOM9 import into purified *Arabidopsis* mitochondria is reduced when the CaMBD is missing. In vitro protein import also showed a reduction of TOM9 import when exogenous CaM is present in the reaction. A simple explanation is that the

CaMBD domain, the TOM20 domain and the specific domain of TOM9 close to its membrane spanning domain that is responsible to target TOM9 into mitochondria all overlap. When this domain is occupied by CaM, the import of TOM9 is inhibited, because TOM cannot longer bind and TOM9 and TOM20 need to interact with each other in order to get imported into the mitochondria. Thus, blocking this interaction by CaM impairs their import. However, this is unlike to be coincidental. It rather indicates that the CaM binding domain is not simply crucial for targeting TOM9 into mitochondria but that this interplay between CaM, TOM9 and TOM20 is a means to negatively regulated TOM complex assembly depending on the presence of both calcium and a specific CaM. This would allow for differential regulation stimuli, developmental as well as tissue dependent if the corresponding CaM is not expressed ubiquitously. Therefore, it would be highly interesting to study mitochondrial insertion of TOM9 in mitochondria isolated from different tissues and various developmental stages under different stress conditions to know under which circumstances mitochondrial targeting of TOM9 is inhibited!

## 6. References

- Abe, Y., Shodai, T., Muto, T., Mihara, K., Torii, H., Nishikawa, S., Endo, T., and Kohda, D. (2000). Structural basis of presequence recognition by the mitochondrial protein import receptor Tom20. *Cell* *100*, 551-560.
- Aich, A., and Shaha, C. (2013). Novel role of calmodulin in regulating protein transport to mitochondria in a unicellular eukaryote. *Mol Cell Biol* *33*, 4579-4593.
- Alconada, A., Gartner, F., Honlinger, A., Kubrich, M., and Pfanner, N. (1995). Mitochondrial receptor complex from *Neurospora crassa* and *Saccharomyces cerevisiae*. *Methods in enzymology* *260*, 263-286.
- Alonso, J.M., Stepanova, A.N., Leisse, T.J., Kim, C.J., Chen, H., Shinn, P., Stevenson, D.K., Zimmerman, J., Barajas, P., Cheuk, R., *et al.* (2003). Genome-wide insertional mutagenesis of *Arabidopsis thaliana*. *Science* *301*, 653-657.
- Arazi, T., Baum, G., Snedden, W.A., Shelp, B.J., and Fromm, H. (1995). Molecular and biochemical analysis of calmodulin interactions with the calmodulin-binding domain of plant glutamate decarboxylase. *Plant Physiol* *108*, 551-561.
- Armbruster, U., Hertle, A., Makarenko, E., Zuhlke, J., Pribil, M., Dietzmann, A., Schliebner, I., Aseeva, E., Fenino, E., Scharfenberg, M., *et al.* (2009). Chloroplast proteins without cleavable transit peptides: rare exceptions or a major constituent of the chloroplast proteome? *Molecular plant* *2*, 1325-1335.
- Arnon, D.I. (1949). COPPER ENZYMES IN ISOLATED CHLOROPLASTS. POLYPHENOLOXIDASE IN BETA VULGARIS. *Plant Physiology* *24*, 1-15.
- Baker, K.P., Schaniel, A., Vestweber, D., and Schatz, G. (1990). A yeast mitochondrial outer membrane protein essential for protein import and cell viability. *Nature* *348*, 605-609.
- Benjamini, Y., and Hochberg, Y. (1995). Controlling the False Discovery Rate: A Practical and Powerful Approach to Multiple Testing. *Journal of the Royal Statistical Society Series B (Methodological)* *57*, 289-300.
- Bevan, M. (1984). Binary *Agrobacterium* vectors for plant transformation. *Nucleic Acids Res* *12*, 8711-8721.

- Blum, H., Beier, H., and Gross, H.J. (1987). Improved silver staining of plant proteins, RNA and DNA in polyacrylamide gels. *ELECTROPHORESIS* 8, 93-99.
- Bolliger, L., Junne, T., Schatz, G., and Lithgow, T. (1995). Acidic receptor domains on both sides of the outer membrane mediate translocation of precursor proteins into yeast mitochondria. *EMBO J* 14, 6318-6326.
- Boyes, D.C., Zayed, A.M., Ascenzi, R., McCaskill, A.J., Hoffman, N.E., Davis, K.R., and Gorlach, J. (2001). Growth stage-based phenotypic analysis of Arabidopsis: a model for high throughput functional genomics in plants. *The Plant cell* 13, 1499-1510.
- Brix, J., Dietmeier, K., and Pfanner, N. (1997). Differential recognition of preproteins by the purified cytosolic domains of the mitochondrial import receptors Tom20, Tom22, and Tom70. *J Biol Chem* 272, 20730-20735.
- Bussemer, J., Chigri, F., and Vothknecht, U.C. (2009). Arabidopsis ATPase family gene 1-like protein 1 is a calmodulin-binding AAA+-ATPase with a dual localization in chloroplasts and mitochondria. *The FEBS journal* 276, 3870-3880.
- Chacinska, A., Koehler, C.M., Milenkovic, D., Lithgow, T., and Pfanner, N. (2009). Importing mitochondrial proteins: machineries and mechanisms. *Cell* 138, 628-644.
- Chew, O., Lister, R., Qbadou, S., Heazlewood, J.L., Soll, J., Schleiff, E., Millar, A.H., and Whelan, J. (2004). A plant outer mitochondrial membrane protein with high amino acid sequence identity to a chloroplast protein import receptor. *FEBS Lett* 557, 109-114.
- Chigri, F., Flosdorff, S., Pilz, S., Kolle, E., Dolze, E., Gietl, C., and Vothknecht, U.C. (2012). The Arabidopsis calmodulin-like proteins AtCML30 and AtCML3 are targeted to mitochondria and peroxisomes, respectively. *Plant Mol Biol* 78, 211-222.
- Clough, S.J., and Bent, A.F. (1998). Floral dip: a simplified method for Agrobacterium-mediated transformation of Arabidopsis thaliana. *The Plant journal : for cell and molecular biology* 16, 735-743.
- Craft, J., Samalova, M., Baroux, C., Townley, H., Martinez, A., Jepson, I., Tsiantis, M., and Moore, I. (2005). New pOp/LhG4 vectors for stringent glucocorticoid-dependent transgene expression in Arabidopsis. *The Plant Journal* 41, 899-918.

- Dekker, P.J., Ryan, M.T., Brix, J., Muller, H., Honlinger, A., and Pfanner, N. (1998). Preprotein translocase of the outer mitochondrial membrane: molecular dissection and assembly of the general import pore complex. *Mol Cell Biol* 18, 6515-6524.
- Dietmeier, K., Honlinger, A., Bomer, U., Dekker, P.J., Eckerskorn, C., Lottspeich, F., Kubrich, M., and Pfanner, N. (1997). Tom5 functionally links mitochondrial preprotein receptors to the general import pore. *Nature* 388, 195-200.
- Dudek, J., Rehling, P., and van der Laan, M. (2013). Mitochondrial protein import: common principles and physiological networks. *Biochimica et biophysica acta* 1833, 274-285.
- Duncan, O., Murcha, M.W., and Whelan, J. (2013). Unique components of the plant mitochondrial protein import apparatus. *Biochimica et biophysica acta* 1833, 304-313.
- Duy, D., Stube, R., Wanner, G., and Philippar, K. (2011). The chloroplast permease PIC1 regulates plant growth and development by directing homeostasis and transport of iron. *Plant Physiol* 155, 1709-1722.
- Eckers, E., Cyrklaff, M., Simpson, L., and Deponte, M. (2012). Mitochondrial protein import pathways are functionally conserved among eukaryotes despite compositional diversity of the import machineries. *Biol Chem* 393, 513-524.
- Ferrandiz, C., Gu, Q., Martienssen, R., and Yanofsky, M.F. (2000). Redundant regulation of meristem identity and plant architecture by FRUITFULL, APETALA1 and CAULIFLOWER. *Development* 127, 725-734.
- Gerbeth, C., Schmidt, O., Rao, S., Harbauer, A.B., Mikropoulou, D., Opalinska, M., Guiard, B., Pfanner, N., and Meisinger, C. (2013). Glucose-induced regulation of protein import receptor Tom22 by cytosolic and mitochondria-bound kinases. *Cell metabolism* 18, 578-587.
- Han, S., Tang, R., Anderson, L.K., Woerner, T.E., and Pei, Z.M. (2003). A cell surface receptor mediates extracellular Ca(2+) sensing in guard cells. *Nature* 425, 196-200.
- Harbauer, A.B., Zahedi, R.P., Sickmann, A., Pfanner, N., and Meisinger, C. (2014). The protein import machinery of mitochondria-a regulatory hub in metabolism, stress, and disease. *Cell metabolism* 19, 357-372.

- Harrison, S.J., Mott, E.K., Parsley, K., Aspinall, S., Gray, J.C., and Cottage, A. (2006). A rapid and robust method of identifying transformed *Arabidopsis thaliana* seedlings following floral dip transformation. *Plant methods* 2, 19.
- Heins, L., and Schmitz, U.K. (1996). A receptor for protein import into potato mitochondria. *The Plant journal : for cell and molecular biology* 9, 829-839.
- Honlinger, A., Kubrich, M., Moczko, M., Gartner, F., Mallet, L., Bussereau, F., Eckerskorn, C., Lottspeich, F., Dietmeier, K., Jacquet, M., *et al.* (1995). The mitochondrial receptor complex: Mom22 is essential for cell viability and directly interacts with preproteins. *Mol Cell Biol* 15, 3382-3389.
- Inoue, H., Nojima, H., and Okayama, H. (1990). High efficiency transformation of *Escherichia coli* with plasmids. *Gene* 96, 23-28.
- Irish, V.F. (2010). The flowering of *Arabidopsis* flower development. *The Plant journal : for cell and molecular biology* 61, 1014-1028.
- Irizarry, R.A., Hobbs, B., Collin, F., Beazer-Barclay, Y.D., Antonellis, K.J., Scherf, U., and Speed, T.P. (2003). Exploration, normalization, and summaries of high density oligonucleotide array probe level data. *Biostatistics (Oxford, England)* 4, 249-264.
- Jansch, L., Kruff, V., Schmitz, U.K., and Braun, H.P. (1998). Unique composition of the preprotein translocase of the outer mitochondrial membrane from plants. *J Biol Chem* 273, 17251-17257.
- Kiebler, M., Keil, P., Schneider, H., van der Klei, I.J., Pfanner, N., and Neupert, W. (1993). The mitochondrial receptor complex: a central role of MOM22 in mediating preprotein transfer from receptors to the general insertion pore. *Cell* 74, 483-492.
- Koop, H.U., Steinmuller, K., Wagner, H., Rossler, C., Eibl, C., and Sacher, L. (1996). Integration of foreign sequences into the tobacco plastome via polyethylene glycol-mediated protoplast transformation. *Planta* 199, 193-201.
- Krizek, B.A., and Meyerowitz, E.M. (1996). The *Arabidopsis* homeotic genes APETALA3 and PISTILLATA are sufficient to provide the B class organ identity function. *Development* 122, 11-22.

- Kuhn, S., Bussemer, J., Chigri, F., and Vothknecht, U.C. (2009). Calcium depletion and calmodulin inhibition affect the import of nuclear-encoded proteins into plant mitochondria. *The Plant journal : for cell and molecular biology* 58, 694-705.
- Kyhse-Andersen, J. (1984). Electroblothing of multiple gels: a simple apparatus without buffer tank for rapid transfer of proteins from polyacrylamide to nitrocellulose. *Journal of biochemical and biophysical methods* 10, 203-209.
- Laemmli, U.K. (1970). Cleavage of structural proteins during the assembly of the head of bacteriophage T4. *Nature* 227, 680-685.
- Lamb, J.R., Tugendreich, S., and Hieter, P. (1995). Tetratricopeptide repeat interactions: to TPR or not to TPR? *Trends in Biochemical Sciences* 20, 257-259.
- Law, S.R., Narsai, R., Taylor, N.L., Delannoy, E., Carrie, C., Giraud, E., Millar, A.H., Small, I., and Whelan, J. (2012). Nucleotide and RNA metabolism prime translational initiation in the earliest events of mitochondrial biogenesis during Arabidopsis germination. *Plant Physiol* 158, 1610-1627.
- Lister, R., Chew, O., Lee, M.N., Heazlewood, J.L., Clifton, R., Parker, K.L., Millar, A.H., and Whelan, J. (2004). A transcriptomic and proteomic characterization of the Arabidopsis mitochondrial protein import apparatus and its response to mitochondrial dysfunction. *Plant Physiol* 134, 777-789.
- Lithgow, T., Junne, T., Suda, K., Gratzler, S., and Schatz, G. (1994). The mitochondrial outer membrane protein Mas22p is essential for protein import and viability of yeast. *Proceedings of the National Academy of Sciences of the United States of America* 91, 11973-11977.
- Liu, Z., Li, X., Zhao, P., Gui, J., Zheng, W., and Zhang, Y. (2011). Tracing the evolution of the mitochondrial protein import machinery. *Computational biology and chemistry* 35, 336-340.
- Logan, D.C., and Knight, M.R. (2003). Mitochondrial and cytosolic calcium dynamics are differentially regulated in plants. *Plant Physiol* 133, 21-24.
- Lohse, M., Nunes-Nesi, A., Kruger, P., Nagel, A., Hannemann, J., Giorgi, F.M., Childs, L., Osorio, S., Walther, D., Selbig, J., *et al.* (2010). Robin: an intuitive wizard application for R-based expression microarray quality assessment and analysis. *Plant Physiol* 153, 642-651.

- Macasev, D., Newbigin, E., Whelan, J., and Lithgow, T. (2000). How do plant mitochondria avoid importing chloroplast proteins? Components of the import apparatus Tom20 and Tom22 from Arabidopsis differ from their fungal counterparts. *Plant Physiol* 123, 811-816.
- Macasev, D., Whelan, J., Newbigin, E., Silva-Filho, M.C., Mulhern, T.D., and Lithgow, T. (2004). Tom22', an 8-kDa trans-site receptor in plants and protozoans, is a conserved feature of the TOM complex that appeared early in the evolution of eukaryotes. *Mol Biol Evol* 21, 1557-1564.
- Mayer, A., Nargang, F.E., Neupert, W., and Lill, R. (1995). MOM22 is a receptor for mitochondrial targeting sequences and cooperates with MOM19. *EMBO J* 14, 4204-4211.
- Milenkovic, D., Muller, J., Stojanovski, D., Pfanner, N., and Chacinska, A. (2007). Diverse mechanisms and machineries for import of mitochondrial proteins. *Biol Chem* 388, 891-897.
- Millar, A.H., Liddell, A., and Leaver, C.J. (2007). Isolation and subfractionation of mitochondria from plants. *Methods in cell biology* 80, 65-90.
- Moczko, M., Bomer, U., Kubrich, M., Zufall, N., Honlinger, A., and Pfanner, N. (1997). The intermembrane space domain of mitochondrial Tom22 functions as a trans binding site for preproteins with N-terminal targeting sequences. *Mol Cell Biol* 17, 6574-6584.
- Moczko, M., Ehmann, B., Gartner, F., Honlinger, A., Schafer, E., and Pfanner, N. (1994). Deletion of the receptor MOM19 strongly impairs import of cleavable preproteins into *Saccharomyces cerevisiae* mitochondria. *J Biol Chem* 269, 9045-9051.
- Murcha, M.W., Kmiec, B., Kubiszewski-Jakubiak, S., Teixeira, P.F., Glaser, E., and Whelan, J. (2014a). Protein import into plant mitochondria: signals, machinery, processing, and regulation. *J Exp Bot* 65, 6301-6335.
- Murcha, M.W., Wang, Y., Narsai, R., and Whelan, J. (2014b). The plant mitochondrial protein import apparatus - the differences make it interesting. *Biochimica et biophysica acta* 1840, 1233-1245.
- Nakamura, Y., Suzuki, H., Sakaguchi, M., and Mihara, K. (2004). Targeting and assembly of rat mitochondrial translocase of outer membrane 22 (TOM22) into the TOM complex. *J Biol Chem* 279, 21223-21232.



- O'Neil, K.T., and DeGrado, W.F. How calmodulin binds its targets: sequence independent recognition of amphiphilic  $\alpha$ -helices. *Trends in Biochemical Sciences* *15*, 59-64.
- Perry, A.J., Hulett, J.M., Likic, V.A., Lithgow, T., and Gooley, P.R. (2006). Convergent evolution of receptors for protein import into mitochondria. *Current biology : CB* *16*, 221-229.
- Perry, A.J., Hulett, J.M., Lithgow, T., and Gooley, P.R. (2005). <sup>1</sup>H, <sup>13</sup>C and <sup>15</sup>N resonance assignments of the cytosolic domain of Tom20 from *Arabidopsis thaliana*. *J Biomol NMR* *33*, 198.
- Perry, A.J., Rimmer, K.A., Mertens, H.D., Waller, R.F., Mulhern, T.D., Lithgow, T., and Gooley, P.R. (2008). Structure, topology and function of the translocase of the outer membrane of mitochondria. *Plant physiology and biochemistry : PPB / Societe francaise de physiologie vegetale* *46*, 265-274.
- Ramage, L., Junne, T., Hahne, K., Lithgow, T., and Schatz, G. (1993). Functional cooperation of mitochondrial protein import receptors in yeast. *The EMBO Journal* *12*, 4115-4123.
- Reiland, S., Messerli, G., Baerenfaller, K., Gerrits, B., Endler, A., Grossmann, J., Gruissem, W., and Baginsky, S. (2009). Large-scale *Arabidopsis* phosphoproteome profiling reveals novel chloroplast kinase substrates and phosphorylation networks. *Plant Physiol* *150*, 889-903.
- Rhoads, A.R., and Friedberg, F. (1997). Sequence motifs for calmodulin recognition. *FASEB journal : official publication of the Federation of American Societies for Experimental Biology* *11*, 331-340.
- Rimmer, K.A., Foo, J.H., Ng, A., Petrie, E.J., Shilling, P.J., Perry, A.J., Mertens, H.D., Lithgow, T., Mulhern, T.D., and Gooley, P.R. (2011). Recognition of mitochondrial targeting sequences by the import receptors Tom20 and Tom22. *J Mol Biol* *405*, 804-818.
- Rodriguez-Cousino, N., Nargang, F.E., Baardman, R., Neupert, W., Lill, R., and Court, D.A. (1998). An import signal in the cytosolic domain of the *Neurospora* mitochondrial outer membrane protein TOM22. *J Biol Chem* *273*, 11527-11532.
- Sabar, M., Balk, J., and Leaver, C.J. (2005). Histochemical staining and quantification of plant mitochondrial respiratory chain complexes using blue-native polyacrylamide gel electrophoresis. *The Plant journal : for cell and molecular biology* *44*, 893-901.

---

Saitoh, T., Igura, M., Obita, T., Ose, T., Kojima, R., Maenaka, K., Endo, T., and Kohda, D. (2007). Tom20 recognizes mitochondrial presequences through dynamic equilibrium among multiple bound states. *EMBO J* 26, 4777-4787.

Samach, A., Onouchi, H., Gold, S.E., Ditta, G.S., Schwarz-Sommer, Z., Yanofsky, M.F., and Coupland, G. (2000). Distinct roles of CONSTANS target genes in reproductive development of Arabidopsis. *Science* 288, 1613-1616.

Sandra van Wilpe, M.T.R., Kerstin Hill, Ammy C. Maarse,, Chris Meisinger, J.B., Peter J. T. Dekker, Martin Moczko,, Richard Wagner, M.M., Bernard Guiard,, and Pfanner, A.H.N. (1999). Tom22 is a multifunctional organizer of the mitochondrial preprotein translocase. *Letters to Nature*.

Schagger, H., and von Jagow, G. (1991). Blue native electrophoresis for isolation of membrane protein complexes in enzymatically active form. *Anal Biochem* 199, 223-231.

Schweiger, R., Soll, J., Jung, K., Heermann, R., and Schwenkert, S. (2013). Quantification of interaction strengths between chaperones and tetratricopeptide repeat domain-containing membrane proteins. *J Biol Chem* 288, 30614-30625.

Seigneurin-Berny, D., Salvi, D., Joyard, J., and Rolland, N. (2008). Purification of intact chloroplasts from Arabidopsis and spinach leaves by isopycnic centrifugation. *Current protocols in cell biology / editorial board, Juan S Bonifacino [et al] Chapter 3, Unit 3 30*.

Shannon, S., and Meeks-Wagner, D.R. (1991). A Mutation in the Arabidopsis TFL1 Gene Affects Inflorescence Meristem Development. *The Plant cell* 3, 877-892.

Shiota, T., Mabuchi, H., Tanaka-Yamano, S., Yamano, K., and Endo, T. (2011). In vivo protein-interaction mapping of a mitochondrial translocator protein Tom22 at work. *Proceedings of the National Academy of Sciences of the United States of America* 108, 15179-15183.

Slater, E.C., and Cleland, K.W. (1953). The calcium content of isolated heart-muscle sarcosomes. *The Biochemical journal* 54, xxii.

Smyth, G.K. (2004). Linear models and empirical bayes methods for assessing differential expression in microarray experiments. *Statistical applications in genetics and molecular biology* 3, Article3.

- Sommer, M.S., Daum, B., Gross, L.E., Weis, B.L., Mirus, O., Abram, L., Maier, U.G., Kuhlbrandt, W., and Schleiff, E. (2011). Chloroplast Omp85 proteins change orientation during evolution. *Proceedings of the National Academy of Sciences of the United States of America* *108*, 13841-13846.
- Stael, S., Rocha, A.G., Wimberger, T., Anrather, D., Vothknecht, U.C., and Teige, M. (2012). Cross-talk between calcium signalling and protein phosphorylation at the thylakoid. *J Exp Bot* *63*, 1725-1733.
- Suarez-Lopez, P., Wheatley, K., Robson, F., Onouchi, H., Valverde, F., and Coupland, G. (2001). CONSTANS mediates between the circadian clock and the control of flowering in *Arabidopsis*. *Nature* *410*, 1116-1120.
- Teper-Bamnolker, P., and Samach, A. (2005). The flowering integrator FT regulates SEPALLATA3 and FRUITFULL accumulation in *Arabidopsis* leaves. *The Plant cell* *17*, 2661-2675.
- Thompson, J.D., Gibson, T.J., Plewniak, F., Jeanmougin, F., and Higgins, D.G. (1997). The CLUSTAL\_X windows interface: flexible strategies for multiple sequence alignment aided by quality analysis tools. *Nucleic Acids Res* *25*, 4876-4882.
- Turck, F., Fornara, F., and Coupland, G. (2008). Regulation and identity of florigen: FLOWERING LOCUS T moves center stage. *Annual review of plant biology* *59*, 573-594.
- Vainonen, J.P., Sakuragi, Y., Stael, S., Tikkanen, M., Allahverdiyeva, Y., Paakkanen, V., Aro, E., Suorsa, M., Scheller, H.V., Vener, A.V., *et al.* (2008). Light regulation of CaS, a novel phosphoprotein in the thylakoid membrane of *Arabidopsis thaliana*. *The FEBS journal* *275*, 1767-1777.
- Valverde, F., Mouradov, A., Soppe, W., Ravenscroft, D., Samach, A., and Coupland, G. (2004). Photoreceptor regulation of CONSTANS protein in photoperiodic flowering. *Science* *303*, 1003-1006.
- Van Larebeke, N., Engler, G., Holsters, M., Van den Elsacker, S., Zaenen, I., Schilperoort, R.A., and Schell, J. (1974). Large plasmid in *Agrobacterium tumefaciens* essential for crown gall-inducing ability. *Nature* *252*, 169-170.

- van Wilpe, S., Ryan, M.T., Hill, K., Maarse, A.C., Meisinger, C., Brix, J., Dekker, P.J., Moczko, M., Wagner, R., Meijer, M., *et al.* (1999). Tom22 is a multifunctional organizer of the mitochondrial preprotein translocase. *Nature* *401*, 485-489.
- Waegemann, K., Popov-Celeketic, D., Neupert, W., Azem, A., and Mokranjac, D. (2015). Cooperation of TOM and TIM23 complexes during translocation of proteins into mitochondria. *J Mol Biol* *427*, 1075-1084.
- Wahl, V., Ponnu, J., Schlereth, A., Arrivault, S., Langenecker, T., Franke, A., Feil, R., Lunn, J.E., Stitt, M., and Schmid, M. (2013). Regulation of flowering by trehalose-6-phosphate signaling in *Arabidopsis thaliana*. *Science* *339*, 704-707.
- Wellmer, F., Alves-Ferreira, M., Dubois, A., Riechmann, J.L., and Meyerowitz, E.M. (2006). Genome-wide analysis of gene expression during early *Arabidopsis* flower development. *PLoS genetics* *2*, e117.
- Werhahn, W., Jansch, L., and Braun, H.-P. (2003). Identification of novel subunits of the TOM complex from *Arabidopsis thaliana*. *Plant Physiology and Biochemistry* *41*, 407-416.
- Werhahn, W., Niemeyer, A., Jansch, L., Kruft, V., Schmitz, U.K., and Braun, H. (2001). Purification and characterization of the preprotein translocase of the outer mitochondrial membrane from *Arabidopsis*. Identification of multiple forms of TOM20. *Plant Physiol* *125*, 943-954.
- Wielopolska, A., Townley, H., Moore, I., Waterhouse, P., and Helliwell, C. (2005). A high-throughput inducible RNAi vector for plants. *Plant Biotechnology Journal* *3*, 583-590.
- Wu, Y., and Sha, B. (2006). Crystal structure of yeast mitochondrial outer membrane translocon member Tom70p. *Nature structural & molecular biology* *13*, 589-593.
- Yamano, K., Yatsukawa, Y., Esaki, M., Hobbs, A.E., Jensen, R.E., and Endo, T. (2008). Tom20 and Tom22 share the common signal recognition pathway in mitochondrial protein import. *J Biol Chem* *283*, 3799-3807.
- Yang, Z., Wang, X., Gu, S., Hu, Z., Xu, H., and Xu, C. (2008). Comparative study of SBP-box gene family in *Arabidopsis* and rice. *Gene* *407*, 1-11.

## Summary

Most of the mitochondrial proteins are encoded in the nuclear genome and synthesized on cytosolic ribosomes. To maintain essential functions mitochondria need to import those proteins and the translocation takes place through protein translocase complexes in the mitochondrial membrane. Therefore, the first point of protein import regulation is the outer membrane localized translocase complex (TOM complex). In plants protein import regulation via calmodulin (CaM) has been shown previously at the inner membrane translocase, but no regulation at the level of TOM complex has been described so far. The present study has identified TOM9, a component of the TOM complex, as a novel CaM-binding protein. It was further shown that the previously described interaction of TOM9 with the major preprotein receptor, TOM20 is negatively regulated by CaM. Analysis of RNAi knock-down lines has shown that the plants experience stress in absence of TOM9.2 and they show several phenotypic abnormalities including shortening of hypocotyl length of the seedlings and early flowering of plants. Gene expression study revealed that plants lacking the *TOM9.2* gene have an elevated level of several genes responsible for regulating flowering. Though unchanged at the transcriptomic level, for some mitochondrial proteins significant changes were observed at protein level in the mutant plants; including TOM20 and OM64 (supposed to be another presequence receptor of the mitochondria). An in depth analysis revealed that in absence of TOM9.2, the TOM complex and the TIM23 complex (a translocase complex located on the inner membrane of mitochondria) are reduced, indicating that they are either not assembled or unstable. Even though, the mitochondria of the mutant plants remain import competent *in vitro*. Taken together, the present study indicates that TOM9 is essential for TOM and TIM23 complex stability/formation and the interference of CaM in TOM9/TOM20 interaction might be evolutionary significant in terms of plant specific adaptation of mitochondrial protein import to stressed condition.

## Zusammenfassung

Die meisten mitochondrialen Proteine werden im Kerngenom kodiert und an zytosolischen Ribosomen synthetisiert. Um ihre Funktionen zu erhalten, müssen die Mitochondrien diese Proteine importieren. Dies erfolgt durch Translokationskomplexe, die in den Membranen der Mitochondrien eingebettet sind. Die Proteine werden dabei zuerst vom TOM (translocon on the outer membrane) Komplex durch die äußere Membran transloziert. Daher stellt der TOM Komplex der erste Punkt der Regulation des Proteinimports in Mitochondrien dar. Für viele Protein, erfolgt eine weitere Translokation über oder in die innere Membran. In Pflanzen wurde eine Regulation des Proteinimports durch Calmodulin (CaM) auf der Ebene der inneren Membran-Translokasen bereits beschrieben. Im Rahmen dieser Arbeit wurde jedoch TOM9, eine Komponente des TOM-Komplexes als CaM-Bindungsprotein identifiziert. Außerdem konnte gezeigt werden, dass eine zuvor beschriebene Interaktion von TOM9 mit TOM20, dem Vorstufenproteine-Rezeptor des TOM Komplexes, durch CaM inhibiert wird. Analysen von *TOM9.2*-RNAi Knock-down Linien zeigten, dass die Pflanzen in Abwesenheit von TOM9.2 mehrere phänotypische Anomalien aufwiesen, einschließlich einer Verkürzung der Hypokotyllänge sowie eine verfrühte Induktion der Blütenbildung. Zusätzlich ergaben Array-basierte Transkriptions-Analysen, dass mehreren Genen, die für die Regulierung der Blütenbildung verantwortlich sind, in *tom9.2*-RNAi Knock-down Pflanzen eine erhöhte Expression zeigen. Dies konnte durch anschließende qPCR Analysen bestätigt werden. Des Weiteren wurde beobachtet, dass, obwohl auf der Transkriptom-Ebene unverändert, einige mitochondrialen Proteine einschließlich TOM20 und OM64 (ein potentieller Vorstufenproteine-Rezeptor in Mitochondrien) signifikante Veränderungen auf der Proteinebene zeigten. Weiterführende Analysen ergaben, dass in Abwesenheit von TOM9.2 die Menge von TOM und TIM23 (eine Translokase an der inneren Membran der Mitochondrien) Komplexen stark reduziert ist. Dies deutet darauf hin, dass beide Komplexe in den Mitochondrien der mutierten Pflanzen entweder nicht assembliert werden oder instabil sind. Dennoch sind die Mitochondrien der *TOM9.2*-Mutante noch in der Lage Proteine zu importieren, wie durch *in vitro* Importexperimente belegt werden konnte. Zusammengefasst zeigen die Ergebnisse der vorliegenden Arbeit, dass TOM9 für die Komplexstabilität bzw. Bildung von TOM und TIM23 unerlässlich ist, und dass die Wirkung von CaM auf die TOM9/TOM20 Interaktion für eine pflanzenspezifische Anpassung des mitochondrialen Proteinimports an Stressbedingungen wesentlich sein könnte.

## **Acknowledgements**

First of all I express my immense gratitude to cordially thank Prof. Dr. Ute C. Vothknecht for giving me the opportunity to work in her group as a PhD student and for kindling a passion in me for the research work and inspiring me with her devotion and dedication as a scientist and project guide.

I wish to express my endless gratitude to my direct advisor Dr. Fatima Chigri who supported me throughout my PhD studies. I gratefully acknowledge her continuous support, guidance, friendliness and patience.

I express my sincerely thanks to the German Academic Exchange Service (DAAD) for granting me a PhD scholarship and Center for Integrated Protein Sciences Munich (CIPSM) for providing partial financial support towards laboratory consumables specially required for my PhD project.

I gratefully acknowledge the help of Dr. Norbert Mehlmer, especially with the First Pressure Liquid Chromatography (FPLC).

I want to express my special thanks to Prof. Dr. Jörg Nickelsen for writing reference letter for me every year for DAAD scholarship extension and for his valuable advice. I would also like to cordially acknowledge the valuable advices from Dr. Ralf Heermann, Dr. Cordelia Bolle, Dr. Katrin Philippar, Dr. Serena Schwenkert, Dr. Chris Carrie and Dr. Gabriel Scaaf.

I owe gratitude to Dr. Agostinho Gomes Rocha and Dr. Sandra Flossdorf for valuable discussion and of course other lab members Henning Ruge, Edoardo Cutolo, Dr. Stephanie Otters, Geraldine Hromatke and Monika Fuchs for their cooperation and for creating friendly working environment.

I wish to extend my thanks to Julia Faltermeier and Claudia Sippel for their technical support.

I express my sincere thanks to Michael, Jasmine, Jessica, Manuela, Martina, Johanna, Anila, Isabelle and Petra who participated in my project and contributed with their dedication.

Lastly, I want to express my heartfelt thanks to Debabrata Laha, who was always there beside me throughout my PhD studies.

I am indebted to my parents Shafikul Hassan and Suraiya Begum and my sister Nadira for their continuous love and support. I dedicate my dissertation to them!

## Appendices

### Appendix I: List of oligomers

Primer name	Sequence	Purpose
<i>TOM9.2 NdeI-Fw</i>	AGTACATATGGCGGCGAAGAGAATCGGAG	cloning
<i>TOM9.2 EcoRI-Rv</i>	ATAGAATTCTTACAATCCCCTTTGCATTGGA GATG	cloning
<i>TOM9.2 StrepII-Rv1</i>	GGTGGCTCCAAGCGCTCAATCCCCTT	cloning
<i>StrepII EcoRI-Rv2</i>	ATAGAATTCTTATTTTTTCGAACTGCGGGTGG CTCCAAG	cloning
<i>TOM9.2 CD StrepII-Rv1</i>	GGTGGCTCCAAGCGCTTGCTTTTCCGG	cloning
<i>TOM9.2 ΔCD NdeI-Fw</i>	ATACATATGGCGTGGATCGCTGGGACAAC	cloning
<i>TOM9.2Δ27-47-1R</i>	CGGTGCTCTCGGAGTTTGAAATCC	cloning
<i>TOM9.2Δ27-47-2F</i>	CTCCGAGAGCACCCGAAAAGCAG	cloning
<i>TOM20.3 NdeI-Fw</i>	ATTCATATGATGGATACGGAAACTGAGTTC GATAGG	cloning
<i>TOM20.3 CD StrepII-Rv1</i>	GGCTCCAAGCGCTGCCTAAGCCTT G	cloning
<i>SNRK2.2 ApaIF</i>	TAA GGG CCC ATG GAT CCG GCG ACT AAT TC	cloning
<i>SNRK2.2 NotIR pBIN</i>	ATT GCG GCC GCC GAG AGC ATA AAC TAT CTC	cloning
<i>FT-qPCR Fw</i>	CAGGGTGGCGCCAGAACTTCAA	qPCR
<i>FT-qPCR Rv</i>	AGTCTTCTTCTCCGCAGCCAC	qPCR
<i>AGL8-qPCR Fw</i>	TGCGATGCTGAGGTTGCTCTCA	qPCR
<i>AGL8-qPCR Rv</i>	CCTCTCCATGCAAGAGTCGGTGGA	qPCR
<i>SPL4-qPCR Fw</i>	GGAGGCGCTTAGCTGGACACAA	qPCR
<i>SPL4-qPCR Rv</i>	TCTGCATCACCACCTGACCATTGA	qPCR
<i>PISTILLATA-qPCR Fw</i>	GCTGTGCGAGCACGCCATTGA	qPCR
<i>PISTILLATA-qPCR Rv</i>	AGTGAGTTGCCGTTGCTCCTCC	qPCR
<i>APETALA3-qPCR Fw</i>	CCGGAICTCAGATCAAGCAGAGGCT	qPCR



<i>APETALA3-qPCR Rv</i>	TGCGCTCGCGAACGAGTTTGA	qPCR
<i>SEPALLATA3-qPCR Fw</i>	TCGAGCATGCTTCGGACACTGG	qPCR
<i>SEPALLATA3-qPCR Rv</i>	AAGGCACATTGGGTTCTGGTGCT	qPCR
CaS-C_373s-aF	GCAGCTTCGAGAGCCTTTGGCACTAGG	Site directed mutagenesis
CaS-C_373s-aR	CCTAGTGCCAAAGGCTCTCGAAGCTGC	Site directed mutagenesis
CaS-C_378s-aF	GGCACTAGGGCCGGAACCAAGTTCCTTC	Site directed mutagenesis
CaS-C_378s-aR	GAAGGAACTTGGTTCCGGCCCTAGTGCC	Site directed mutagenesis
CaS-C_378s/a-80s/aF	GCACTAGGGCCGGAGTCAAGTTCCTTC	Site directed mutagenesis
CaS-C_378s/a-80s/aR	GAAGGAACTTGACTCCGGCCCTAGTGC	Site directed mutagenesis
CaS-C_373s/a_378s/a_380t/vF	GCTTCGAGAGCCTTTGGCACTAGGGCCGGA GTCAAGTTCC	Site directed mutagenesis
CAS 373s/a_378s/a_380t/v	GGAAGTCTGACTCCGGCCCTAGTGCCAAAGG CTCTCGAAGC	Site directed mutagenesis

## Appendix II: Microarray data

Comparison of DNA microarray analysis (ATH1 GeneChip) between induced (+Dex, n = 5) versus non-induced (-Dex, n = 6) *TOM9* RNAi lines in 18-day-old rosette leaves. Reporter Identifiers (Affymetrix ATH1 probeset) are provided. Functional categories are according to MAPMAN/TAIR 2010 (Ath\_AGI\_LOCUS\_TAIR10\_Aug2012 download). Arabidopsis Genome Initiative (AGI) codes are also listed below. The sample mean values are tabulated for induced (mean +dex) and non-induced (mean -dex) *TOM9* RNAi lines. In addition to that, fold changes (FCH) are also presented.

### Upregulated genes

Identifier	functional category	GeneName	mean +dex	mean -dex	FCH	
254197_at	3 minor CHO metabolism	At4g24040	322.86	147.01	2.20	
254146_at		At4g24260	92.20	69.03	1.34	
246994_at		At5g67460	183.39	123.09	1.49	
265441_at	10 cell wall	At2g20870	320.82	96.38	3.33	
255080_at		At4g09030	1417.65	778.12	1.82	
252971_at		At4g38770	6305.51	5065.05	1.24	
251317_at		At3g61490	390.39	105.94	3.69	
250780_at		At5g05290	142.95	60.24	2.37	
250992_at		At5g02260	72.48	49.61	1.46	
248263_at		At5g53370	1583.82	862.51	1.84	
261826_at		At1g11580	410.73	232.99	1.76	
259616_at		At1g47960	783.16	539.37	1.45	
262630_at		11 lipid metabolism	At1g06520	70.60	36.84	1.92
253309_at			At4g33790	82.18	51.13	1.61
245322_at	26.21 lipid transfer protein	At4g14815	52.34	35.87	1.46	
251928_at		At3g53980	955.05	507.95	1.88	
256145_at		At1g48750	775.06	556.60	1.39	
257066_at		At3g18280	314.31	215.42	1.46	
245842_at	28.28 GDSL-motif lipiase	At1g58430	36.89	19.57	1.88	
259786_at		At1g29660	4396.49	2090.47	2.10	

262736_at		At1g28570	396.00	241.69	1.64
262745_at		At1g28600	1133.98	948.37	1.20
262749_at		At1g28580	1608.52	839.46	1.92
257194_at	13 amino acid metabolism	At3g13110	3343.22	1737.70	1.92
251260_at		At3g62130	658.45	379.73	1.73
249112_at	14 S-assimilation	At5g43780	987.58	729.91	1.35
248779_at	16 secondary metabolism	At5g47720	390.21	329.68	1.18
245258_at		At4g15340	73.65	24.12	3.05
264100_at		At1g78970	2153.11	1617.73	1.33
247038_at		At5g67160	108.16	64.06	1.69
245690_at		At5g04230	310.04	176.67	1.75
249489_at		At5g39090	115.69	66.05	1.75
248431_at	17 hormone metabolism	At5g51470	37.73	24.68	1.53
261776_at		At1g76190	73.17	47.28	1.55
248011_at		At5g56300	43.03	19.17	2.24
261150_at		At1g19640	42.76	26.91	1.59
251021_at	20 stress (biotic/abiotic)	At5g02140	27.57	21.71	1.27
266118_at		At2g02130	3304.19	2702.35	1.22
254361_at		At4g22212	107.96	53.37	2.02
258727_at		At3g11930	4052.90	2689.84	1.51
248172_at		At5g54660	316.66	201.40	1.57
252047_at		At3g52490	300.66	113.49	2.65
258519_at		At3g06760	733.52	342.91	2.14
254234_at		At4g23680	314.59	164.10	1.92
258879_at		At3g03270	253.91	152.30	1.67
252629_at	26.1 misc redox metabolism	At3g44970	237.37	70.47	3.37
254331_s_at		At4g22710	3455.85	2381.91	1.45
257636_at		At3g26200	168.68	117.25	1.44
250646_at		At5g06720	37.05	30.07	1.23
260060_at		At1g73680	561.83	211.60	2.66
261023_at		At1g12200	692.70	222.56	3.11
247814_at	26.8 misc metabolism	At5g58310	784.43	629.30	1.25
264436_at		At1g10370	199.46	121.76	1.64
264988_at		At1g27140	47.06	37.06	1.27

256564_at		At3g29770	136.54	103.25	1.32
260297_at		At1g80280	1733.67	386.12	4.49
266363_at		At2g41250	386.31	276.15	1.40
249034_at	27 RNA regulation of transcription (8 associated with floral development)	At5g44160	36.44	29.09	1.25
250396_at		At5g10970	84.30	65.18	1.29
267291_at		At2g23740	145.35	103.52	1.40
258198_at		At3g14020	119.31	90.86	1.31
262378_at		At1g72830	121.68	75.42	1.61
246215_at		At4g37180	580.28	408.23	1.42
245901_at		At5g11060	667.01	564.10	1.18
256081_at		At1g20700	134.38	35.05	3.83
259165_at		At3g01470	1418.88	1086.95	1.31
252081_at		At3g51910	66.78	41.64	1.60
246531_at		At5g15800	43.56	32.18	1.35
259124_at		At3g02310	30.99	21.39	1.45
264872_at		At1g24260	40.87	27.22	1.50
262096_at		At1g56010	415.93	57.44	7.24
261375_at		At1g53160	217.78	113.71	1.92
246072_at		At5g20240	34.29	23.81	1.44
258571_at		At3g04420	33.29	26.15	1.27
247227_at		At5g65130	37.66	29.59	1.27
266606_at		At2g46310	87.48	63.01	1.39
258068_at		At3g25990	35.74	26.17	1.37
250666_at		At5g07100	73.77	46.82	1.58
264390_at		At1g11950	94.51	54.80	1.72
248564_at		At5g49700	88.68	72.09	1.23
256720_at		At2g34140	76.02	42.44	1.79
266216_at		At2g28810	451.96	271.81	1.66
254391_at	28 DNA	At4g21590	66.61	52.10	1.28
257356_s_at		At2g32490	47.98	36.15	1.33
256597_at	29 protein	At3g28500	261.31	133.18	1.96
262615_at		At1g13950	231.83	126.99	1.83
261116_at		At1g75370	496.86	354.65	1.40
250633_at		At5g07460	1107.48	411.59	2.69

249448_at		At5g39420	25.29	19.23	1.32
250900_at		At5g03470	496.69	385.76	1.29
255631_at		At4g00710	577.17	488.55	1.18
258901_at		At3g05640	1740.54	133.79	13.01
261401_at		At1g79640	74.94	57.41	1.31
263416_at		At2g17170	24.12	15.89	1.52
264369_at		At1g70430	47.60	19.44	2.45
248017_at		At5g56460	197.78	131.18	1.51
255115_at		At4g08840	51.08	34.99	1.46
248819_at		At5g47050	363.15	236.03	1.54
254695_at		At4g17910	211.01	122.13	1.73
262726_at		At1g43640	35.93	26.16	1.37
262208_at		At1g74800	243.89	180.84	1.35
259329_at	30 signalling	At3g16360	300.86	128.34	2.34
245202_at		At1g67720	241.75	122.59	1.97
259912_at		At1g72670	181.99	72.74	2.50
246891_at		At5g25490	298.95	192.14	1.56
261460_at		At1g07880	188.27	73.19	2.57
261917_at	31 cell division	At1g65920	120.99	58.88	2.06
250869_at	33 development	At5g03840	105.81	34.99	3.02
264638_at		At1g65480	571.29	301.08	1.90
258008_at		At3g19430	486.54	38.53	12.63
247212_at		At5g65040	129.37	86.98	1.49
255129_at		At4g08290	356.48	167.80	2.12
255578_at		At4g01450	399.69	232.96	1.72
245090_at		At2g40900	299.94	163.41	1.84
261576_at		At1g01070	207.49	105.23	1.97
265962_at		At2g37460	222.05	148.21	1.50
260693_at	34 transport	At1g32450	163.23	91.40	1.79
259953_at		At1g74810	207.07	47.73	4.34
262456_at		At1g11260	7454.40	2493.12	2.99
248496_at		At5g50790	68.92	50.85	1.36
252327_at		At3g48740	4421.43	3135.62	1.41
248467_at		At5g50800	335.81	53.60	6.27

267093_at		At2g38170	6870.29	5559.09	1.24
246260_at		At1g31820	214.82	168.22	1.28
249791_at		At5g23810	82.98	57.93	1.43
263318_at		At2g24762	791.84	619.24	1.28
264901_at		At1g23090	1229.18	183.99	6.68
247128_at		At5g66110	478.67	76.80	6.23
258100_at		At3g23550	282.30	165.11	1.71
263866_at		At2g36950	688.91	421.47	1.63
246273_at		At4g36700	46.97	21.29	2.21
263285_at		At2g36120	338.03	237.34	1.42
248967_at		At5g45350	1645.37	1328.27	1.24
249939_at		At5g22430	119.87	30.53	3.93
252185_at		At3g50780	498.31	379.14	1.31
253182_at		At4g35190	73.88	57.63	1.28
253582_at		At4g30670	53.11	41.37	1.28
264466_at		At1g10380	156.05	101.98	1.53
265355_at	35 unknown	At2g16760	57.56	44.96	1.28
253525_at		At4g31330	332.71	182.09	1.83
259766_at		At1g64360	993.00	551.64	1.80
261772_at		At1g76240	60.49	37.12	1.63
262386_at		At1g49370	39.34	24.31	1.62
245871_at		At1g26290	91.74	35.75	2.57
248525_s_at		At5g50710	16.00	13.13	1.22
249332_at		At5g40980	207.59	104.11	1.99
250796_at		At5g05300	39.91	33.08	1.21

**Down regulated genes**

<b>Identifier</b>	<b>functional category</b>	<b>GeneName</b>	<b>mean +dex</b>	<b>mean -dex</b>	<b>FCH</b>
259970_at	1 photosynthesis	At1g76570	303.40	357.07	1.18
265228_s_at	9 mitochondrial electron transport	At2g07698	274.74	376.37	1.37
266012_s_at		At2g07741	113.84	135.62	1.19
257339_s_at		At2g07671	480.97	757.78	1.58
265230_s_at		At2g07707	189.09	298.87	1.58
261949_at		10 cell wall	At1g64670	214.68	270.37
247450_at	At5g62350		3648.35	4571.52	1.25
259391_s_at	11 lipid metabolism	At1g06350	726.25	977.04	1.35
255692_at		At4g00400	463.48	551.18	1.19
249527_at	13 amino acid metabolism	At5g38710	42.39	65.08	1.54
254512_at	16 secondary metabolism	At4g20230	44.25	56.94	1.29
263927_s_at		At2g21890	45.45	57.65	1.27
251658_at		At3g57020	307.35	429.18	1.40
249942_at		At5g22300	176.76	304.81	1.72
246481_s_at	17 hormone metabolism	At5g15960	6448.76	10123.14	1.57
255645_at		At4g00880	413.29	680.14	1.65
260547_at	20 stress (biotic/abiotic)	At2g43550	1530.64	2040.13	1.33
256340_at		At1g72070	33.38	42.56	1.28
248337_at		At5g52310	305.88	652.99	2.13
263495_at		At2g42530	1498.03	3065.46	2.05
263497_at		At2g42540	987.75	3075.01	3.11
247948_at		At5g57130	91.02	116.17	1.28
249477_s_at		At5g38930	32.45	53.15	1.64
246464_at	26.1 misc redox metabloism	At5g16980	36.69	55.24	1.51
260831_at	21 redox:glutaredoxins	At1g06830	140.32	247.08	1.76
263168_at		At1g03020	113.33	164.30	1.45
266516_at		At2g47880	119.74	247.74	2.07
263595_at	26.8 misc metabolism	At2g01890	81.89	175.05	2.14
253367_at		At4g33180	204.37	248.52	1.22
266485_at		At2g47630	228.26	284.04	1.24
245029_at		At2g26580	258.27	322.91	1.25

246069_at	27 RNA regulation of transcription	At5g20220	226.43	284.14	1.25
263797_at		At2g24570	68.06	89.62	1.32
265454_at		At2g46530	147.75	188.96	1.28
255694_at		At4g00050	283.78	381.28	1.34
260034_at		At1g68810	164.28	211.86	1.29
264264_at		At1g09250	137.23	181.71	1.32
256452_at		At1g75240	271.51	347.36	1.28
253617_at		At4g30410	49.88	68.75	1.38
256980_at		At3g26932	58.44	78.39	1.34
257519_at		At3g01210	195.10	245.91	1.26
254300_at	29 protein	At4g22780	62.33	87.51	1.40
249076_at		At5g43970	224.24	499.57	2.23
255923_at		At1g22180	64.41	83.19	1.29
259163_at		At3g01490	261.35	327.50	1.25
245088_at		At2g39850	494.42	732.36	1.48
247922_at		At5g57500	21.77	26.55	1.22
250277_at	30 signalling	At5g12940	270.15	330.43	1.22
267596_s_at		At2g33050	278.45	360.19	1.29
252280_at		At3g49260	333.02	430.00	1.29
256731_at	33 development	At3g30340	97.28	126.20	1.30
248888_at	34 transport	At5g46240	79.22	132.41	1.67
247304_at		At5g63850	399.61	560.14	1.40
257271_at		At3g28007	106.41	165.26	1.55
245912_at		At5g19600	100.32	121.00	1.21
254697_at		At4g17970	99.71	161.33	1.62
259968_at		At1g76530	78.33	116.18	1.48
260363_at	35 unknown	At1g70550	106.59	147.71	1.39
255621_at		At4g01390	232.50	368.96	1.59
263693_at		At1g31200	27.84	37.57	1.35
262250_at		At1g48280	146.10	174.06	1.19
246487_at		At5g16030	1147.45	1547.15	1.35
247882_at		At5g57785	455.85	598.91	1.31
248646_at		At5g49100	156.07	215.33	1.38
249932_at		At5g22390	86.34	124.55	1.44



---

250481_at		At5g10310	62.88	89.92	1.43
250734_at		At5g06270	138.34	177.02	1.28
251010_at		At5g02550	77.15	113.79	1.47
252134_at		At3g50910	271.98	323.92	1.19
253401_at		At4g32870	90.97	125.70	1.38
256456_at		At1g75180	185.15	263.36	1.42
259093_at		At3g04860	203.07	240.38	1.18
260883_at		At1g29270	62.10	88.41	1.42

## Appendix III: Mass spectrometric data

### Identification of CaM binding protein- TOM9.2

#### *{MATRIX}* *{SCIENCE}* Mascot Search Results

##### Protein View

Match to: gi|15240059 Score: 140  
 TOM22-V (TRANSLOCASE OF OUTER MEMBRANE 22-V); P-P-bond-hydrolysis-driven protein transmembrane transporter [Arabidopsis thaliana]  
 Found in search of C:\Documents and Settings\Lars.Israel.ZFP.000\My Documents\Data Orbitrap + QStar\NParvin\_SID954\_030311\SID954\_220211\_NP-b.RAW

Nominal mass ( $M_r$ ): 10372; Calculated pI value: 9.81  
 NCBI BLAST search of gi|15240059 against nr  
 Unformatted [sequence string](#) for pasting into other applications

Taxonomy: [Arabidopsis thaliana](#)  
 Links to retrieve other entries containing this sequence from NCBI Entrez:  
[gi|24212685](#) from [Arabidopsis thaliana](#)  
[gi|9758556](#) from [Arabidopsis thaliana](#)  
[gi|15529292](#) from [Arabidopsis thaliana](#)  
[gi|16974415](#) from [Arabidopsis thaliana](#)  
[gi|21595230](#) from [Arabidopsis thaliana](#)

Fixed modifications: Carbamidomethyl (C)  
 Variable modifications: Oxidation (M)  
 Cleavage by Trypsin/P: cuts C-term side of KR  
 Sequence Coverage: 33%

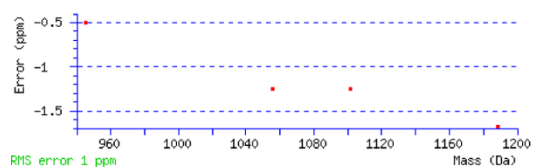
Matched peptides shown in **Bold Red**

1 MAAKRIGAGK **SGGGDPNILA RISNSEIVSQ GRRAAGDAVE VSK**KLLRSTG  
 51 KAAWIAGTTF LILVPLIIE MDREAQINEI ELQQASLLGA PPSPMQRGL

Show predicted peptides also

Sort Peptides By  Residue Number  Increasing Mass  Decreasing Mass

Start - End	Observed	Mr (expt)	Mr (calc)	ppm	Miss	Sequence	
11 - 21	528.7746	1055.5346	1055.5360	-1	0	<b>K.SGGDPNILAR.I</b>	( <a href="#">Ions score 71</a> )
22 - 32	595.3112	1188.6078	1188.6098	-2	0	<b>R.ISNSEIVSQGR.R</b>	( <a href="#">Ions score 77</a> )
33 - 43	551.7955	1101.5764	1101.5778	-1	1	<b>R.RAAGDAEVSK.K</b>	( <a href="#">Ions score 27</a> )
34 - 43	473.7454	945.4762	945.4767	-0	0	<b>R.AAGDAEVSK.K</b>	( <a href="#">Ions score 44</a> )



## Identification of CaM binding protein- RISP

### **MASCOT** Mascot Search Results

#### Protein View

Match to: [gi|15240627](#) Score: 1030

ubiquinol-cytochrome C reductase iron-sulfur subunit, mitochondrial, putative / Rieske iron-sulfur protein, putative [Arabidopsis thaliana]

Found in search of C:\Documents and Settings\Lars.Israel.ZFP.000\My Documents\Data Orbitrap + QStar\NParvin\_SID954\_030311\SID954\_220211\_NP-a.RAW

Nominal mass ( $M_r$ ): 30111; Calculated pI value: 8.86

NCBI BLAST search of [gi|15240627](#) against nr

Unformatted [sequence string](#) for pasting into other applications

Taxonomy: [Arabidopsis thaliana](#)

Links to retrieve other entries containing this sequence from NCBI Entrez:

[gi|13899077](#) from [Arabidopsis thaliana](#)

[gi|7543911](#) from [Arabidopsis thaliana](#)

[gi|20148363](#) from [Arabidopsis thaliana](#)

Fixed modifications: Carbamidomethyl (C)

Variable modifications: Oxidation (M)

Cleavage by Trypsin/P: cuts C-term side of KR

Sequence Coverage: 42%

Matched peptides shown in **Bold Red**

```

1 MLRVAGRRLF SVSQRSSSTAT SFVLRSRDHL SDGGNSSSAS RSVPSADLSS
51 FNSYHRVIR GFASQVITQG NEIGFGSEVP ATVEAVKTPN SKIVYDDHNNH
101 ERYPPGDPSK RAFAYFVLSG GRFYASVLR LLVLLIVSM SASKDVLALA
151 SLEVDLGSIE PGTIVTKWNR GKPVFIRRRRT EDDIKLANSV DVGSLRDPQE
201 DSVRVKNPEW LIVVGVCTHL GCIPLNAGD YGGWFCPCHG SHYDISGRIR
251 KGPAPYNLEV PTYSFLEENK LLIG

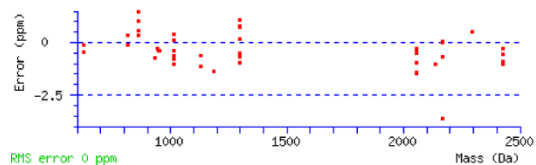
```

Show predicted peptides also

Sort Peptides By  Residue Number  Increasing Mass  Decreasing Mass

Start - End	Observed	Mr (expt)	Mr (calc)	ppm	Miss	Sequence
93 - 102	649.2990	1296.5834	1296.5847	-1	0	K.IVYDDHNER.Y ( <a href="#">Ions score 44</a> )
93 - 102	649.2992	1296.5838	1296.5847	-1	0	K.IVYDDHNER.Y ( <a href="#">Ions score 36</a> )
93 - 102	649.2993	1296.5840	1296.5847	-1	0	K.IVYDDHNER.Y ( <a href="#">Ions score 32</a> )
93 - 102	649.2993	1296.5840	1296.5847	-1	0	K.IVYDDHNER.Y ( <a href="#">Ions score 50</a> )
93 - 102	649.2993	1296.5840	1296.5847	-1	0	K.IVYDDHNER.Y ( <a href="#">Ions score 48</a> )
93 - 102	325.1535	1296.5849	1296.5847	0	0	K.IVYDDHNER.Y ( <a href="#">Ions score 2</a> )
93 - 102	433.2025	1296.5857	1296.5847	1	0	K.IVYDDHNER.Y ( <a href="#">Ions score 33</a> )
93 - 102	433.2025	1296.5857	1296.5847	1	0	K.IVYDDHNER.Y ( <a href="#">Ions score 34</a> )
93 - 102	325.1537	1296.5857	1296.5847	1	0	K.IVYDDHNER.Y ( <a href="#">Ions score 2</a> )
93 - 102	325.1538	1296.5861	1296.5847	1	0	K.IVYDDHNER.Y ( <a href="#">Ions score 2</a> )
93 - 110	713.6671	2137.9795	2137.9817	-1	1	K.IVYDDHNERYPFGDPSK.R ( <a href="#">Ions score 2</a> )
103 - 110	430.7112	859.4078	859.4076	0	0	R.YPPGDPSK.R ( <a href="#">Ions score 31</a> )
103 - 110	430.7112	859.4078	859.4076	0	0	R.YPPGDPSK.R ( <a href="#">Ions score 30</a> )
103 - 110	430.7113	859.4080	859.4076	1	0	R.YPPGDPSK.R ( <a href="#">Ions score 24</a> )
103 - 110	430.7113	859.4080	859.4076	1	0	R.YPPGDPSK.R ( <a href="#">Ions score 35</a> )
103 - 110	430.7113	859.4080	859.4076	1	0	R.YPPGDPSK.R ( <a href="#">Ions score 35</a> )
103 - 110	430.7115	859.4084	859.4076	1	0	R.YPPGDPSK.R ( <a href="#">Ions score 47</a> )
103 - 110	430.7117	859.4088	859.4076	1	0	R.YPPGDPSK.R ( <a href="#">Ions score 31</a> )
103 - 111	508.7611	1015.5076	1015.5087	-1	1	R.YPPGDPSKR.A ( <a href="#">Ions score 31</a> )
103 - 111	508.7612	1015.5078	1015.5087	-1	1	R.YPPGDPSKR.A ( <a href="#">Ions score 37</a> )
103 - 111	508.7612	1015.5078	1015.5087	-1	1	R.YPPGDPSKR.A ( <a href="#">Ions score 30</a> )
103 - 111	508.7613	1015.5080	1015.5087	-1	1	R.YPPGDPSKR.A ( <a href="#">Ions score 28</a> )
103 - 111	508.7613	1015.5080	1015.5087	-1	1	R.YPPGDPSKR.A ( <a href="#">Ions score 22</a> )
103 - 111	508.7614	1015.5082	1015.5087	-0	1	R.YPPGDPSKR.A ( <a href="#">Ions score 21</a> )
103 - 111	339.5102	1015.5088	1015.5087	0	1	R.YPPGDPSKR.A ( <a href="#">Ions score 25</a> )
103 - 111	339.5103	1015.5091	1015.5087	0	1	R.YPPGDPSKR.A ( <a href="#">Ions score 18</a> )
103 - 111	339.5103	1015.5091	1015.5087	0	1	R.YPPGDPSKR.A ( <a href="#">Ions score 18</a> )
103 - 111	339.5103	1015.5091	1015.5087	0	1	R.YPPGDPSKR.A ( <a href="#">Ions score 24</a> )
103 - 111	339.5103	1015.5091	1015.5087	0	1	R.YPPGDPSKR.A ( <a href="#">Ions score 19</a> )
112 - 122	594.3132	1186.6118	1186.6135	-1	0	R.AFAYFVLSGGR.F ( <a href="#">Ions score 73</a> )
123 - 130	477.7738	953.5330	953.5334	-0	0	R.FVYASVLR.L ( <a href="#">Ions score 48</a> )
123 - 130	477.7738	953.5330	953.5334	-0	0	R.FVYASVLR.L ( <a href="#">Ions score 55</a> )
136 - 144	468.2648	934.5150	934.5157	-1	0	K.LIVSMSASK.D ( <a href="#">Ions score 25</a> )
136 - 144	476.2624	950.5102	950.5107	-0	0	K.LIVSMSASK.D Oxidation (M) ( <a href="#">Ions score 54</a> )
145 - 168	809.7783	2426.3131	2426.3156	-1	0	K.DVLALASLEVDLGSIEPGTTTVK.W ( <a href="#">Ions score 71</a> )
145 - 168	1214.1640	2426.3134	2426.3156	-1	0	K.DVLALASLEVDLGSIEPGTTTVK.W ( <a href="#">Ions score 58</a> )
145 - 168	1214.1640	2426.3134	2426.3156	-1	0	K.DVLALASLEVDLGSIEPGTTTVK.W ( <a href="#">Ions score 40</a> )
145 - 168	809.7787	2426.3143	2426.3156	-1	0	K.DVLALASLEVDLGSIEPGTTTVK.W ( <a href="#">Ions score 79</a> )
145 - 168	809.7789	2426.3149	2426.3156	-0	0	K.DVLALASLEVDLGSIEPGTTTVK.W ( <a href="#">Ions score 78</a> )
171 - 177	408.7581	815.5016	815.5018	-0	1	R.GKPVFIR.R ( <a href="#">Ions score 14</a> )
171 - 177	408.7583	815.5020	815.5018	0	1	R.GKPVFIR.R ( <a href="#">Ions score 32</a> )
171 - 177	408.7583	815.5020	815.5018	0	1	R.GKPVFIR.R ( <a href="#">Ions score 20</a> )
173 - 177	316.1998	630.3850	630.3853	-0	0	K.PVFIR.R ( <a href="#">Ions score 17</a> )
173 - 177	316.1999	630.3852	630.3853	-0	0	K.PVFIR.R ( <a href="#">Ions score 22</a> )

186 - 196	565.8112	1129.6078	1129.6091	-1	0	K.LANSVDVGS LR.D	( <a href="#">Ions score 85</a> )
186 - 196	565.8115	1129.6084	1129.6091	-1	0	K.LANSVDVGS LR.D	( <a href="#">Ions score 89</a> )
186 - 204	1029.0150	2056.0154	2056.0185	-1	1	K.LANSVDVGS LRDPQEDSVR.V	( <a href="#">Ions score 23</a> )
186 - 204	686.3458	2056.0156	2056.0185	-1	1	K.LANSVDVGS LRDPQEDSVR.V	( <a href="#">Ions score 34</a> )
186 - 204	686.3458	2056.0156	2056.0185	-1	1	K.LANSVDVGS LRDPQEDSVR.V	( <a href="#">Ions score 44</a> )
186 - 204	686.3461	2056.0165	2056.0185	-1	1	K.LANSVDVGS LRDPQEDSVR.V	( <a href="#">Ions score 45</a> )
186 - 204	1029.0160	2056.0174	2056.0185	-1	1	K.LANSVDVGS LRDPQEDSVR.V	( <a href="#">Ions score 42</a> )
186 - 204	686.3465	2056.0177	2056.0185	-0	1	K.LANSVDVGS LRDPQEDSVR.V	( <a href="#">Ions score 46</a> )
186 - 204	686.3466	2056.0180	2056.0185	-0	1	K.LANSVDVGS LRDPQEDSVR.V	( <a href="#">Ions score 59</a> )
197 - 204	473.2171	944.4196	944.4199	-0	0	R.DPQEDSVR.V	( <a href="#">Ions score 26</a> )
251 - 270	1148.5790	2295.1434	2295.1423	1	1	R.KGPAPYNLEVPTYSFLEENK.L	( <a href="#">Ions score 71</a> )
252 - 270	1084.5270	2167.0394	2167.0473	-4	0	K.GPAPYNLEVPTYSFLEENK.L	( <a href="#">Ions score 40</a> )
252 - 270	723.3559	2167.0459	2167.0473	-1	0	K.GPAPYNLEVPTYSFLEENK.L	( <a href="#">Ions score 40</a> )
252 - 270	723.3564	2167.0474	2167.0473	0	0	K.GPAPYNLEVPTYSFLEENK.L	( <a href="#">Ions score 59</a> )
252 - 270	1084.5310	2167.0474	2167.0473	0	0	K.GPAPYNLEVPTYSFLEENK.L	( <a href="#">Ions score 53</a> )
252 - 270	1084.5310	2167.0474	2167.0473	0	0	K.GPAPYNLEVPTYSFLEENK.L	( <a href="#">Ions score 84</a> )



## Identification of calcium dependent protein kinases in chloroplasts- SNRK2.2

### *{MATRIX}* Mascot Search Results

#### Protein View

Match to: [gi|15229772](#) Score: 27  
**SNRK2.2 (SNF1-RELATED PROTEIN KINASE 2.2); kinase/ protein kinase [Arabidopsis thaliana]**  
 Found in search of C:\Documents and Settings\ZFP Guest PC\My Documents\Data Orbitrap + QStar\NParvin\_SID1899\_020813\SID1899\_190713\_D7-1.RAW

Nominal mass ( $M_r$ ): **41580**; Calculated pI value: **4.71**  
 NCBI BLAST search of [gi|15229772](#) against nr  
 Unformatted [sequence string](#) for pasting into other applications

Taxonomy: [Arabidopsis thaliana](#)  
 Links to retrieve other entries containing this sequence from NCBI Entrez:  
[gi|75319453](#) from [Arabidopsis thaliana](#)  
[gi|166817](#) from [Arabidopsis thaliana](#)  
[gi|6561990](#) from [Arabidopsis thaliana](#)  
[gi|94442423](#) from [Arabidopsis thaliana](#)

Fixed modifications: Carbamidomethyl (C)  
 Variable modifications: Oxidation (M)  
 Cleavage by Trypsin/P: cuts C-term side of KR  
 Sequence Coverage: 2%

Matched peptides shown in **Red**

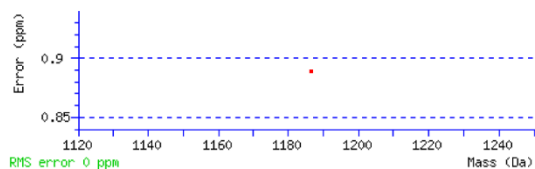
```

1 MDPATNSPIM PIDLPIMHDS DRYDFVKDIG SGNFGVARLM TDRVTKELVA
51 VKYIERGEKI DENVQREIIN HRSLRHPNIV RFKEVILTPT HLAIVMEYAA
101 GGLYERICN AGRFSEDEAR FFFQQLISGV SYCHAMQICH RDLKLENTLL
151 DGSPPAPRLKI CDFGYSKSSV LHSQPKSTVG TPAYIAPEIL LRQEYDGKLA
201 DVWSCGVTLY VMLVGAYPFE DPQEPRDYRK TIQRILSVTY SIPEDLHLSP
251 ECRHLISRIF VADPATRITI PEITSDKWFL KNLPGLMDE NRMGSQFQEP
301 EQPMQSLDTI MQIISEATIP TVRNRLDDF MADNLDLDDD MDDFSESEI
351 DVDSSEIVY AL
    
```

Show predicted peptides also

Sort Peptides By  Residue Number  Increasing Mass  Decreasing Mass

Start - End	Observed	Mr (expt)	Mr (calc)	ppm	Miss	Sequence
57 - 66	594.3049	1186.5952	1186.5942	1	1	<b>R.GEKIDENVQR.E</b> ( <a href="#">Ions score 27</a> )



## Identification of calcium dependent protein kinases in chloroplasts- TAK-1

### **MASCOT** Mascot Search Results

#### Protein View

Match to: [gi|15235432](#) Score: 29

protein kinase family protein [*Arabidopsis thaliana*]

Found in search of C:\Documents and Settings\ZFP Guest PC\My Documents\Data Orbitrap + QStar\NParvin\_SID1899\_020813\SID1899\_190713\_D7-2.RAW

Nominal mass ( $M_r$ ): 54872; Calculated pI value: 7.28

NCBI BLAST search of [gi|15235432](#) against nr

Unformatted [sequence string](#) for pasting into other applications

Taxonomy: [Arabidopsis thaliana](#)

Links to retrieve other entries containing this sequence from NCBI Entrez:

[gi|2262143](#) from [Arabidopsis thaliana](#)

[gi|7269023](#) from [Arabidopsis thaliana](#)

[gi|28393613](#) from [Arabidopsis thaliana](#)

[gi|28973357](#) from [Arabidopsis thaliana](#)

Fixed modifications: Carbamidomethyl (C)

Variable modifications: Oxidation (M)

Cleavage by Trypsin/P: cuts C-term side of KR

Sequence Coverage: 1%

Matched peptides shown in **Bold Red**

```

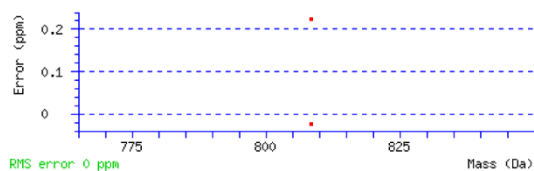
1 MADSHSVNNQ LSRHTSIFGL RLWVVLGVCV GAATVLLLVL ISLWFIYRRS
51 NKNKSLESSS KSNHTIVPVV SKETQEIRPP IQPDPTPEPH QNQQREDDNK
101 IHIEIGKDHR IAYPERGGWT GSGSGSGSD QGLMLSGPE VSHLWGHWY
151 TLRELEVSTN GFADENVIGQ GGYGIVYRGV LEDKSMVAIK NLLNRRQAE
201 KEFKVEVEAI GRVRHKNLVR LLGYCVGAH RMLVVEYVDN GNLEQWIHGG
251 GLGFKSPLTW EIRMNIVLGT AKGLMYLHEG LEPKVVRDI KSSNILLDKQ
301 WNSKVSDFGL AKLLGSEMSY VTTRVMGTFG YVAPYVASTG MLNERSDVYS
351 FGVLMVEIIS GRSPVDYSRA PGEVNLVEWL KRLVTNRDAE GVLDRPMVDK
401 PSLRSLKRTL LVALRCVDPN AQKRPKMGHI IHMLEADLV SKDDRRNSGG
451 GGGGIEQGRS PRRKTNVNES EDESGNSVLI NNDQLALENK QN

```

Show predicted peptides also

Sort Peptides By  Residue Number  Increasing Mass  Decreasing Mass

Start	End	Observed	Mr (expt)	Mr (calc)	ppm	Miss	Sequence	
101	107	405.2476	808.4806	808.4807	-0	0	<b>K.IHIEIGK.D</b>	( <a href="#">Ions score 29</a> )
101	107	405.2477	808.4808	808.4807	0	0	<b>K.IHIEIGK.D</b>	( <a href="#">Ions score 3</a> )



# Identification of calcium dependent protein kinases in chloroplasts- LRRLK

## *MATRIX* SCIENCE Mascot Search Results

### Protein View

Match to: [gi|15226197](#) Score: 33  
 leucine-rich repeat transmembrane protein kinase, putative [Arabidopsis thaliana]  
 Found in search of C:\Documents and Settings\ZFP Guest PC\My Documents\Data Orbitrap + QStar\NParvin\_SID1899\_020813\SID1899\_190713\_D7-2.RAW

Nominal mass (M<sub>r</sub>): 79284; Calculated pI value: 5.75  
 NCBI BLAST search of [gi|15226197](#) against nr  
 Unformatted [sequence string](#) for pasting into other applications

Taxonomy: [Arabidopsis thaliana](#)  
 Links to retrieve other entries containing this sequence from NCBI Entrez:  
[gi|4262228](#) from [Arabidopsis thaliana](#)  
[gi|224589493](#) (no taxonomy information for this entry)

Fixed modifications: Carbamidomethyl (C)  
 Variable modifications: Oxidation (M)  
 Cleavage by Trypsin/P: cuts C-term side of KR  
 Sequence Coverage: 6%

Matched peptides shown in **Bold Red**

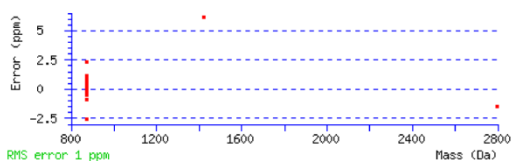
```

1 MLASLIIFVA LLCNVTVISG LNDEGFALL FKQSVHDDPT GSLNNWSSD
51 ENACSWNGVT CKELRVVSLV IPRKNLYGSL PSSLGFLSSL RHLNLRNRF
101 YGSLPIQLFH LQGLQSLVLY GNSFDGSLSE EIGKLLKLT LDLSQNLFNG
151 SPLSLIQLCN RLKTLDSVRN NLSGGLPDGF GSAFVSLKLEK DLAFNQFNFS
201 IPSDIGNLSN LQGTADFVSHN HFTGSIPPAL GDLPEKVYID LTFNNLSGPI
251 PQTGALMNRG PTAFIGNTGL CGPPLKDLQC GYQLGLNASY PFIPSNPPE
301 DSDSTNSETK QKSSGLSKSA VIAIVLQVDF GICLVGLLFT YCYSKFCACN
351 RENQFVGEKE SKKRASECLC FRKDESETPS ENVEHCDIVP LDAQVAFNLE
401 ELLKASAFVL GKSIGIVYK VVLENGTLA VRRLGEGGSQ RFKEFQTEVE
451 AIGKLPKPHI ASLRAYWVSV DEKLLIYDVV SNGNLATALH KPGMMTIAP
501 LTWSELRIM KGIATGLVYL HEFSPKVVH GDLKPSNILI GQDMEPKISS
551 FGLARLANIA GGSSPTIQSN RIIQTDQPPQ ERQQHHHKSV SSEFTAHSSS
601 GSYQAPETL KMWKPSQKWD VVSYGILILE LIAGRSPAVE VGTSEMDLVR
651 WVQVCIIEKK PLCDVLDPLC APEAETEDEI VAVLKIAISC VNSSPEKRPRT
701 MRHVSDTLDR LPVAGD
    
```

Show predicted peptides also

Sort Peptides By  Residue Number  Increasing Mass  Decreasing Mass

Start - End	Observed	Mr (expt)	Mr (calc)	ppm	Miss	Sequence
66 - 73	435.7729	869.5312	869.5334	-3	0	R.VVSLSIPR.K ( <a href="#">Ions score 22</a> )
66 - 73	435.7736	869.5326	869.5334	-1	0	R.VVSLSIPR.K ( <a href="#">Ions score 12</a> )
66 - 73	435.7738	869.5330	869.5334	-0	0	R.VVSLSIPR.K ( <a href="#">Ions score 10</a> )
66 - 73	435.7739	869.5332	869.5334	-0	0	R.VVSLSIPR.K ( <a href="#">Ions score 13</a> )
66 - 73	435.7739	869.5332	869.5334	-0	0	R.VVSLSIPR.K ( <a href="#">Ions score 3</a> )
66 - 73	435.7740	869.5334	869.5334	0	0	R.VVSLSIPR.K ( <a href="#">Ions score 1</a> )
66 - 73	435.7740	869.5334	869.5334	0	0	R.VVSLSIPR.K ( <a href="#">Ions score 0</a> )
66 - 73	435.7740	869.5334	869.5334	0	0	R.VVSLSIPR.K ( <a href="#">Ions score 2</a> )
66 - 73	435.7740	869.5334	869.5334	0	0	R.VVSLSIPR.K ( <a href="#">Ions score 6</a> )
66 - 73	435.7740	869.5334	869.5334	0	0	R.VVSLSIPR.K ( <a href="#">Ions score 27</a> )
66 - 73	435.7740	869.5334	869.5334	0	0	R.VVSLSIPR.K ( <a href="#">Ions score 4</a> )
66 - 73	435.7740	869.5334	869.5334	0	0	R.VVSLSIPR.K ( <a href="#">Ions score 1</a> )
66 - 73	435.7740	869.5334	869.5334	0	0	R.VVSLSIPR.K ( <a href="#">Ions score 8</a> )
66 - 73	435.7741	869.5336	869.5334	0	0	R.VVSLSIPR.K ( <a href="#">Ions score 0</a> )
66 - 73	435.7741	869.5336	869.5334	0	0	R.VVSLSIPR.K ( <a href="#">Ions score 0</a> )
66 - 73	435.7742	869.5338	869.5334	0	0	R.VVSLSIPR.K ( <a href="#">Ions score 2</a> )
66 - 73	435.7742	869.5338	869.5334	0	0	R.VVSLSIPR.K ( <a href="#">Ions score 4</a> )
66 - 73	435.7742	869.5338	869.5334	0	0	R.VVSLSIPR.K ( <a href="#">Ions score 7</a> )
66 - 73	435.7742	869.5338	869.5334	0	0	R.VVSLSIPR.K ( <a href="#">Ions score 28</a> )
66 - 73	435.7742	869.5338	869.5334	0	0	R.VVSLSIPR.K ( <a href="#">Ions score 8</a> )
66 - 73	435.7743	869.5340	869.5334	1	0	R.VVSLSIPR.K ( <a href="#">Ions score 9</a> )
66 - 73	435.7744	869.5342	869.5334	1	0	R.VVSLSIPR.K ( <a href="#">Ions score 3</a> )
66 - 73	435.7744	869.5342	869.5334	1	0	R.VVSLSIPR.K ( <a href="#">Ions score 2</a> )
66 - 73	435.7744	869.5342	869.5334	1	0	R.VVSLSIPR.K ( <a href="#">Ions score 6</a> )
66 - 73	435.7744	869.5342	869.5334	1	0	R.VVSLSIPR.K ( <a href="#">Ions score 15</a> )
66 - 73	435.7744	869.5342	869.5334	1	0	R.VVSLSIPR.K ( <a href="#">Ions score 12</a> )
66 - 73	435.7745	869.5344	869.5334	1	0	R.VVSLSIPR.K ( <a href="#">Ions score 12</a> )
66 - 73	435.7750	869.5354	869.5334	2	0	R.VVSLSIPR.K ( <a href="#">Ions score 24</a> )
352 - 363	711.8692	1421.7238	1421.7150	6	2	R.ENQFVGEKESKK.R ( <a href="#">Ions score 1</a> )
661 - 685	932.7929	2795.3569	2795.3609	-1	0	K.PLCDVLDPLCAPEAETEDEIVAVLK.I ( <a href="#">Ions score 0</a> )



# Identification of calcium dependent protein kinases in chloroplasts- PKF-1

## *MATRIX* Mascot Search Results

### Protein View

Match to: [gi|15235312](#) Score: 18  
 HAE (HAESA); ATP binding / kinase/ protein kinase/ protein serine/threonine kinase [Arabidopsis thaliana]  
 Found in search of C:\Documents and Settings\ZFP Guest PC\My Documents\Data Orbitrap + QStar\NParvin\_SID1899\_020813\SID1899\_190713\_D7-3.RAW

Nominal mass (M<sub>r</sub>): 110338; Calculated pI value: 6.39  
 NCBI BLAST search of [gi|15235312](#) against nr  
 Unformatted [sequence string](#) for pasting into other applications

Taxonomy: [Arabidopsis thaliana](#)  
 Links to retrieve other entries containing this sequence from NCBI Entrez:  
[gi|1350783](#) from [Arabidopsis thaliana](#)  
[gi|166850](#) from [Arabidopsis thaliana](#)  
[gi|2842492](#) from [Arabidopsis thaliana](#)  
[gi|7269703](#) from [Arabidopsis thaliana](#)  
[gi|224589632](#) (no taxonomy information for this entry)

Fixed modifications: Carbamidomethyl (C)  
 Variable modifications: Oxidation (M)  
 Cleavage by Trypsin/P: cuts C-term side of KR  
 Sequence Coverage: 1%

Matched peptides shown in **Red**

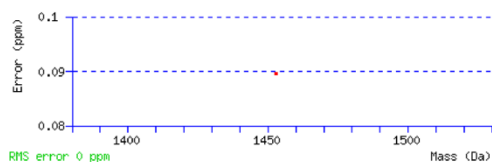
```

1  MLYCLILLLC  LSSTYLPSSL  LNQDATILRQ  AKLGLSDPAQ  SLSSWSDNND
51  VTPCKLWLVG  CDATSNVVSV  DLSSFMLVGP  FPSILCHLPS  LHSLSLYNNS
101  INGSLSADDF  DTCHNLISLD  LSENLLVGSV  PKSLPFNLPN  LKFLEISGNN
151  LSDTIPSSFG  EFRKLESLNL  AGNFLSGTIP  ASLGNVTTLK  ELKLAYNLF5
201  PSQIPSQLGN  LTELQVLWLA  GCNLVGPIPP  SLSRLTSLVN  LDLTFNQLTG
251  SIPSWITQLK  TVEQIELFNN  SFSGELPESM  GNMTTLKRFD  ASMNKLTGKI
301  PDNLNLNLE  SLNLFENMLE  GPLPESITRS  KTLSELKLFN  NRTLGVLP5Q
351  LGANSPLQYV  DLSYNRFSGE  IPANVCGEK  LEYLILIDNS  FSGEISNNLG
401  KCKSLTRVRL  SNNKLSGQIP  HGFWGLPRLS  LLELSDNSFT  GSIPKTIIGA
451  KNLSNLRISK  NRFSGSIPNE  IGSNLGIIIE  SGAENDFSGE  IPESLVK1KQ
501  LSRDL5KNQ  LSGEIPRELR  GWKLNLELNL  ANNHLSGEIP  KEVGIPLVLN
551  YLDLSSNQFS  GEIPELQNL  KLNVLNLSYN  HLSGKIPPLY  ANKIYAHDFI
601  GNPGLCVDLD  GLCRKITRSK  NIGYVWILLT  IFLLAGLVFV  VGIVMFIACK
651  RKLRAKLSST  LAASKWRSFH  KLFHSEHEIA  DCLDEKNVIG  FGSSGKVYKV
701  ELRGGEVVAV  KKLNSVKVGG  DDEYS5D5LN  RDVFAAEVET  LGTIRK5IV
751  RLWGCCSSGD  CKLLVYEVMP  NGS1ADVLHG  DRKGGVVLGW  PERLIRIALDA
801  AEGLSYLHHD  CVPPIVHRDV  KSSNLLDSD  YGAKVADFGI  AKVGQMSGSK
851  TPEAMSGIAG  SCGYIAPEYV  YTLRVNEKSD  IY5FGVLLLE  LVTGKQPTDS
901  ELGDKDMAKW VCTALDKCGL  EPVIDPKLDL  KFKEEISKVI  HIGLLCT5PL
951  PLNRPSMRKV  VIMLQEVSGA  VPCSSPNTSK  RSKTGGK1LSP  YYTEDLNSV
    
```

Show predicted peptides also

Sort Peptides By  Residue Number  Increasing Mass  Decreasing Mass

Start - End	Observed	Mr (expt)	Mr (calc)	ppm	Miss Sequence
906 - 917	727.3444	1452.6742	1452.6741	0	1 <b>K.DMAKWVCTALDK.C</b> Oxidation (M) ( <a href="#">Ions score 18</a> )





## Identification of calcium dependent protein kinases in chloroplasts- PKF-2

### **MASCOT** Mascot Search Results

#### Protein View

Match to: [gi|15242720](#) Score: 15  
**protein kinase, putative [Arabidopsis thaliana]**  
 Found in search of C:\Documents and Settings\ZFP Guest PC\My Documents\Data Orbitrap + QStar\NParvin\_SID1899\_020813\SID1899\_190713\_F7-6.RAW

Nominal mass ( $M_r$ ): 47261; Calculated pI value: 9.34

NCBI BLAST search of [gi|15242720](#) against nr  
 Unformatted [sequence string](#) for pasting into other applications

Taxonomy: [Arabidopsis thaliana](#)  
 Links to retrieve other entries containing this sequence from NCBI Entrez:  
[gi|7378612](#) from [Arabidopsis thaliana](#)  
[gi|9757783](#) from [Arabidopsis thaliana](#)  
[gi|114050627](#) from [Arabidopsis thaliana](#)

Fixed modifications: Carbamidomethyl (C)  
 Variable modifications: Oxidation (M)  
 Cleavage by Trypsin/P: cuts C-term side of KR  
 Sequence Coverage: 3%

Matched peptides shown in **Bold Red**

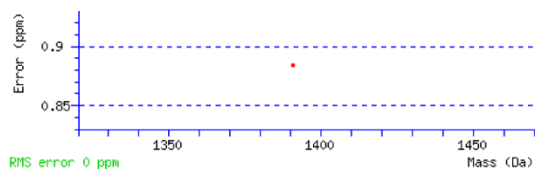
```

1 MKCFLFPLGD KKDEQRSPKP VSPSTSNFSDV NKSQSDFSR DVSQTSTVSS
51 TGRNSNTSMS ARENNLREFT IGDLSATR N FSRSGMIGEG GFGCVFWGTI
101 KNLEDPSKKI EVAVKQLGKR GLQGHKEWVT EVNFLGVVEH SNLVKLLGHC
151 AEDDERGIQR LLVVEYMPNQ SVEFHLSPRS PTVLTWDLRL RIAQDAARGL
201 TYLHEEMDFQ IIFRDFKSSN ILLDENWTAK LSDFGLARLG PSPGSSHVST
251 DVVGTMGYAA PEYIQTGRLT SKSDVWGYGV FIYELITGRR PLDRNPKPGE
301 QKLEWVRPY LSDTRRFRLI VDPRLLEGKYM IKSQKLA VV ANLCLTRNAK
351 ARPKMSEVLE MVTKIVEASS PNGGKKPQL VPLKSQETSR VEEGKNNKVL
401 DGAEGGWLEK LWNPNVVRAC
  
```

Show predicted peptides also

Sort Peptides By  Residue Number  Increasing Mass  Decreasing Mass

Start	End	Observed	Mr (expt)	Mr (calc)	ppm	Miss	Sequence
20	32	348.6758	1390.6741	1390.6729	1	0	<b>K.PVSPSTSNFSDVKNK.S</b> ( <a href="#">Ions score 15</a> )



## Curriculum Vitae

Name: Nargis Parvin  
 Date of Birth: July 24, 1986  
 Place of Birth: Gorapara, India

### Education:

Since Oct, 2010 PhD studies in the lab of Prof. Ute C. Vothknecht, Department-Biology I, Botany, Biocentre of LMU on `` Identification and Functional Characterization of Calcium Regulated Processes in Plant Organelle`` with DAAD PhD scholarship

2009-2010 Worked on ``Stomatal Signalling in *Commelina benghalensis*`` in the lab of Prof. Rup Kumar Kar, Department of Botany, Visva-Bharati, Santiniketan, India

2007-2009 Master of Science (M.Sc) in Botany with specialization in Plant Physiology, Biochemistry and Molecular Biology with 1<sup>st</sup> class from Visva-Bharati University, India

2004-2007 Bachelor of Science (B.Sc) in Life Science with 1<sup>st</sup> class from Visva- Bharati University, India

### Scientific Publications:

**Parvin.N.**, Laha D., Bolle C., Heermann R., Jung K., Philippar K., Vothknecht U.C., and Chigri F., (2015) TOM9: a calmodulin-regulated protein involved in TOM complex integrity in *Arabidopsis thaliana*. (Manuscript in preparation).

Rocha A.G., Mehlmer N., Stael S., Mair A., **Parvin N.**, Chigri F., Teige M. And Vothknecht U.C., (2013) Phosphorylation of Arabidopsis transketolase at Ser-428 provides a potential paradigm for metabolic control of chloroplast carbon metabolism. Biochemical Journal. (Published online on 13 Dec 2013 as manuscript BJ20130631).

Mehlmer N., **Parvin N.**, Hurst C.H., Knight M.R., Teige M. and Vothknecht U.C. (2012) A toolset of aequorin expression vectors for in planta studies of subcellular calcium concentrations in *Arabidopsis thaliana*. Journal of Experimental Botany 63 (4), 1751-1761

Laha D., **Parvin N.** and Kar R.K. (2009) Role of ethylene and its interaction with hydrogen peroxide and calcium in light-induced stomatal opening of *Commelina benghalensis*. Journal of Theoretical and Experimental Biology. 5(3&4):115-120

### Academic awards:

- Qualified for CSIR-UGC NET (India) for Junior Research Fellowship (not availed) and lectureship, 2009
- UGC merit scholarship for University rank holders (for standing first in B.Sc) 2007- 2009
- DAAD PhD scholarship 2010